

**CHAPTER 4
BASIN MODELING**



Principles and Workflow

General Principles and Workflow:

Basin modeling is numerical forward modeling of physical and chemical processes in sedimentary basins over geological time spans. Based on the geometrical reconstruction of sedimentary basins, it simulates and predicts the thermal regimen and fluid flows (water and hydrocarbons) through time in order to assess source rock maturity, pore pressure and hydrocarbon charge. The main objective of basin modeling is to estimate exploration risk for hydrocarbon charge by testing various assumptions regarding source rock characteristics, impact of faults, lithofacies, permeability, etc.

The first step of basin modeling is geometrical reconstruction, a 3D structural restoration (generally vertical shear displacement) that takes into account internal stratigraphic architecture, eroded thicknesses, paleo-bathymetries, lithofacies distribution and their associated compaction laws. The structural and facies models depict static petroleum system elements such as source rock, reservoirs, seal and traps. The reconstruction defines burial and porosity/permeability evolution, drainage areas and migration pathways.

The second step addresses thermal regime history and maturity calibration. It provides a first estimate of the basin's hydrocarbon potential by estimating hydrocarbon mass expelled through time. The thermal model is constrained at the base with lithospheric characteristics (geometrical and radiogenic heat production) and at the top with a definition of paleo-temperature. The present day thermal regime is calibrated using well temperatures while the past thermal regime is calibrated on maturity indicators (generally vitrinite data).

The third step of basin modeling is fluid flow simulation and calibration of hydrocarbon accumulation. Hydrocarbon migration is driven through a generalized Darcy law that takes into account permeability, relative permeability, viscosity, hydrodynamism, capillarity and buoyancy. As a consequence, hydrocarbon migration is conditioned by internal stratigraphic architecture, lithofacies distribution and water pressure gradient (hydrodynamism). Calibration consists in recreating hydrocarbon accumulations known in the basin (and even shows and seeps) in order to be predictive.

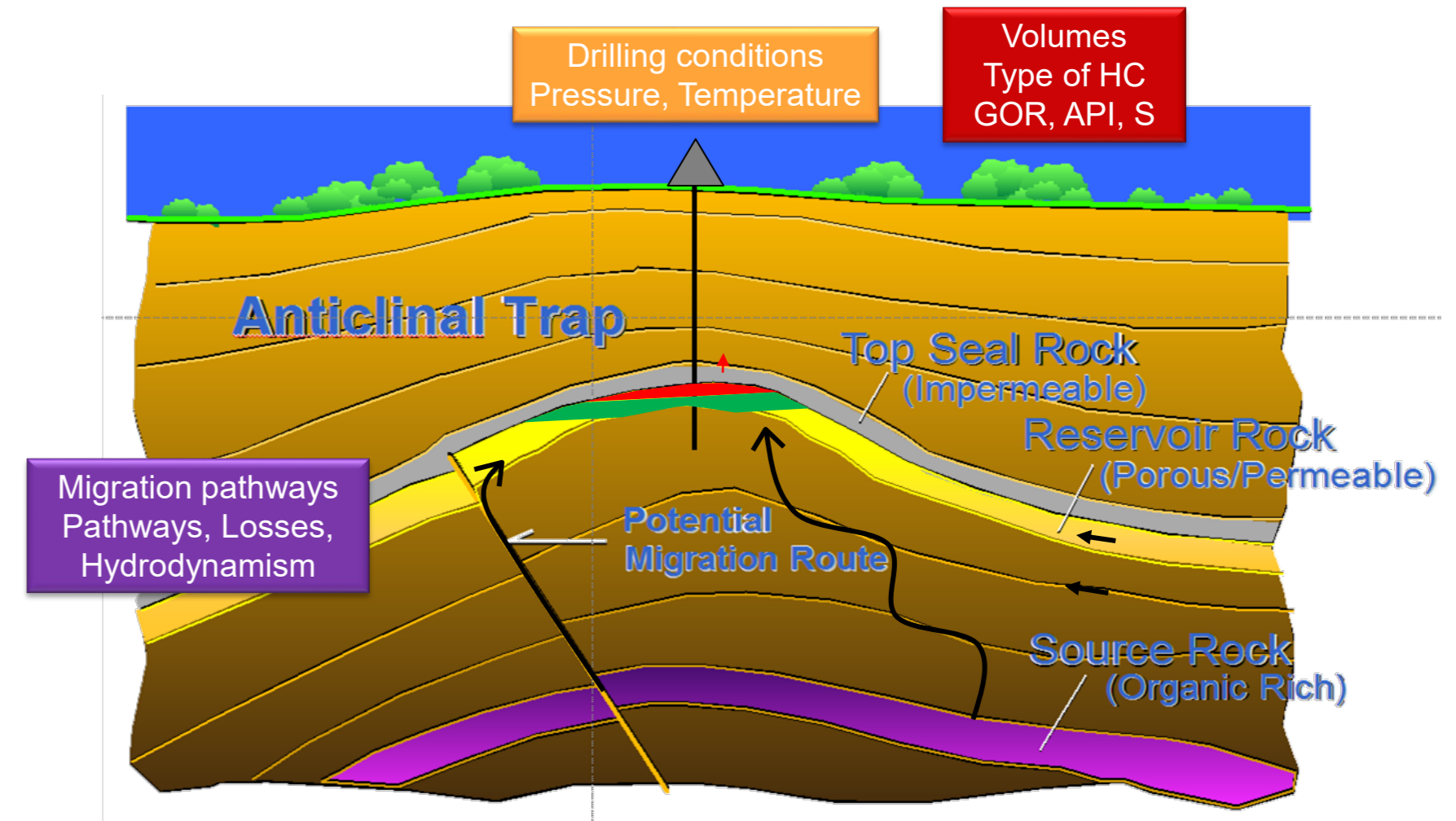


Figure 1: Principle of Petroleum System Model

Armentrout, 2000

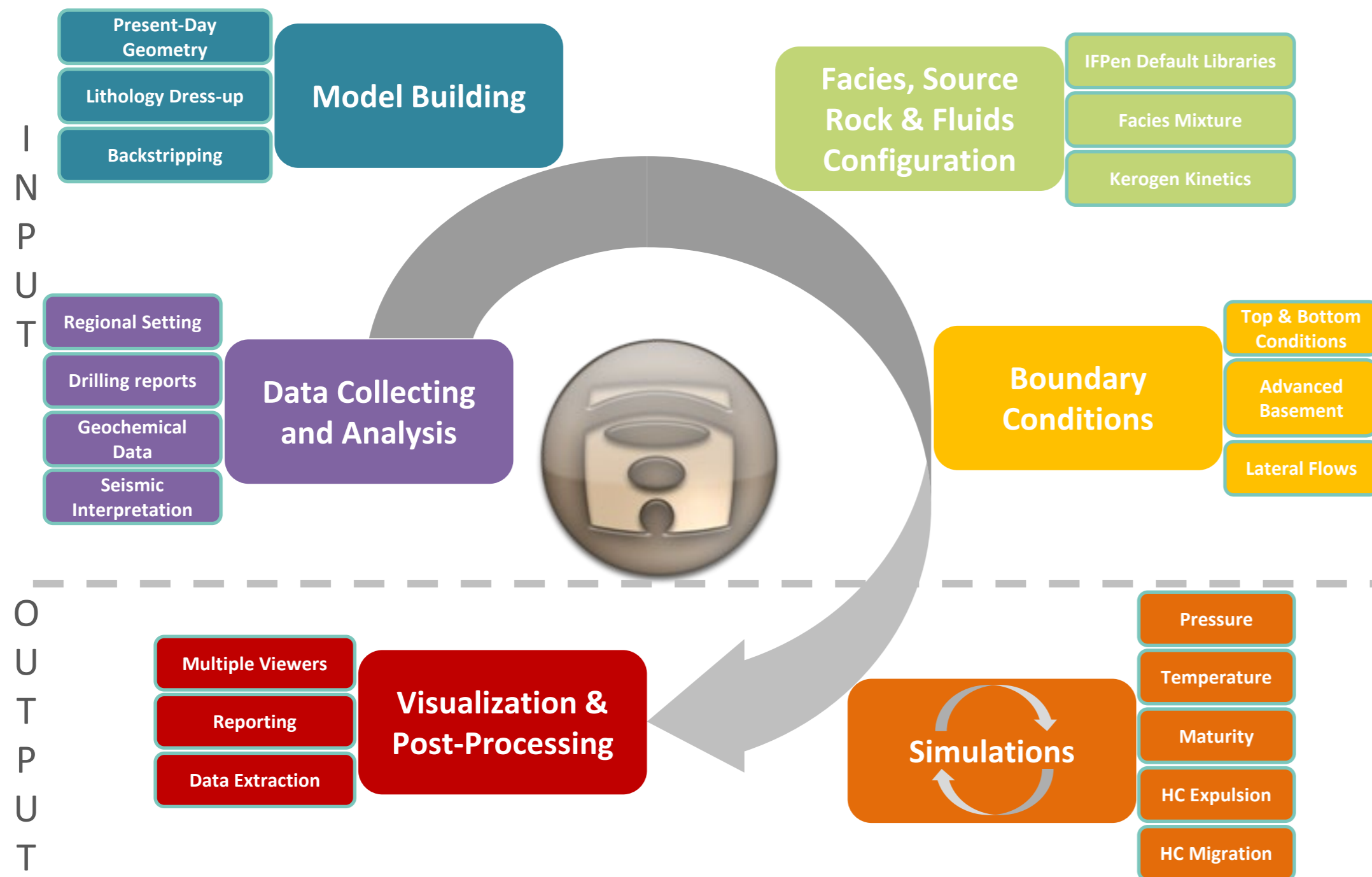


Figure 2: Basin Modeling workflow

Example of a 3D Temisflow Model

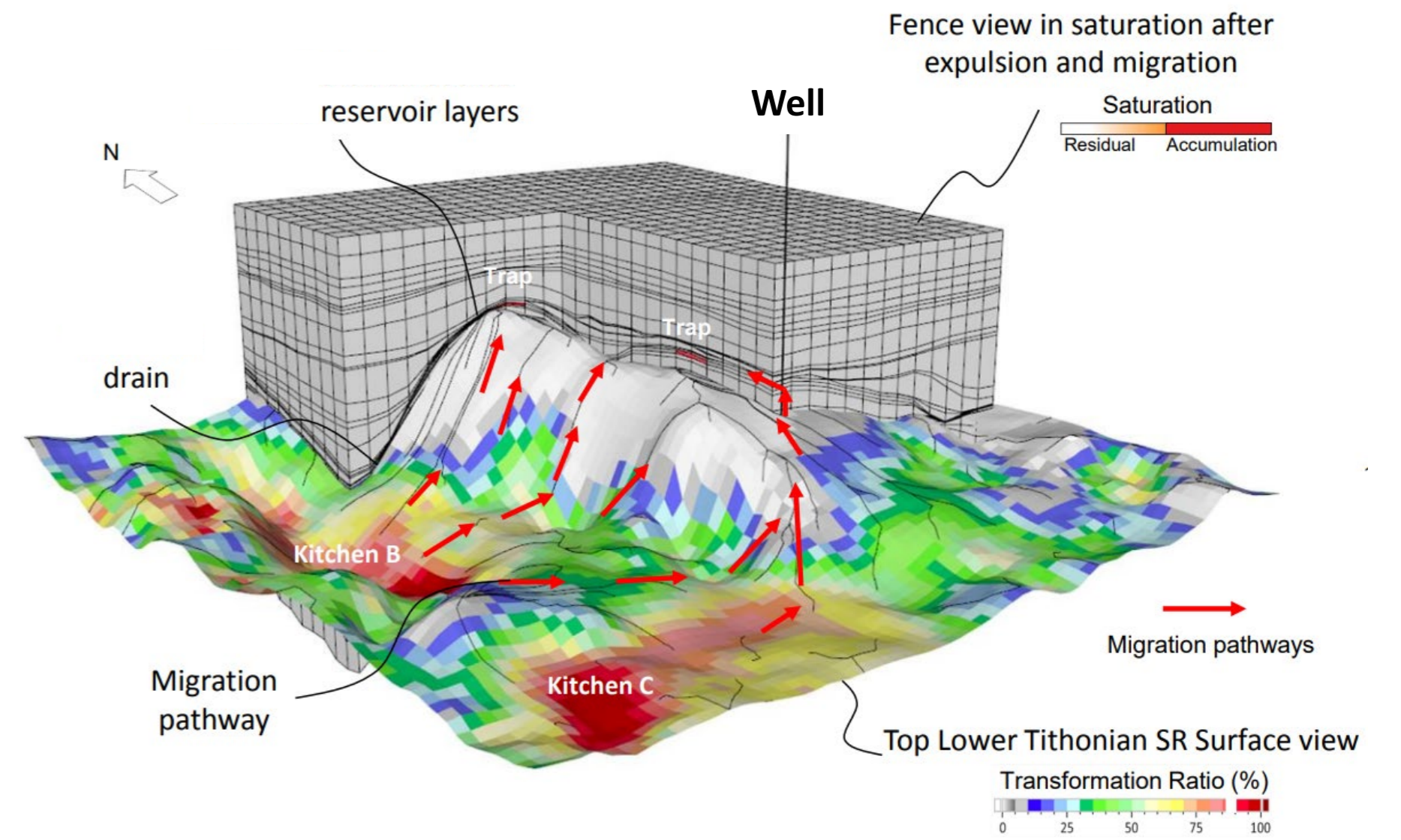


Figure 3: Example of Basin Modeling result



CHAPTER 4.1 INTRODUCTION

Kilometers

0 100 200



Introduction

Objectives:

Hydrocarbon discoveries and numerous Direct Hydrocarbon Indicators demonstrate that offshore Nova Scotia has active petroleum systems. Nevertheless, the deep-water setting is still under-explored with only thirteen exploration wells. The basin modeling objective was to assess the basin's hydrocarbon potential with the most up to date information and analysis. The aim was to assess the potential for trapped hydrocarbons in deep water and to estimate associated risks. To do so, basin modeling will, first, evaluate source rock maturity, timing and hydrocarbon quantity expelled, and secondly, hydrocarbon volume in place, fluid types (oil, and gas) at standard condition.

This 3D basin model is based on sedimentological, petrophysical and structural analyses done earlier in this study and detailed in previous chapters. It simulates and predicts the thermal regime, pore-pressure, hydrocarbon migration pathways and trapping.

Tool: TemisFlow™

The IFP Group pioneered the development and use of Petroleum System Analysis and Basin Modeling techniques in the late 1980's. These techniques include the modeling of burial, thermal history, oil and gas generation and migration processes with the TemisFlow technology. TemisFlow is the leading industrial tool in its domain, widely used by oil and gas companies and consulting firms around the globe. With a long proven track record, TemisFlow is the next-generation solution for basin modeling. It excels in assessing regionally-controlled petroleum systems while identifying local drilling opportunities and quantifying the associated commercial and technical risks. (<http://www.beicjp.com/basin-modeling-and-petroleum-system-analysis>).

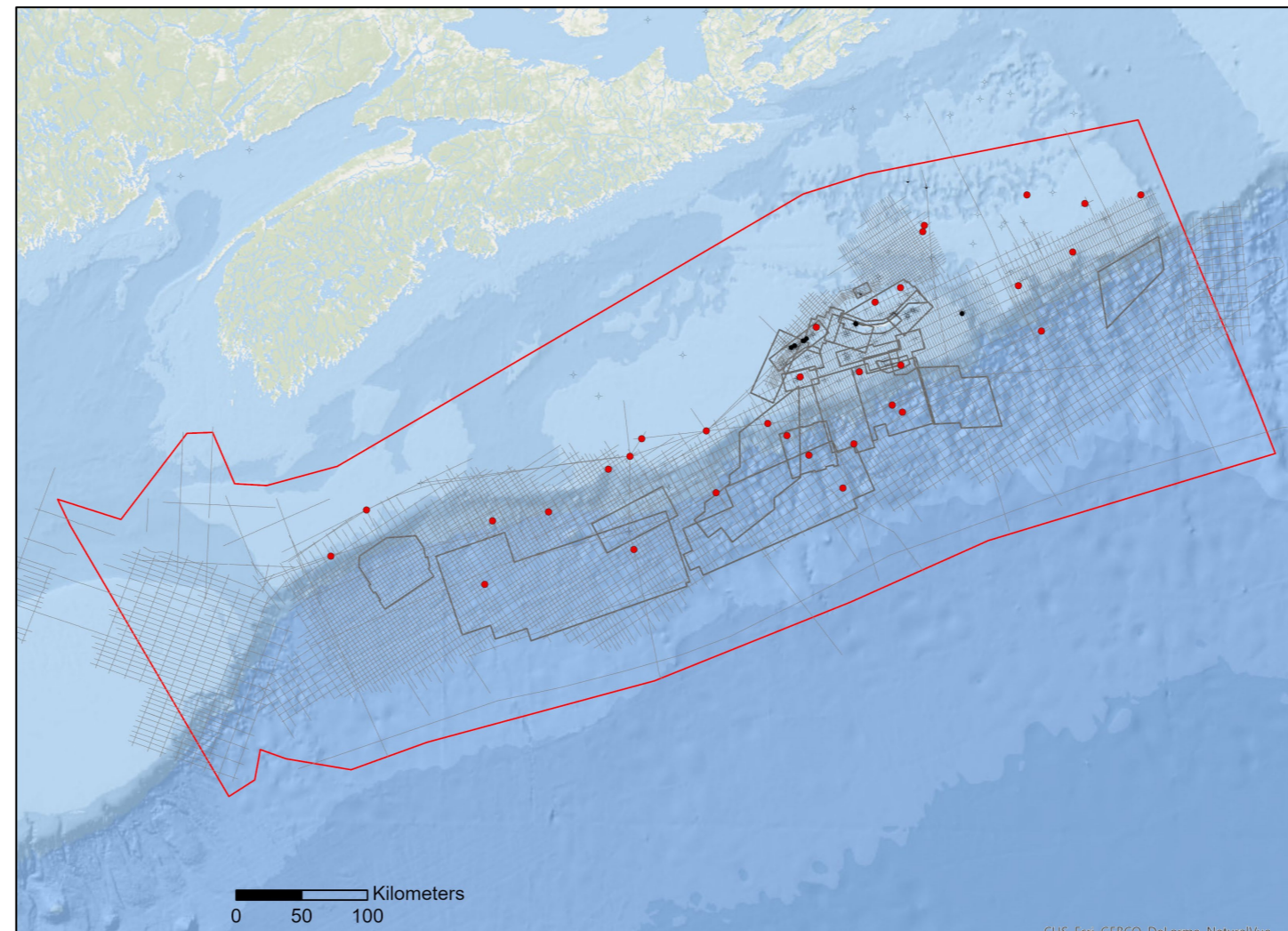


Figure 4: Basin modeling study area

Wells	Temperature	Pressure	Maturity
ALBATROSS B-13	x	x	x
ALMA F-67	x	x	x
ANNAPOLIS G-24	x	x	x
ASPY D-11/D-11A		x	
BALVENIE B-79	x	x	x
BANQUEREAU C-21	x	x	x
BONNET P-23	x	x	x
CHEBUCTO K-90	x	x	x
CHESHIRE L-97/L-97A	x	x	x
CHIPPEWA G-67	x	x	
COHASSET L-97	x	x	x
COMO P-21	x	x	
CREE E-35	x		
CRIMSON F-81	x	x	x
DAUNTLESS D-35	x	x	x
EVANGELINE H-98	x	x	x
GLENELG J-48	x	x	x
GLOOSCAP C-63	x	x	x
HESPER P-52	x	x	x
LOUISBOURG J-47	x	x	x
MIC MAC H-86	x	x	x
MIC MAC J-77	x	x	x
MISSISSAUGA H-54	x	x	
MOHAWK B-93	x	x	x
MOHEIDA P-15	x	x	x
MOHICAN I-100	x	x	x
MONTAGNAIS I-94	x	x	
MONTEREY JACK E-43/E-43A	x	x	x
NASKAPI N-30	x	x	x
NEWBURN H-23	x	x	x
ONEIDA O-25	x		x
PANUKE F-99	x	x	
SACHEM D-76	x		
SHELBURNE G-29	x	x	x
SHUBENACADIE H-100	x	x	x
SOUTH DESBARRES O-76	x	x	x
SOUTH WEST BANQUEREAU F-34	x	x	x
TANTALLON M-41	x	x	x
TORBROOK C-15	x	x	x
UNIACKE G-72	x	x	x
WENONAH J-75	x		
WEST ESPERANTO B-78	x	x	x
WEYMOUTH A-45	x	x	x

Figure 5: Well Data Base for Basin Modeling

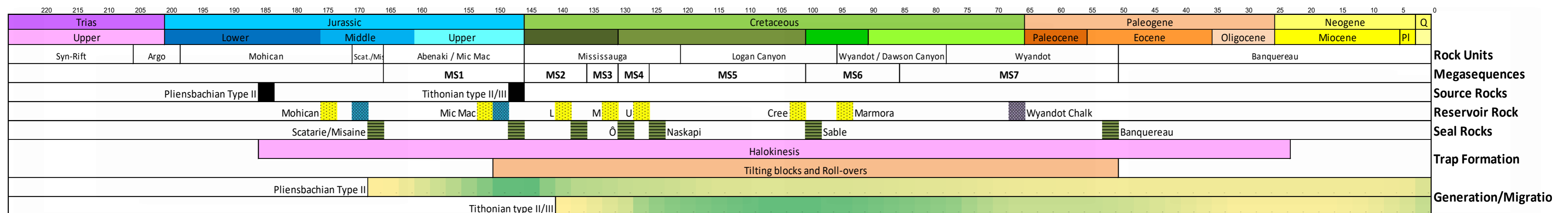


Figure 6: Generalized Nova Scotia Petroleum system chart



CHAPTER 4.2
3D MODEL CONSTRUCTION



3D Model Construction

Static Model:

The Temisflow static model was built from regional seismic horizons, GDE maps, sequence stratigraphic analysis and well data. The 3D grid covers 230 000 km² with a 1x1km cell size resolution.

- Architecture** : 12 Structural depth maps based on the 3D and 2D seismic line interpretations from basement to sea bottom (Chapter 1, PL. 1.2) were used. These maps correspond to the main tectono-sequences and are the foundation of the 3D model architecture for the 3D basin model. Horizon ages originate from the stratigraphic interpretation (Chapter 3. PL. 3.9). The horizons are: Basement (≈225Ma), Base Autochthonous Salt (≈205Ma), Top Autochthonous (≈196Ma), Salt, J163, J145, K125, K112, K101, K94, K78, T50 and Sea Bottom. Moreover, allochthonous salt was interpreted from the seismic as polygons for each horizons to be incorporated in the 3D grid.
- Internal stratigraphic architecture** : Subdivisions between horizons was based on the sequence stratigraphic analysis (PL 3.9, Chapter 3) that provides the main system tract (FRST, HST, TST) and associated relative thickness. Sequence stratigraphic analysis was critical for identifying reservoirs, seals and source rock layers.
- Lithofacies distribution**: Lithofacies distribution was defined using GDE maps (Chapter 3) from the Middle Jurassic (J163) to lower Banquereau (T50) for FRST and HST system tracts. The Lower to Middle Jurassic was defined from previous PFA studies (PFA 2011 Chapter 6-2, PFA 2015 Chapter 6.2, PFA 2016 Chapter 6.2.5) driven Seismic stratigraphic analysis and by Forward Stratigraphic Modeling (Dionisoflow).
- Source Rocks**: Two source rocks were defined in the Temisflow model. One in the Lower Jurassic at the Pliensbachian with a type II restricted marine kerogen and the second of Tithonian age with a kerogen of type II/III (deltaic marine environment).
- Reservoirs**: The main reservoirs were integrated into the Temisflow model based on seismic, sedimentology and sequence stratigraphic analysis. Reservoir layers were included at Forced Regression System Tract (FRST) and correspond to net thickness reservoir.
- Seals**: Lithofacies distribution for transgressive system tracts (TST) corresponds to regional shaly environment and defines the potential seal interval that was validated by well data over-pressure analysis. Salt diapirs and canopies also provide lateral and top seal for hydrocarbon trapping.

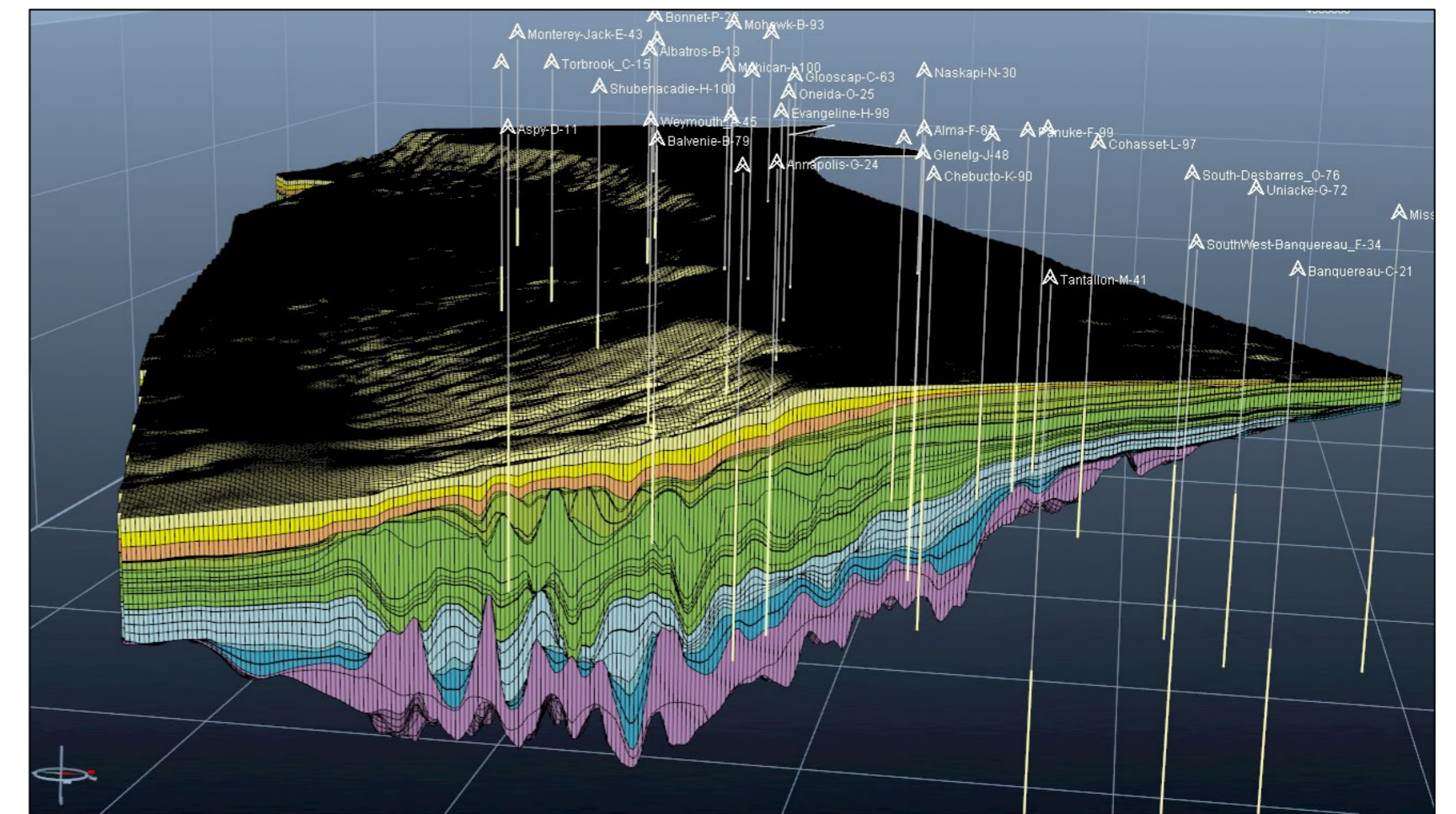
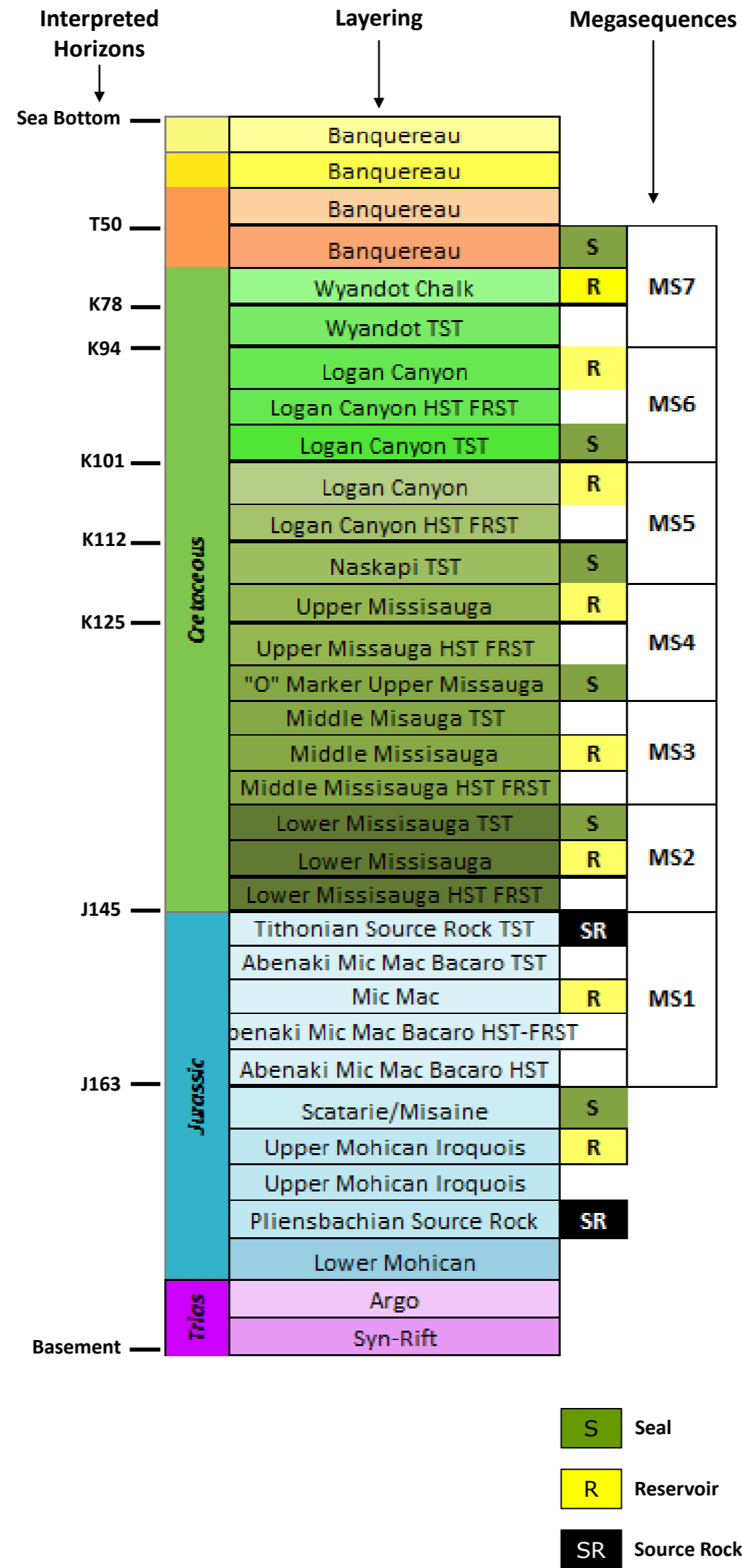


Figure 7: 3D view of Temisflow model displaying stratigraphy

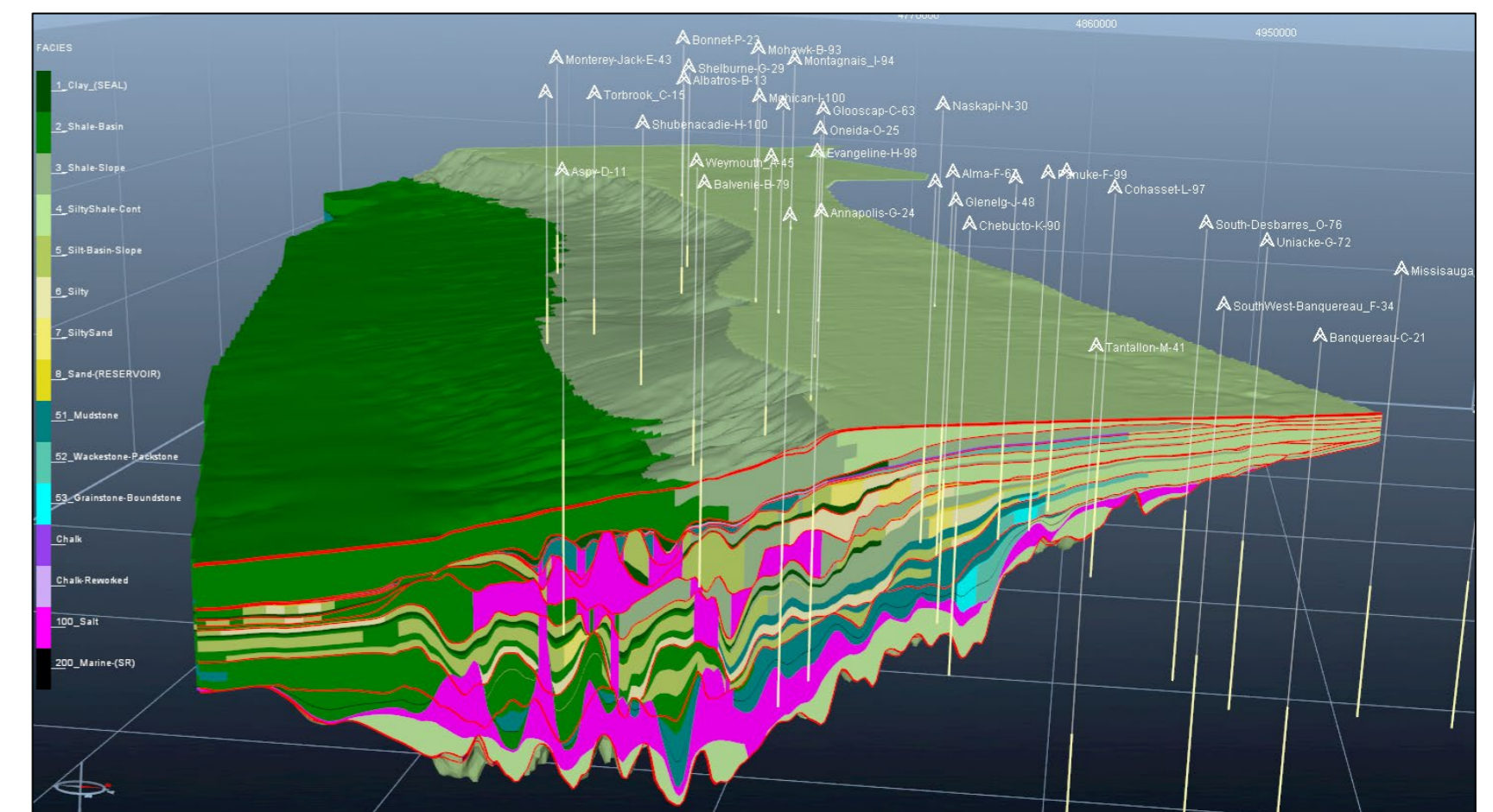
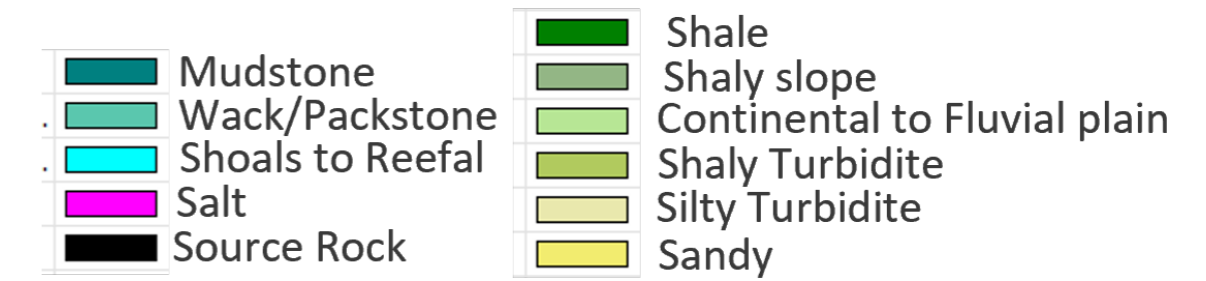


Figure 8: 3D view of Temisflow model displaying lithofacies



3D Model Construction

Kinematic Model:

The kinematic model corresponds to the basin geometry evolution through time. The kinematic reconstruction is performed through a backstripping process taking into account paleobathymetries, thickness maps, sediment compaction and salt diapirism restoration. The kinematic model defines the paleo-drainage areas and paleo-structures until present geometry, defining migration pathways history (migration and dismigration).

- Paleobathymetry maps were defined using GDE maps and Dionisoflow results from previous PFA projects from Basement to Present day. Maps were calibrated on biostratigraphic data, tectonic and thermal subsidence history. 11 maps are used as key paleobathymetry maps (171Ma, 151Ma, 145Ma, 137Ma, 130Ma, 125Ma, 101Ma, 94Ma, 78Ma, 50Ma and 29Ma). Intermediate ages are extrapolated between two key maps.
- Salt **restoration** was performed for autochthonous and allochthonous salt in order to model the diapirism and its impact on structural evolution. The initial salt thickness was estimated based on present day salt volume (autochthonous and allochthonous) taking into account the loss due to dissolution and non interpreted bodies. Additionally, distribution of the initial salt thickness take into account the rifting accommodation space. The timing of salt deformation is based on seismic interpretation and gives intervals from Lower Jurassic (around 163Ma) to Upper Cretaceous (78Ma).
- Lithofacies properties such as compaction and porosity/permeability laws were defined for each lithofacies and calibrated to measurements at well locations. Petrophysical parameters were adjusted to take into account upscaling effects.

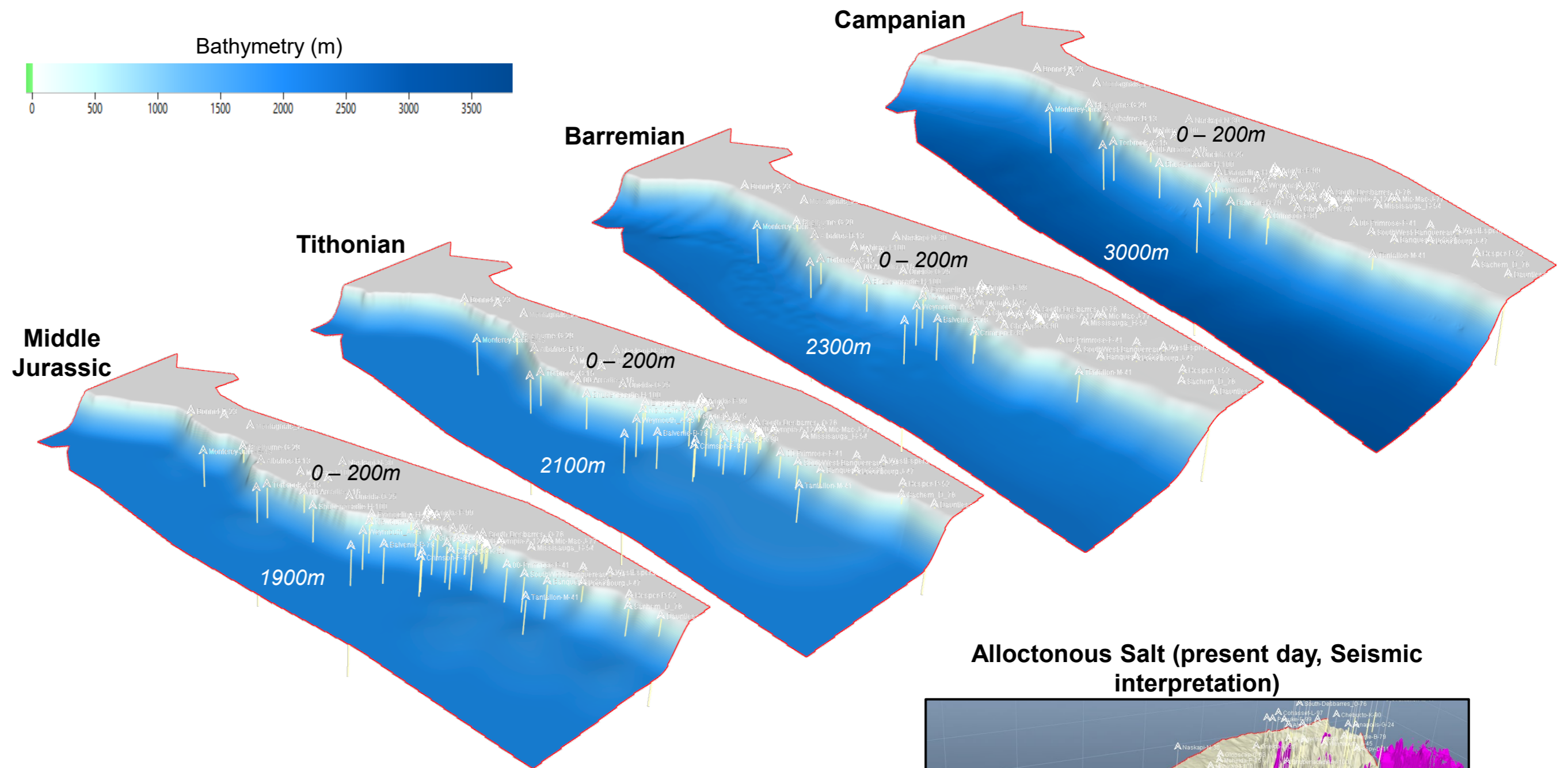


Figure 9: Example of some paleobathymetry maps

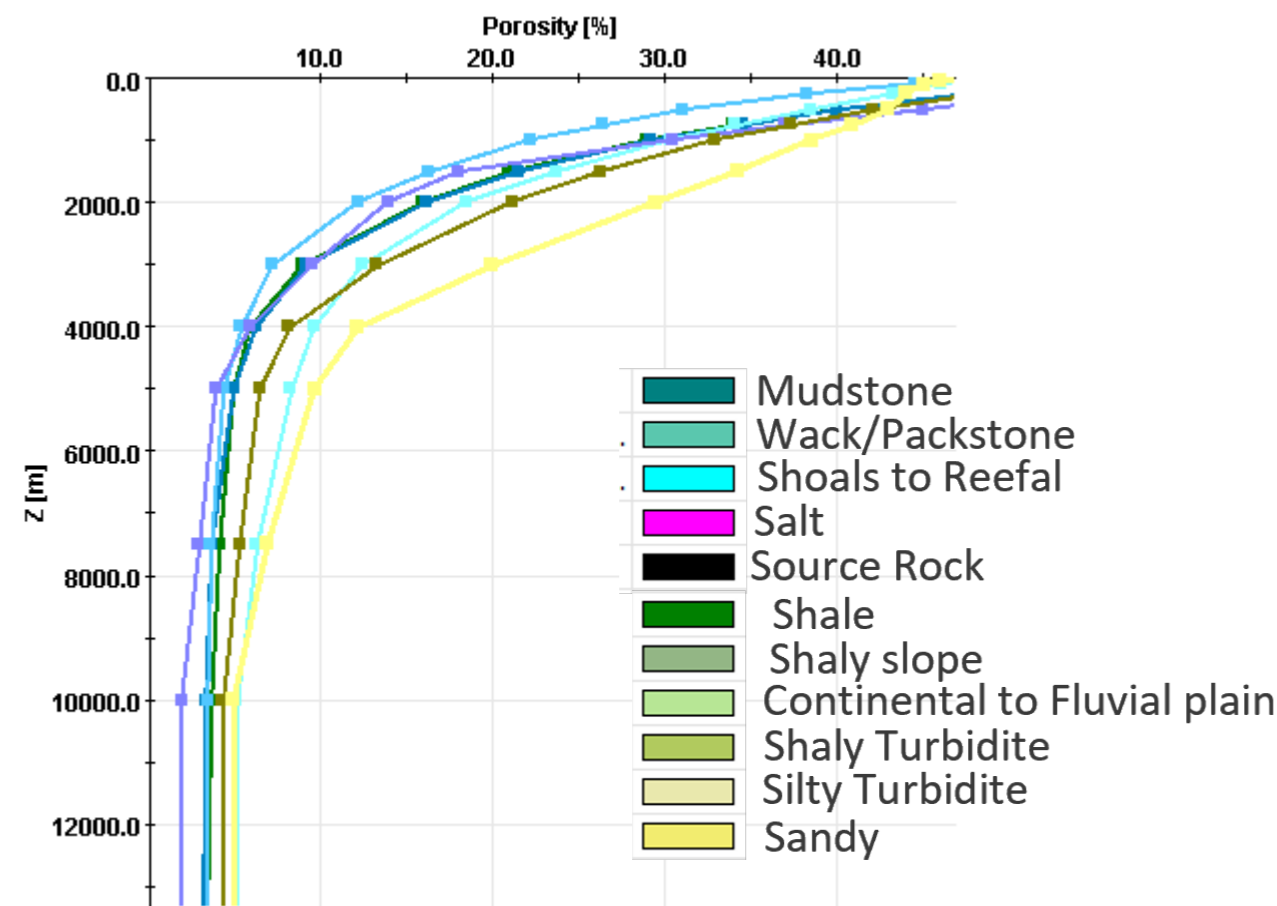
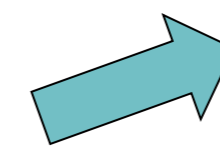
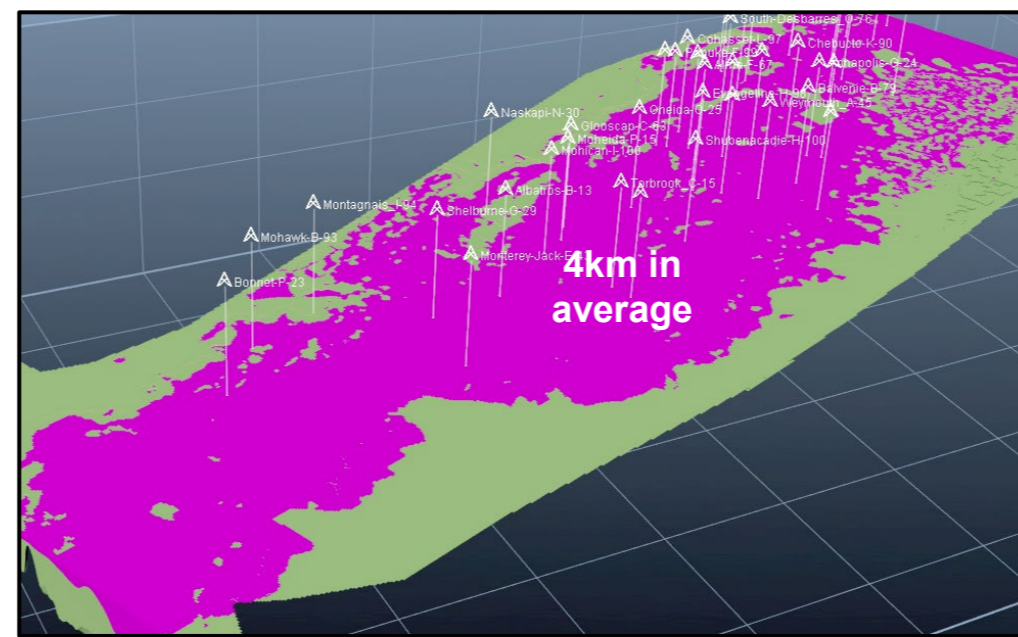
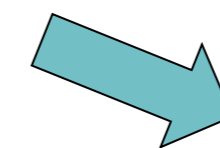
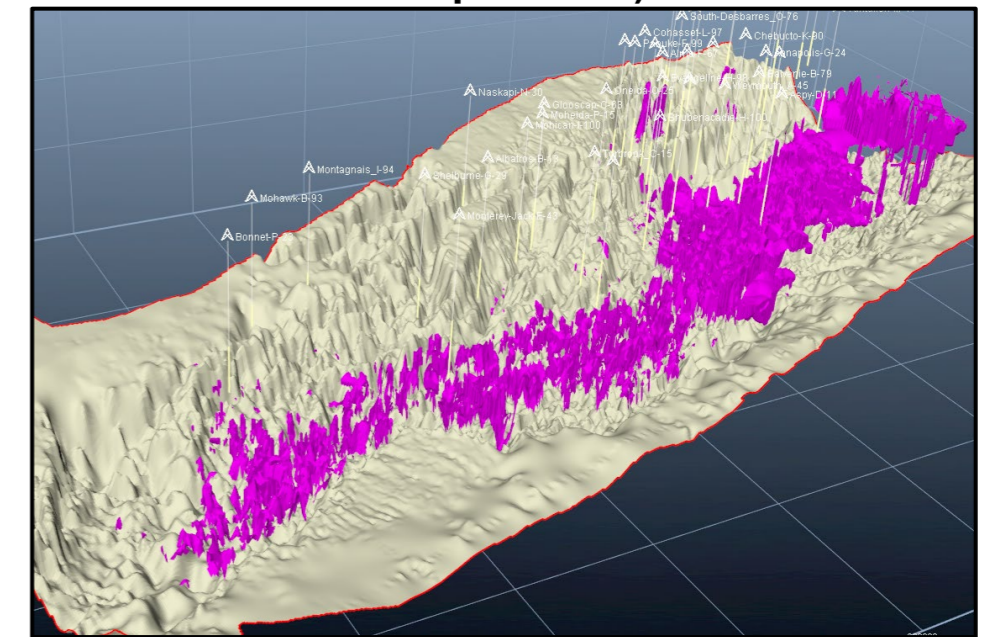


Figure 10: Lithofacies compaction curves

Salt distribution at time of deposition (196Ma)



Allochthonous Salt (present day, Seismic interpretation)



Autochthonous Salt (present day, Seismic interpretation)

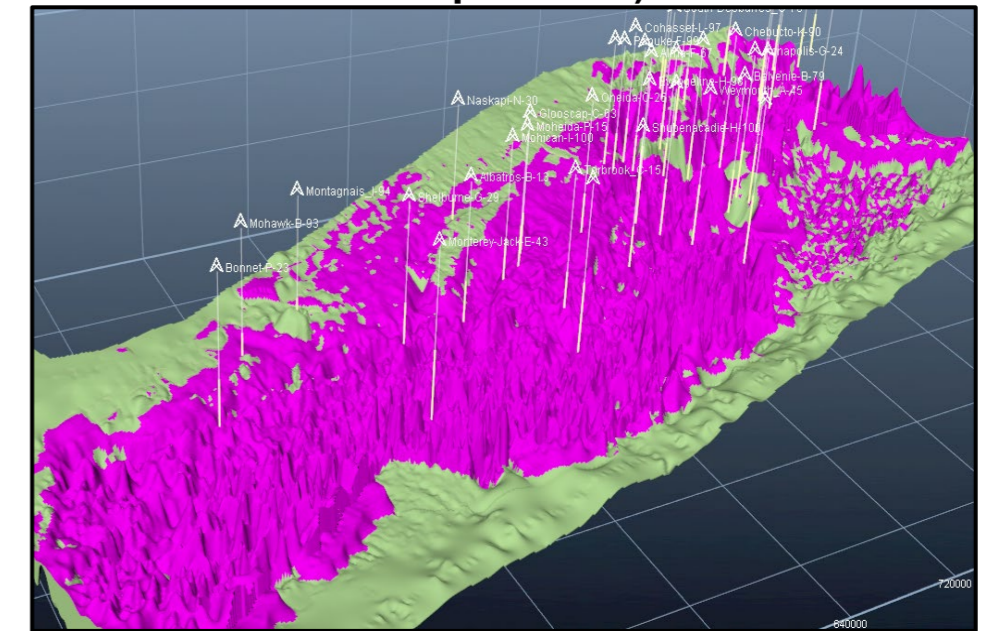


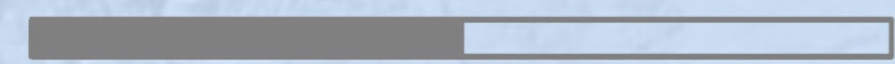
Figure 11: 3D view of autochthonous salt restoration in Temisflow model



CHAPTER 4.3 SOURCE ROCKS

Kilometers

0 100 200



Tithonian source rock :

The Tithonian source consists of a type II/III kerogen deposited in an open marine environment with terrestrial influx. Based on recent wells (Monterey Jack and Cheshire) organic matter preservation in the western deep marine environment appeared to be limited probably due to extremely low sedimentation rates and possible deep marine currents. The eastern part of the province shows nutrient rich environments and favorable sedimentation rate conditions for preservation. Hence the TOC and net thickness distribution map is mainly driven by the Upper Jurassic thickness map. TOC (wt%) ranges from 0 to 5% and net thickness varies from 0 to 20m.

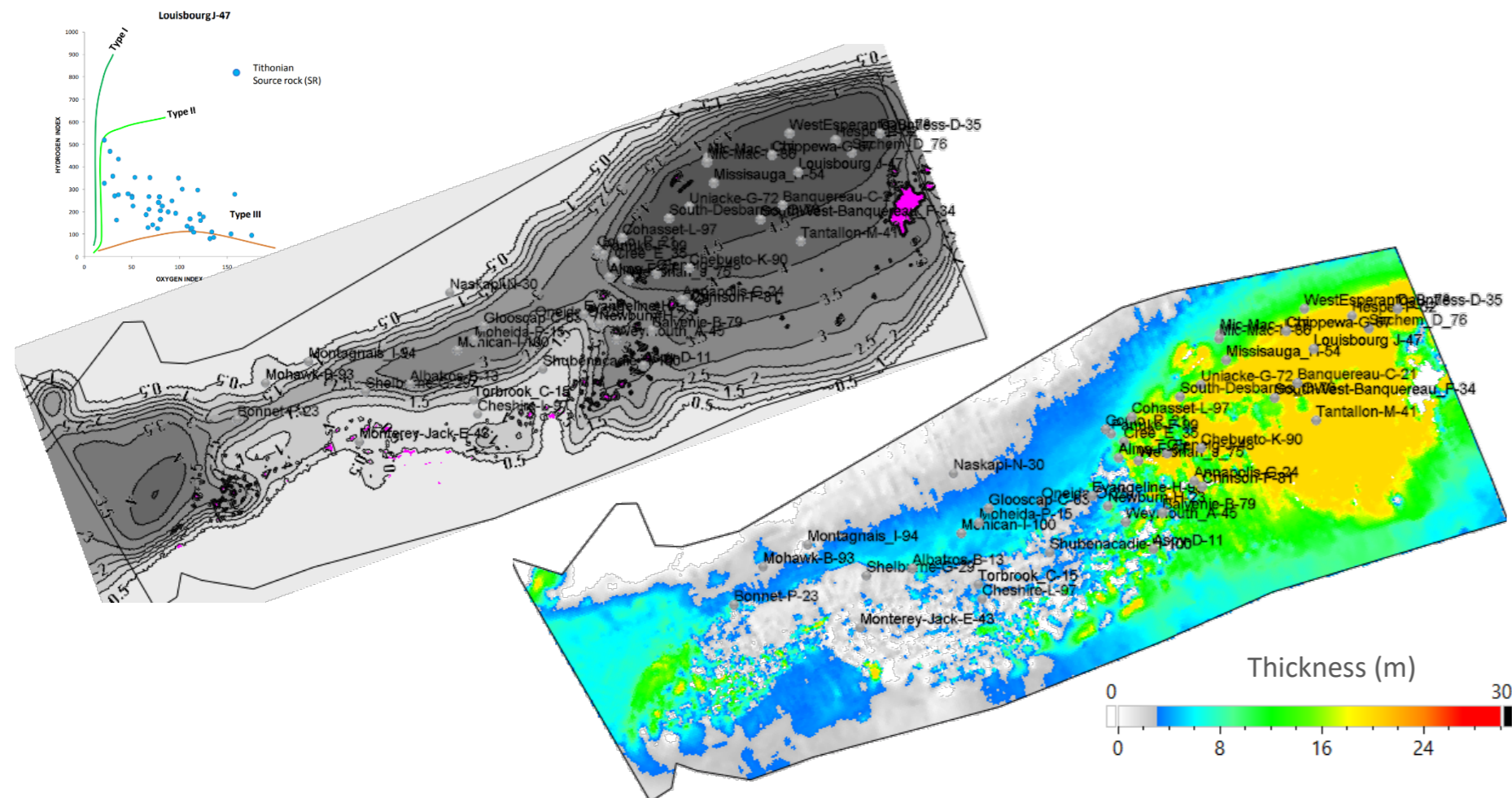


Figure 12: Tithonian source rock distribution in TOC (%wt) and Net thickness (m)

Pliensbachian source rock :

The Pliensbachian source rock consists of a type II kerogen deposited in a restricted marine environment. This source rock is inferred by analogy to source rocks recognized on the conjugate margins of Newfoundland and Nova Scotia, in Portugal and Morocco. See Chapter 2.3 “Jurassic Source Rock – Synthesis and new model” for more details. Source rock parameters used in this study are: TOC around 3 to 4% , HI from 300 to 500 mg/g and a net thickness from 10 to 30m.

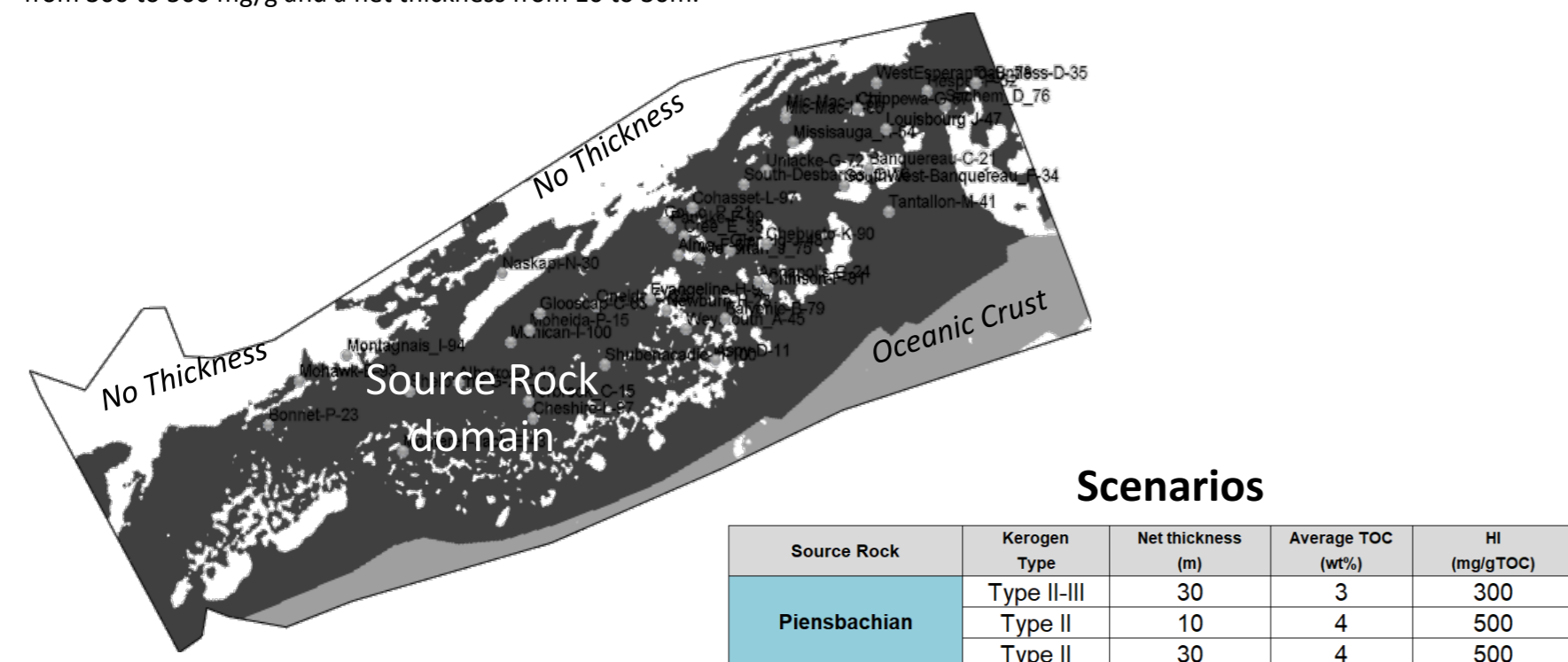


Figure 13: Pliensbachian source rock distribution and associated scenarios (TOC, HI and Net Thickness)

Source Rock	Depositional Environment	Kerogen Type	Net thickness (m)	Average TOC (wt%)	HI (mg/gTOC)
Tithonian	Regional Open Marine	Type II / III	0 to 20m	0 to 5%	400
Pliensbachian	Restricted Marine	Type II	0 to 30m	3 to 4%	300 to 500

Figure 14: Synthesis of Nova Scotia source rock potential

Compositional Kinetic Scheme :

- Tithonian source rock type II-III kinetic scheme was defined as a mixture between Mesnil 2 (type II Toarcian France, Behar et al 1997) and Brent (type III Dogger. North Sea - Vandenbrouke et al., 1999) from IFPEN library.
- Pliensbachian source rock type II kinetic scheme was defined as Mesnil 2 (type II Toarcian France, Behar et al 1997) from IFPEN library.

In this study, kerogen maturation generates five families of hydrocarbons; heavy oil, normal oil, condensate oil, gas and coke (considered only in the secondary cracking). The kinetic scheme of each source rock is detailed below. The histogram shows reaction frequency (thermal cracking) as a function of activation energy (temperature) and associated products from kerogen (Heavy (C14+), Normal (C8-C13), Condensate (C5-C8) and Gas (C1-C4). Secondary cracking generates lighter components and coke from heavy, normal and condensate oil until complete secondary cracking if the conditions are favorable. These schemes were edited from the IFPEN Default Library (specific data not available for Nova Scotia).

The graph below shows the source rock transformation rate as a function of temperature for each Tithonian and Pliensbachian source rocks.

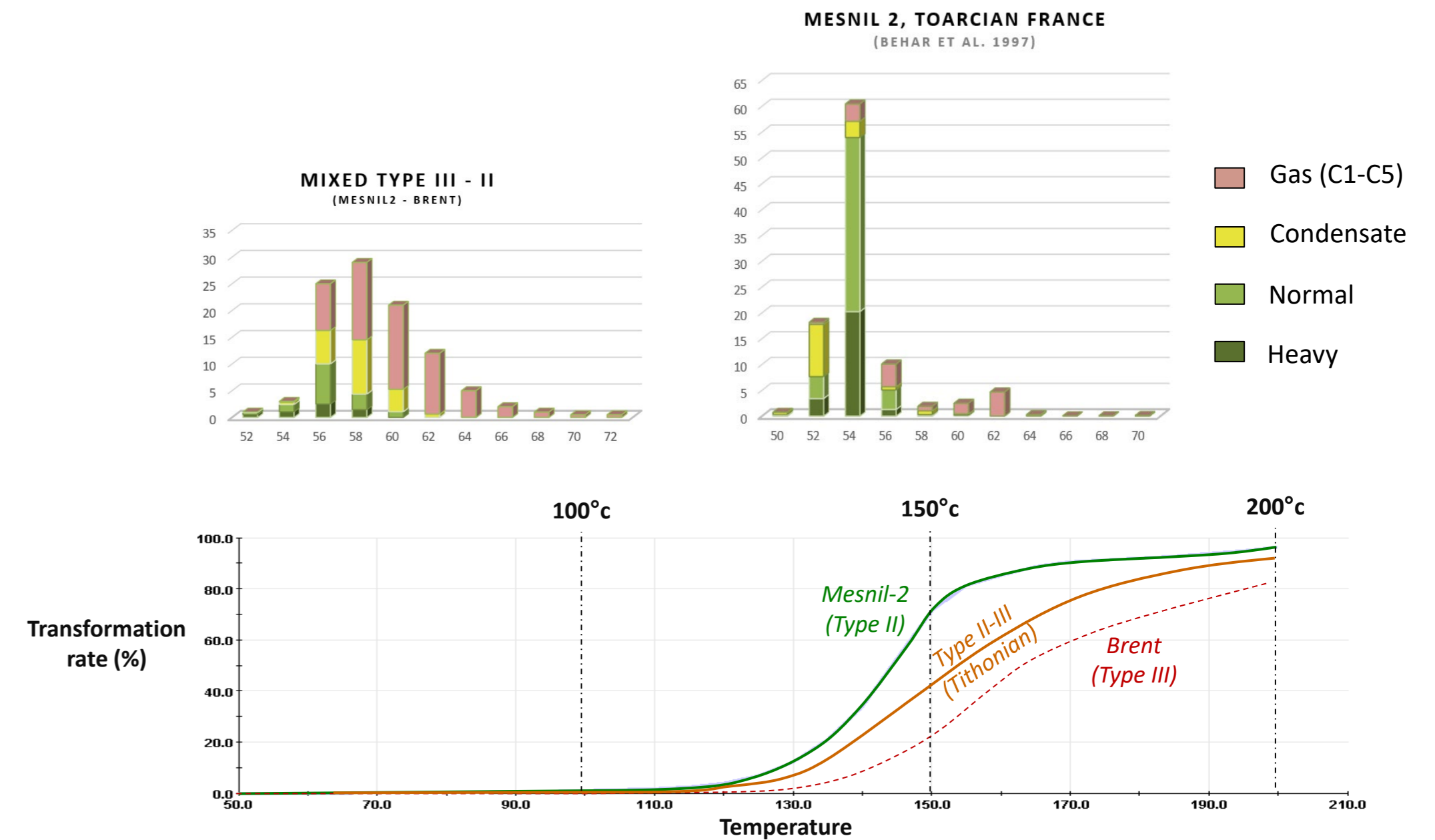


Figure 15: Kinetic scheme selected for the Tithonian and Pliensbachian source rocks



CHAPTER 4.4
THERMAL AND PRESSURE MODEL



Thermal Model Inputs

The history of the sedimentary basin thermal regime was constrained by thermal boundary conditions with an advanced lithospheric model, sea bottom temperatures and lithofacies petrophysical parameters (thermal conductivity, mass heat capacity and radiogenic heat production). Additionally, convection is simulated during the fluid flow migration modeling (Darcy migration).

Paleo-seabed temperature maps

Paleo-seabed temperature defines the thermal boundary condition at the top of the sedimentary model. Paleo-seabed temperatures are calculated from paleo-climate, paleo-latitude, meridional oceanic change in the Atlantic ocean and paleo-water depth. It defines the paleo-surface temperature from continental to deep water environment.

First, paleo-surface temperature was defined from paleo-climate combined with the paleo-latitude evolution of Nova Scotia (www.paleolatitude.org). The paleo-climate graph (Wygrala, 1989) gives mean surface temperature as a function of age and latitude. The position of the Nova Scotia basin latitude was plotted on the paleo-climate graph in order to extract the evolution of basin surface temperature. Meridional oceanic change in the Atlantic creates a colder environment in the west Atlantic and this was taken into account by decreasing the reference paleo-temperature. It gives the reference paleo-temperature from Triassic to Present day at 0m (sea level).

Then, Paleo-seabed temperatures maps were calculated from paleo-bathymetries defined in the model using the following equation:

$$T = T_{min} + A \cdot e^{(-z/B)}$$

Where:

- **T** is temperature
- **A** is a regional coefficient
- **Tmin** is the minimum attained temperature
- **z** is the depth
- **B** is the curvature (empirical calibration of the depth at which T_0 is reached)
- $T_{min} + A$ when $z = 0$ is the maximum temperature

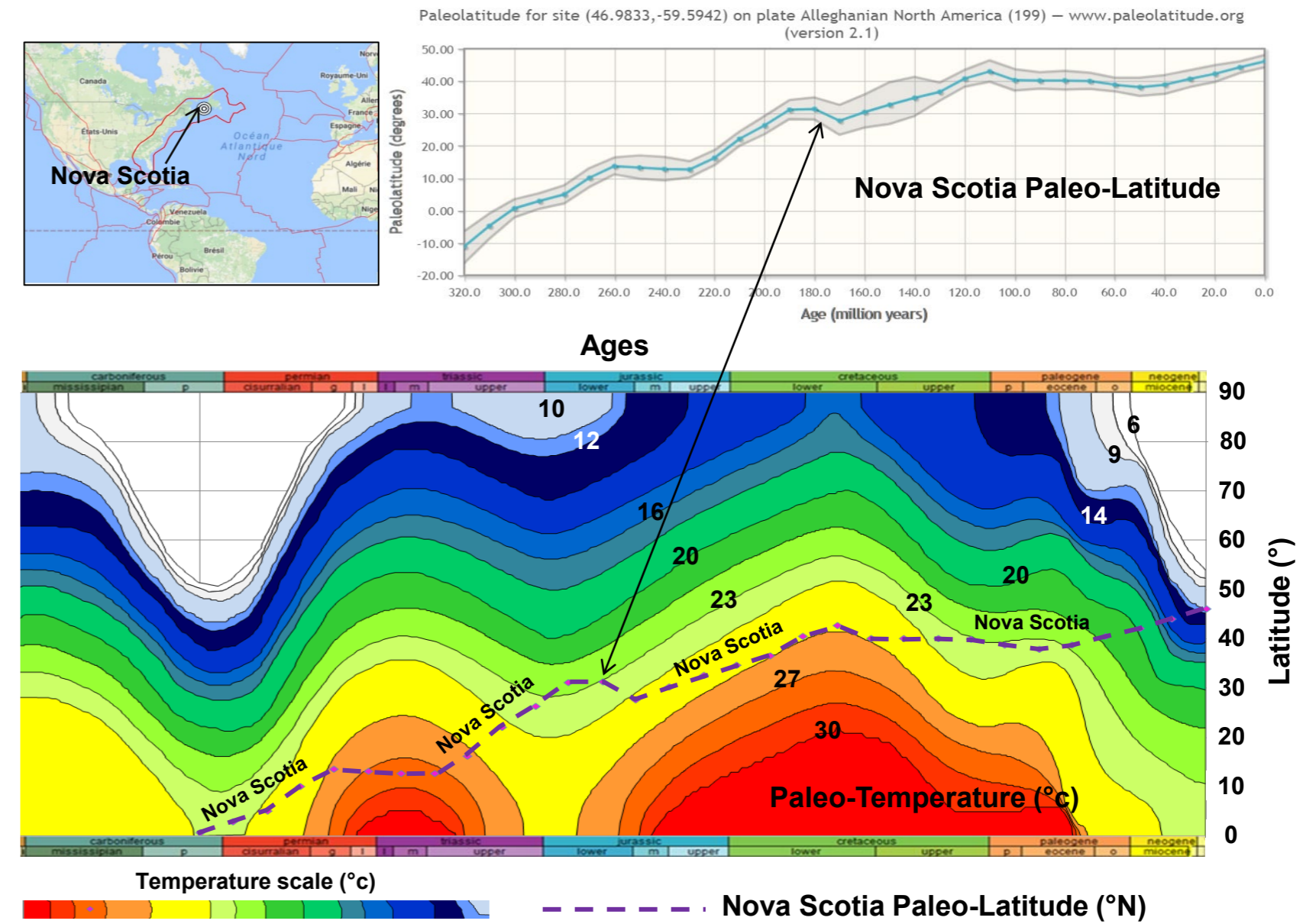


Figure 16: Paleo-temperature and Paleo-latitude

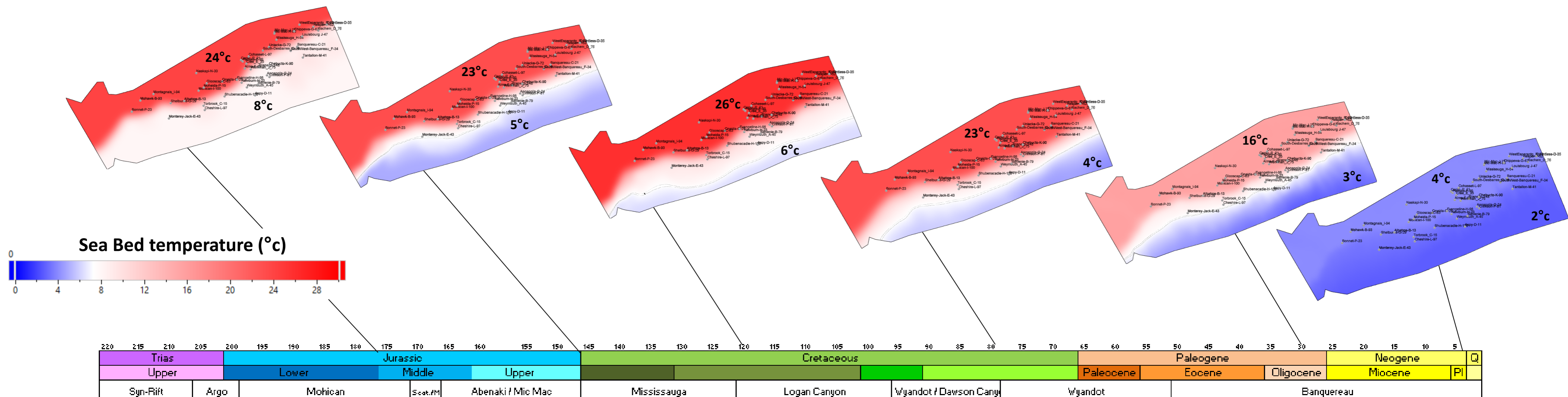


Figure 17: Paleo-surface temperature maps (Thermal model boundary conditions)

Thermal Model Inputs

Lithospheric Model

The lithospheric model defines the thermal boundary condition at the base of the sedimentary model. Lithosphere geometrical and lithological evolution were defined from late Triassic to Present day. In effect, stretching of the lithosphere during rifting phase generates a strong increase of heat flow due to the uplift of the upper mantle. This stretching is defined by the Beta Factor map (Figure 18 D). As well as mantle uplift, heat also gains a significant contribution from radiogenic sources in the crust (Figure 19). The elements of the lithospheric model are:

- Basement depth (Figure 18 A) : Seismic interpretation from CNSOPB
- Moho depth (Figure 18 B): The Moho depth was modelled by a team at Cergy University (Appendix 4.8). This model was based on gravity inversion and flexural backstripping and post rift reverse thermal subsidence modelling results. Moho depths varies between 13 and 44 km
- Crust thickness (Figure 18 C); i.e. the interval between the Moho and the Basement depth. Crustal thickness varies from 3km to 44km.
- Initial crust thickness (Pre-Rift) : estimated to be ≈44km
- Rifting period from 225Ma to 196Ma and associated Beta Factor. This defines the thinning of the crust and the asthenospheric uplift which causes the rise of the isotherms modelled in TemisFlow®.
- Upper mantle thickness: estimated to be around ≈ 100km

The crust was divided vertically into upper and lower crust (Figure 19). The crustal architecture is varied from continental crust, to transitional crust and oceanic crust in order to properly model radiogenic heat production. The distribution of crustal lithologies (Figure 18 E and F) is estimated from deep refraction seismic data together with estimated rock densities and observations of seaward dipping reflectors. Thermal calibration was achieved using well data. The temperature at the base of the lithosphere were defined at 1330°C.

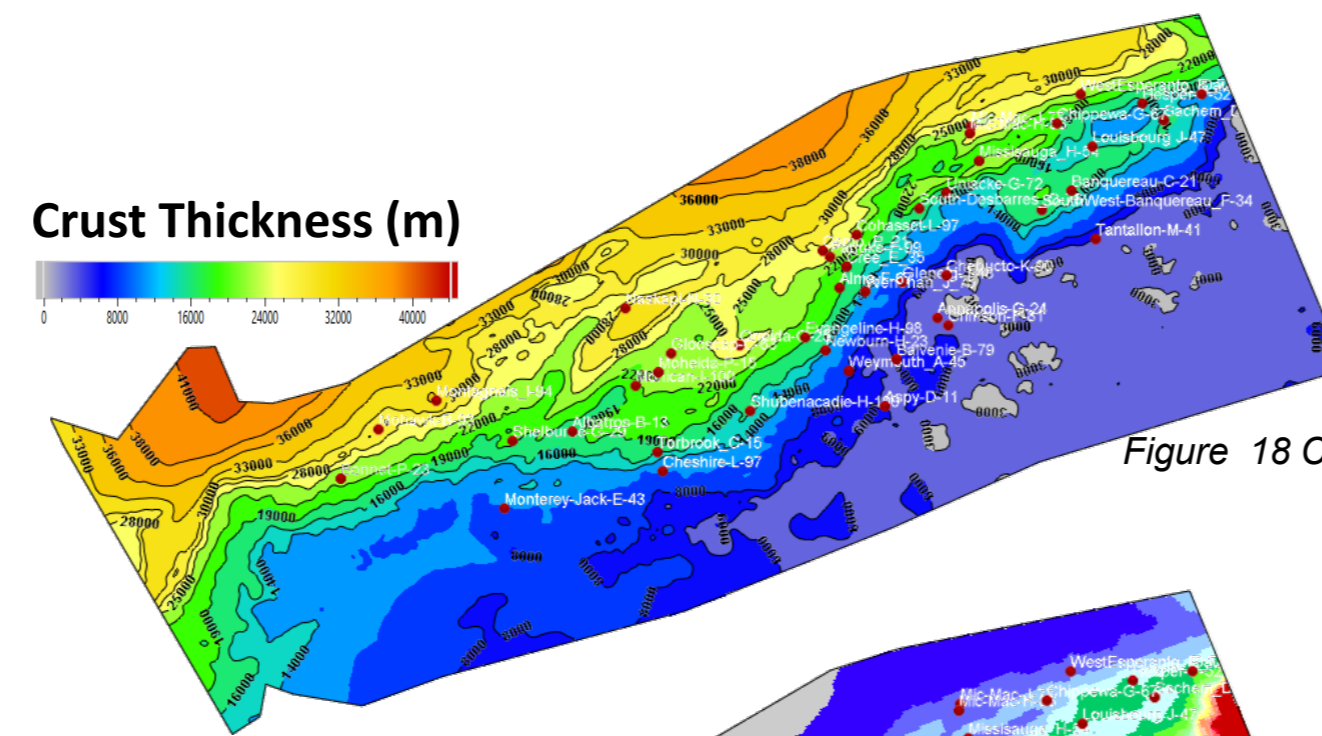


Figure 18 C

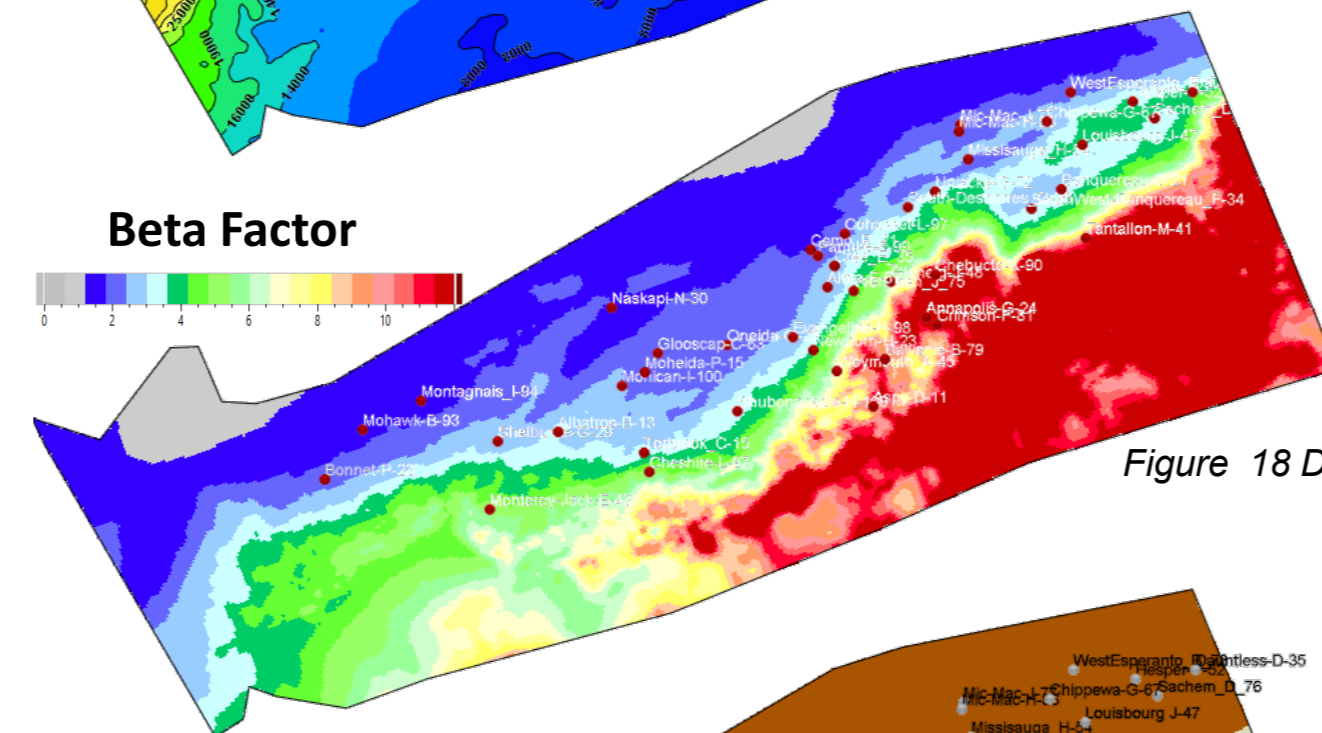


Figure 18 D

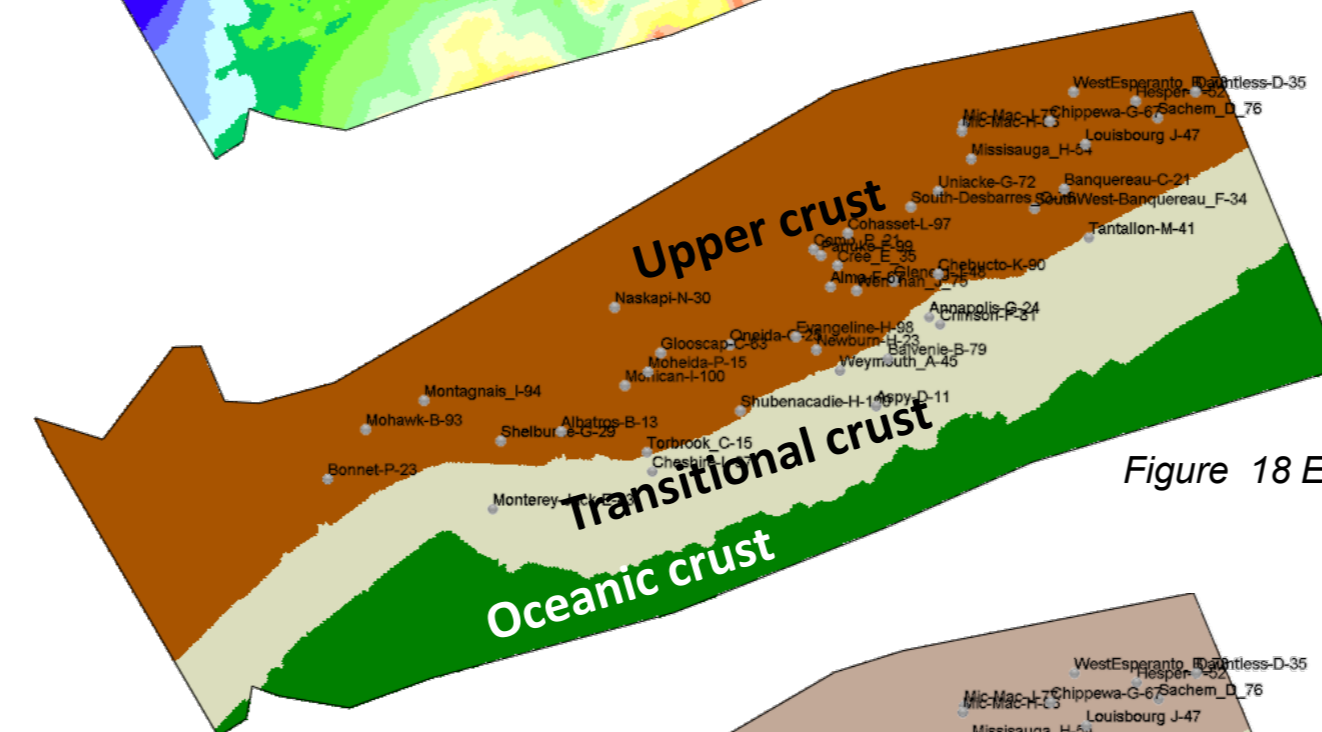


Figure 18 E

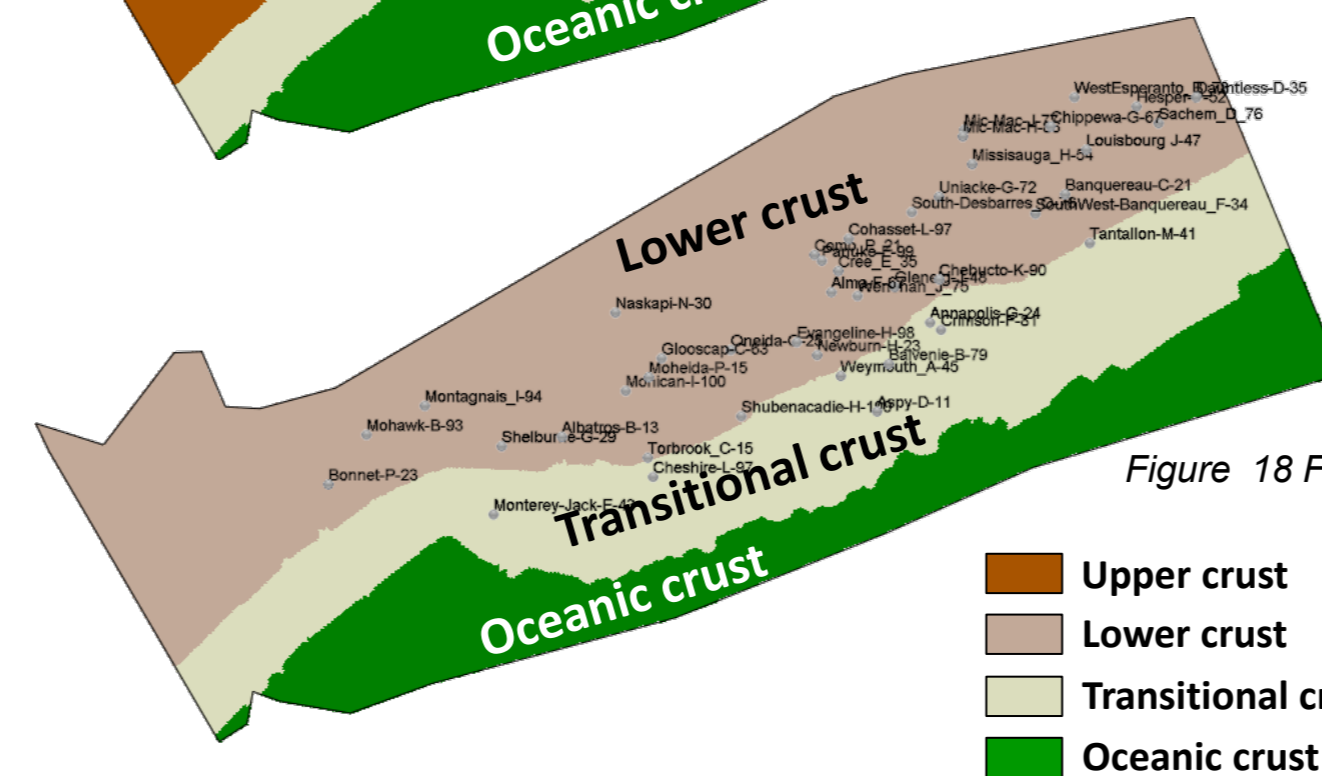


Figure 18 F

- Upper crust
- Lower crust
- Transitional crust
- Oceanic crust

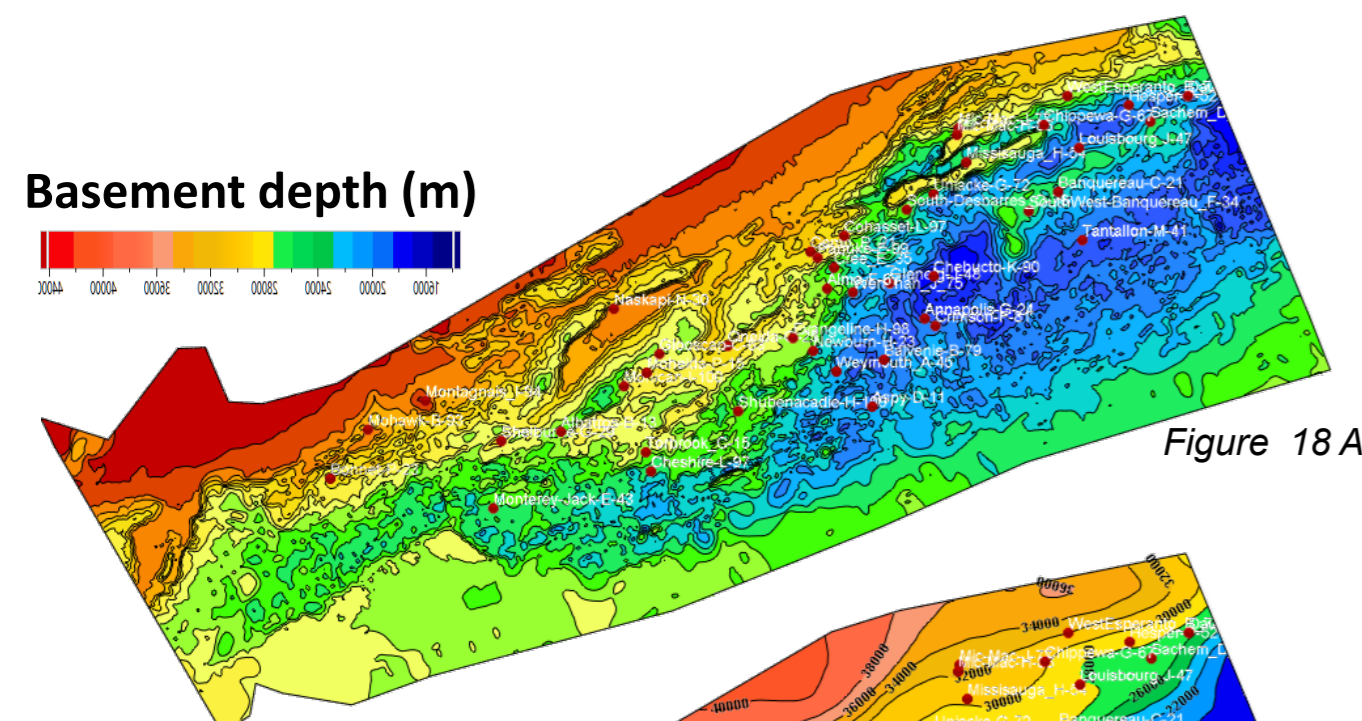


Figure 18 A

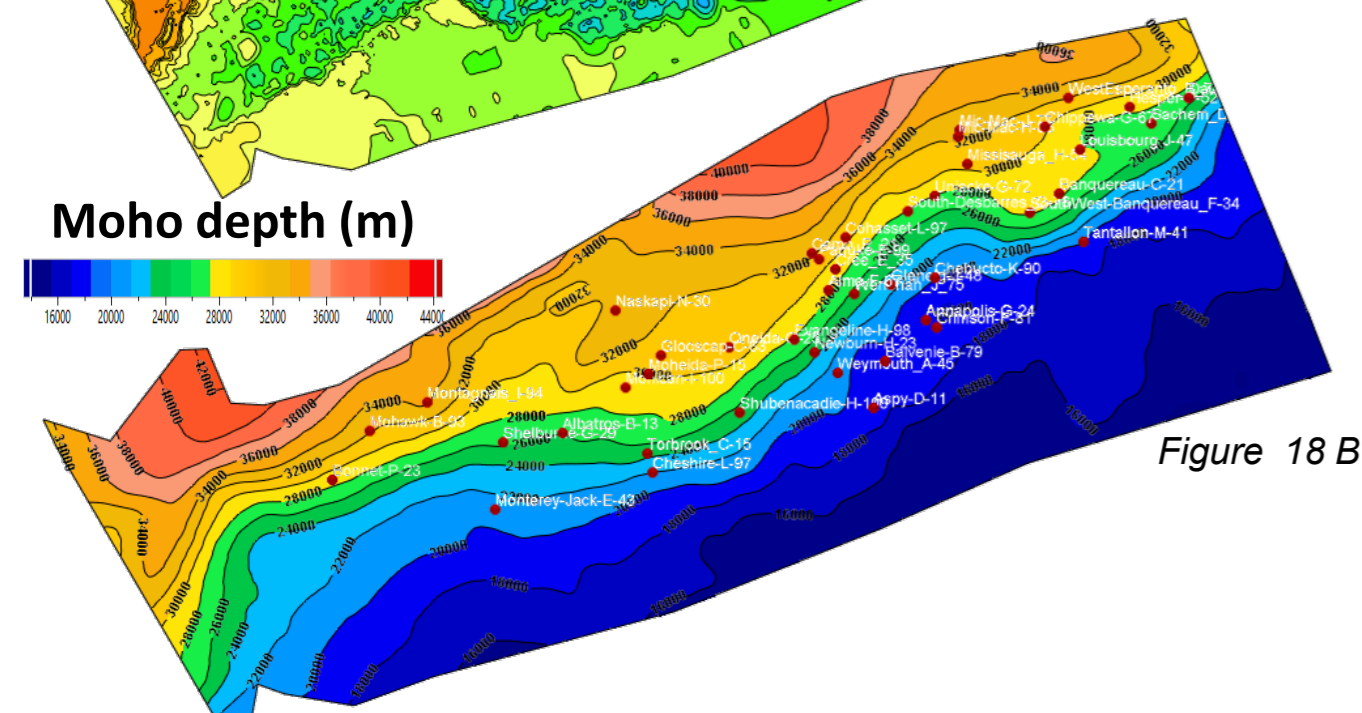


Figure 18 B

Figure 18: Maps used to build the lithospheric model (A, B, C, D, E and F)

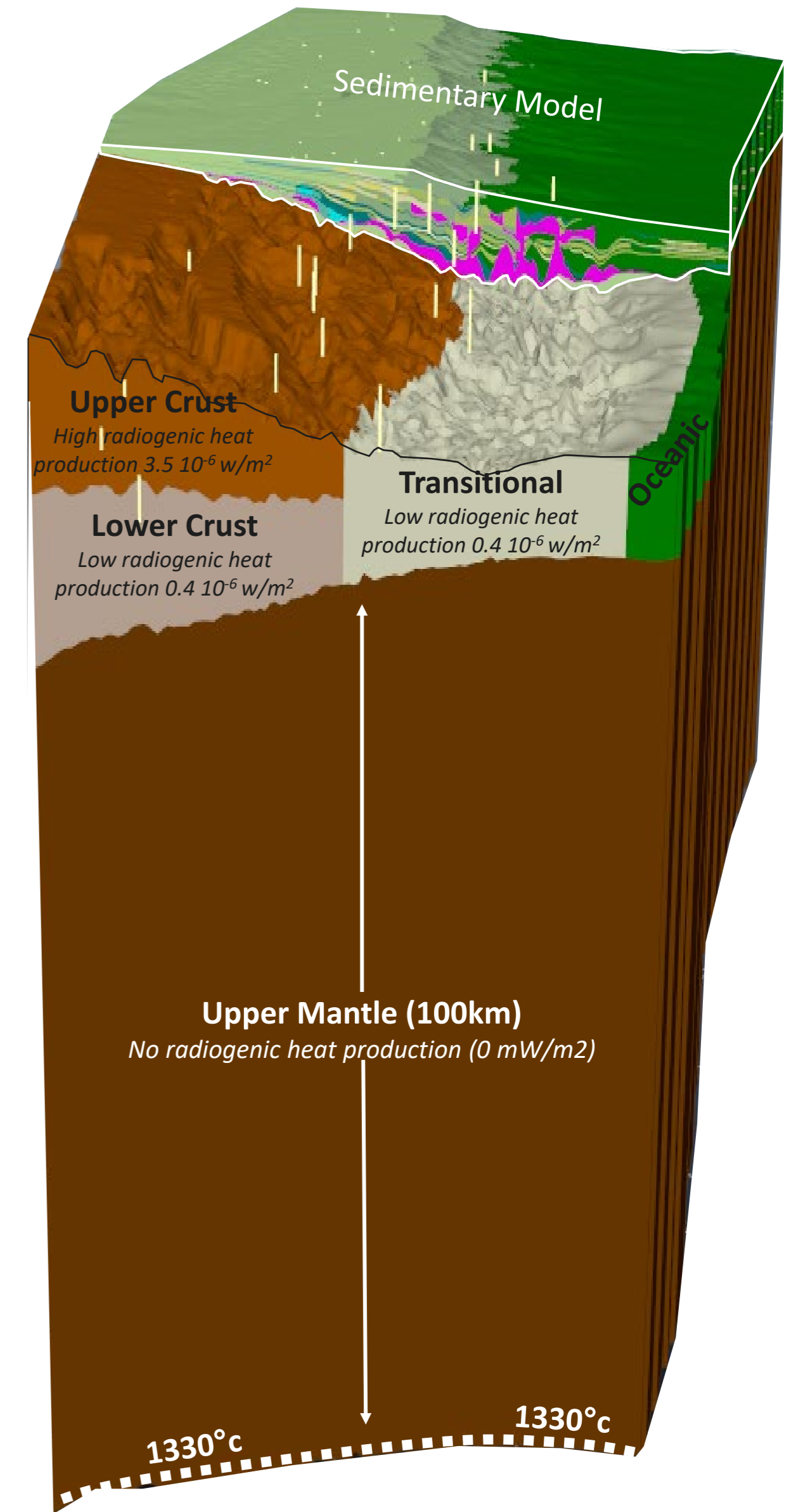
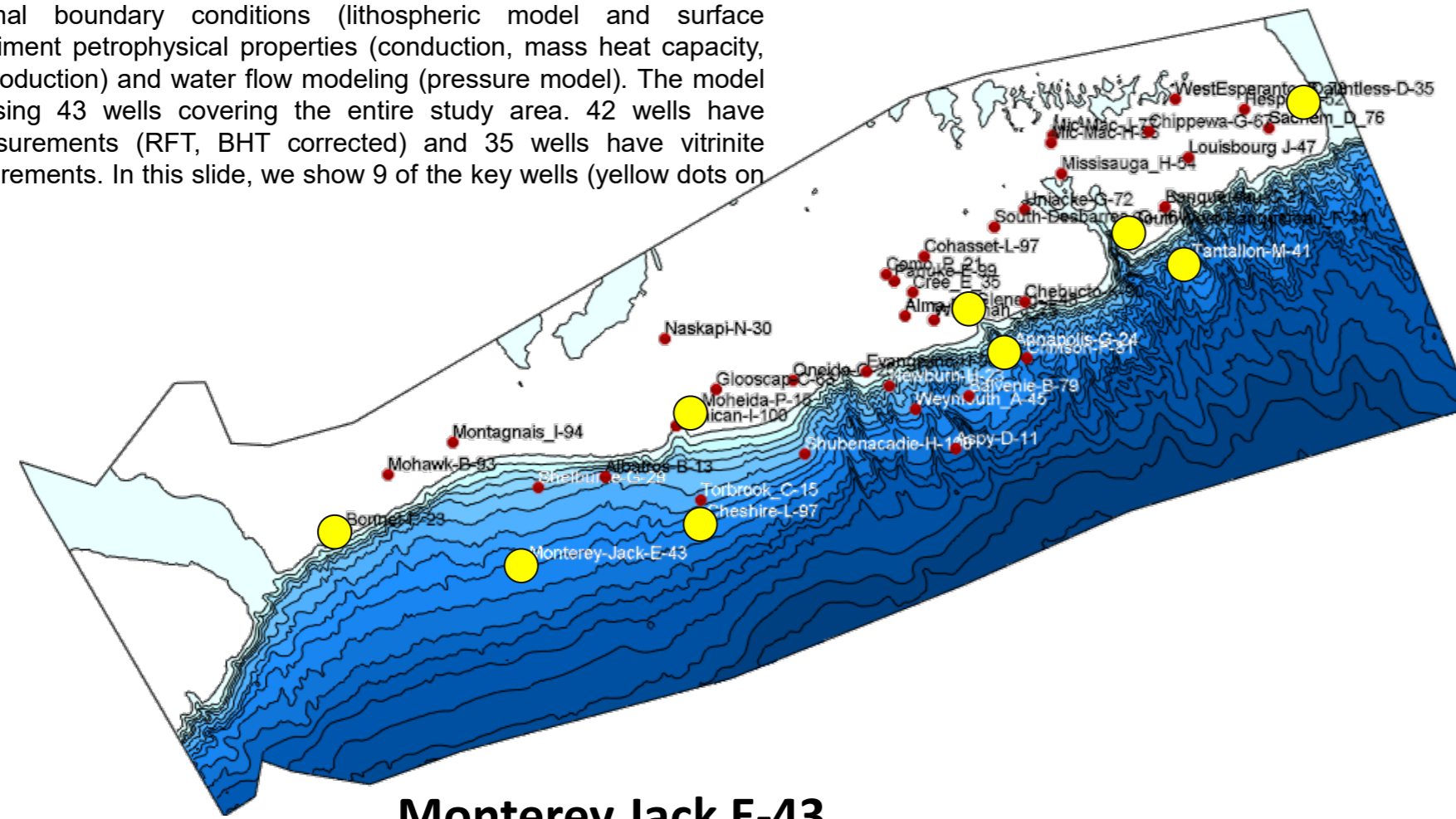


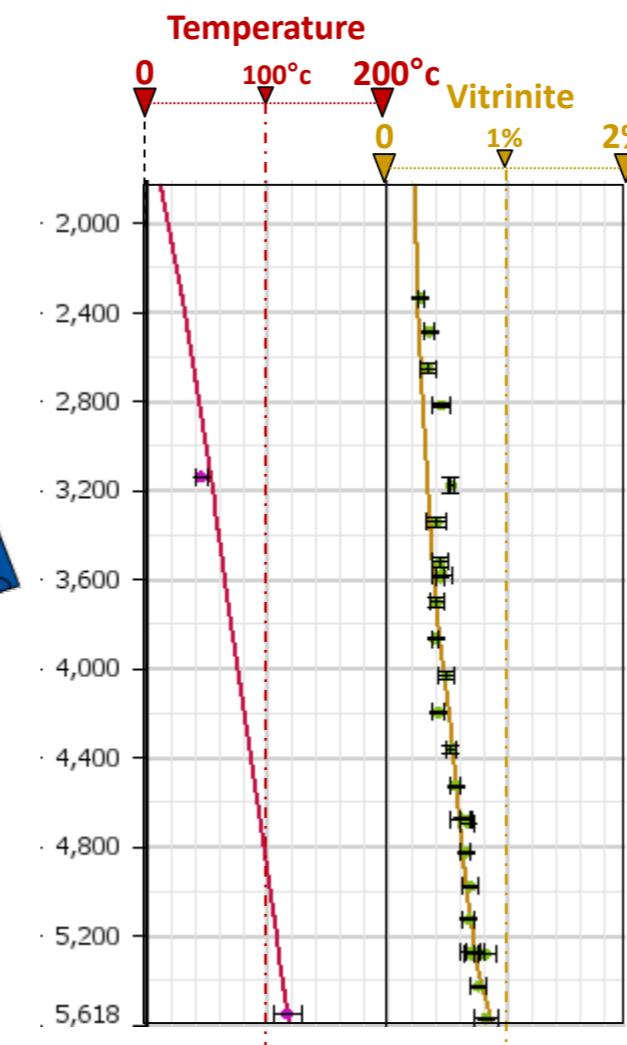
Figure 19: 3D view of the lithospheric and sedimentary model

Thermal Model Calibration

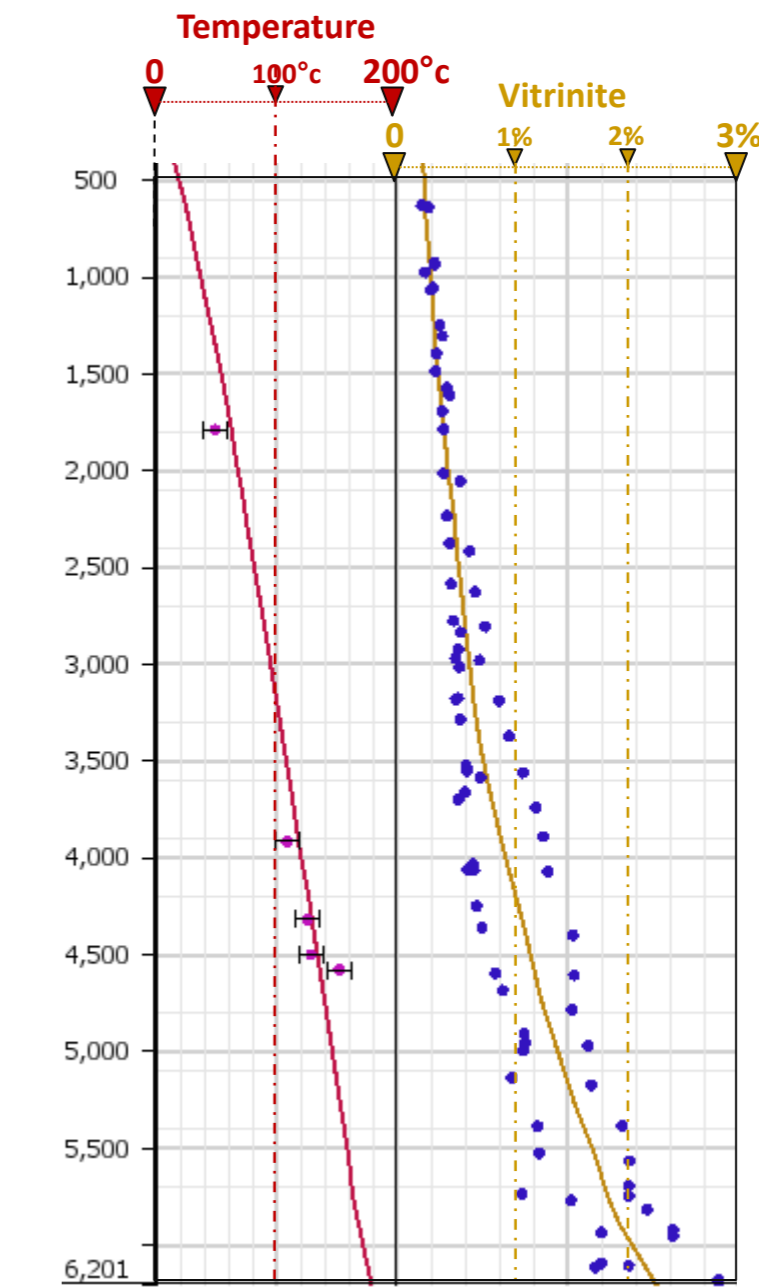
The thermal model simulates temperature, heat flow, thermal gradient and maturity based on thermal boundary conditions (lithospheric model and surface temperature), sediment petrophysical properties (conduction, mass heat capacity, radiogenic heat production) and water flow modeling (pressure model). The model was calibrated using 43 wells covering the entire study area. 42 wells have temperature measurements (RFT, BHT corrected) and 35 wells have vitrinite reflectance measurements. In this slide, we show 9 of the key wells (yellow dots on the location map).



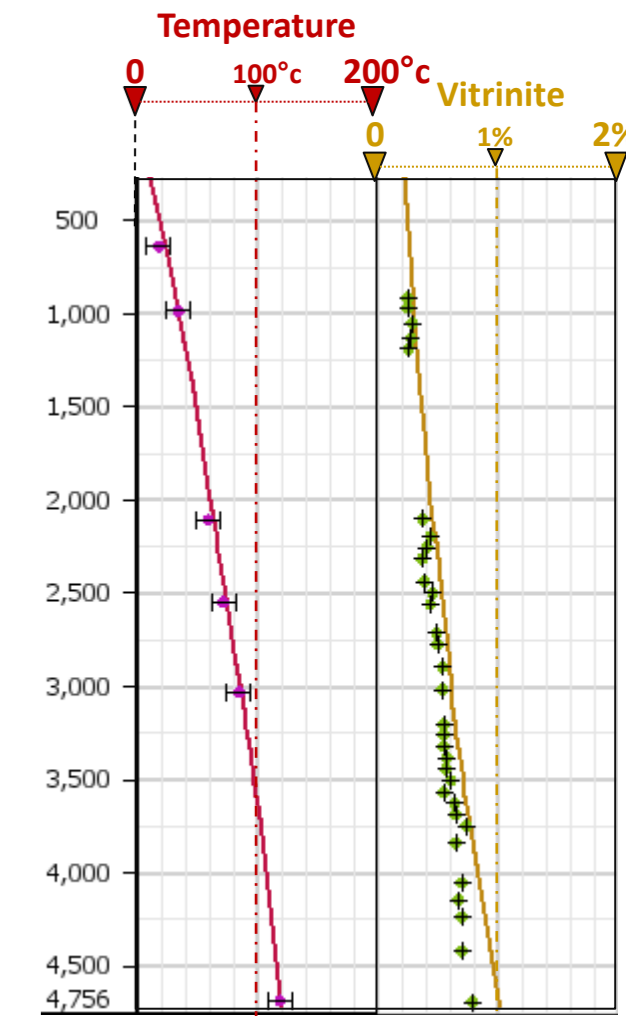
Tantaloon M-41



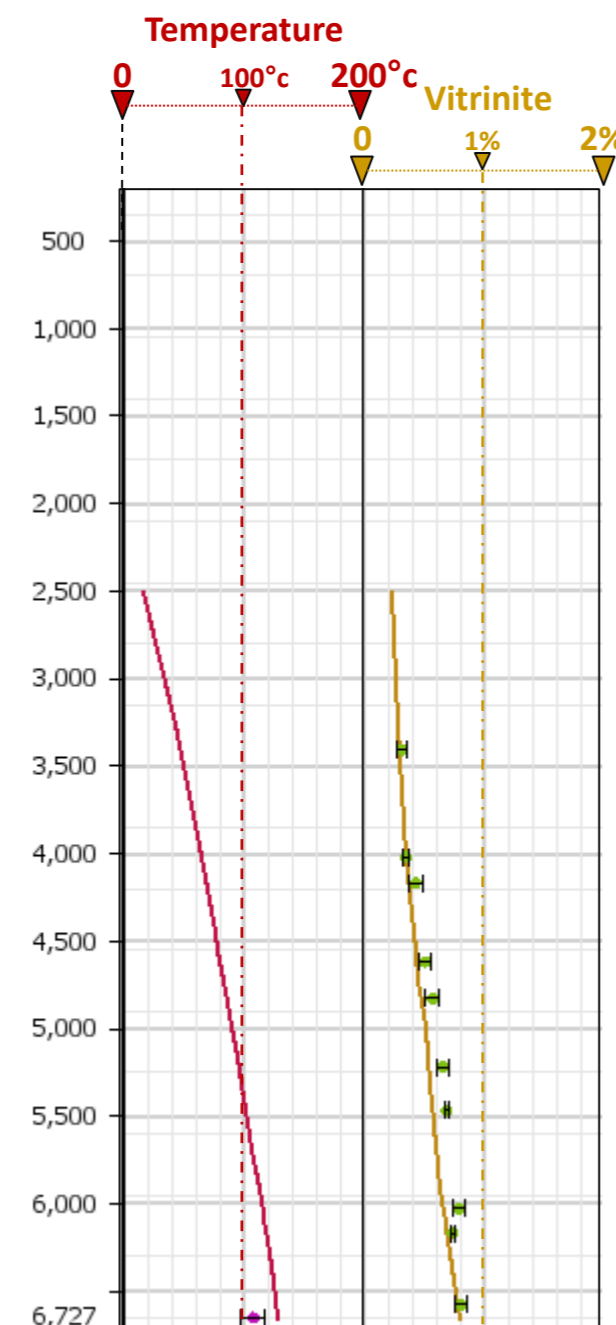
South West Banquereau F-34



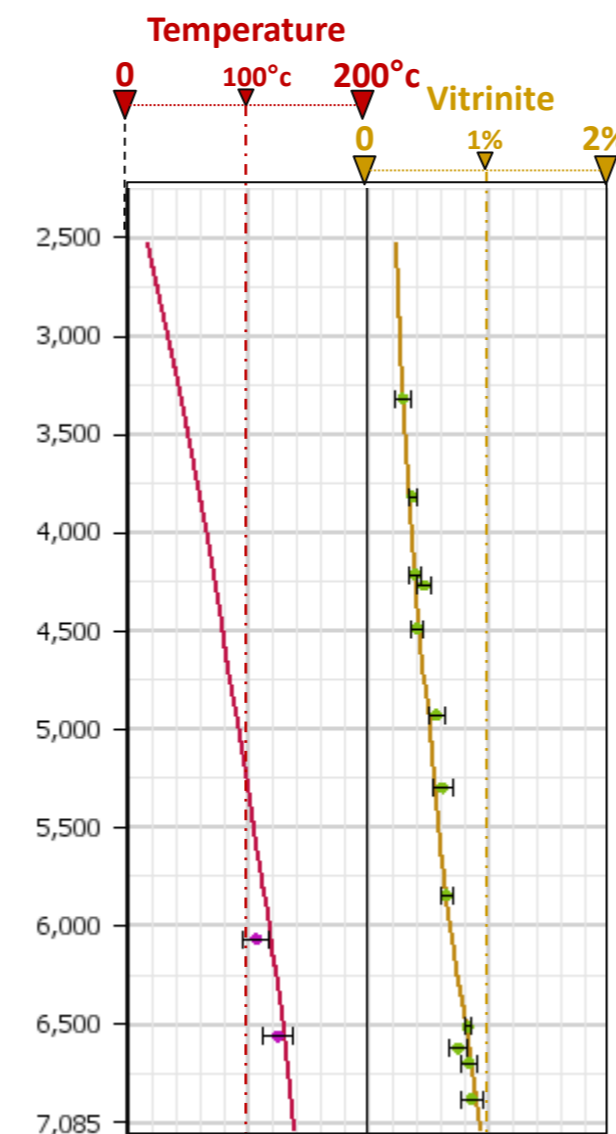
Dauntless D-35



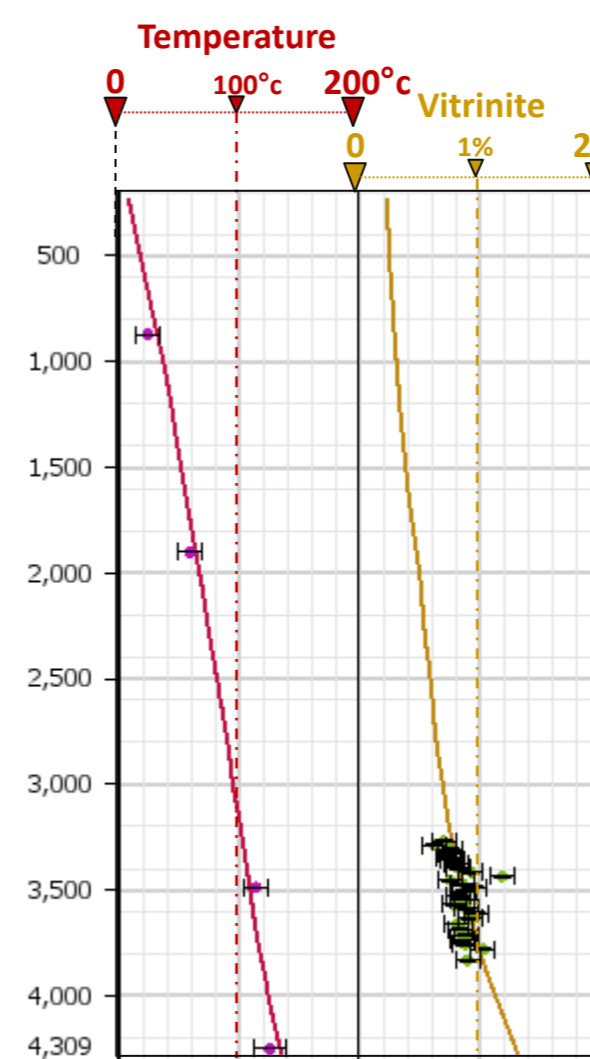
Monterey Jack E-43



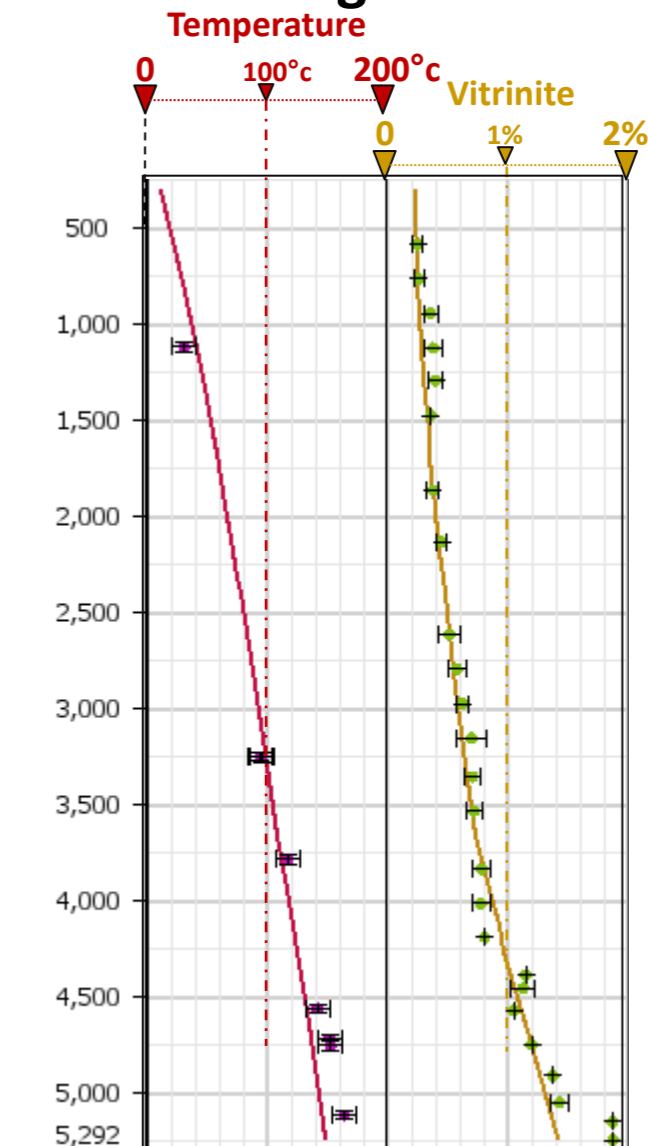
Cheshire L-97



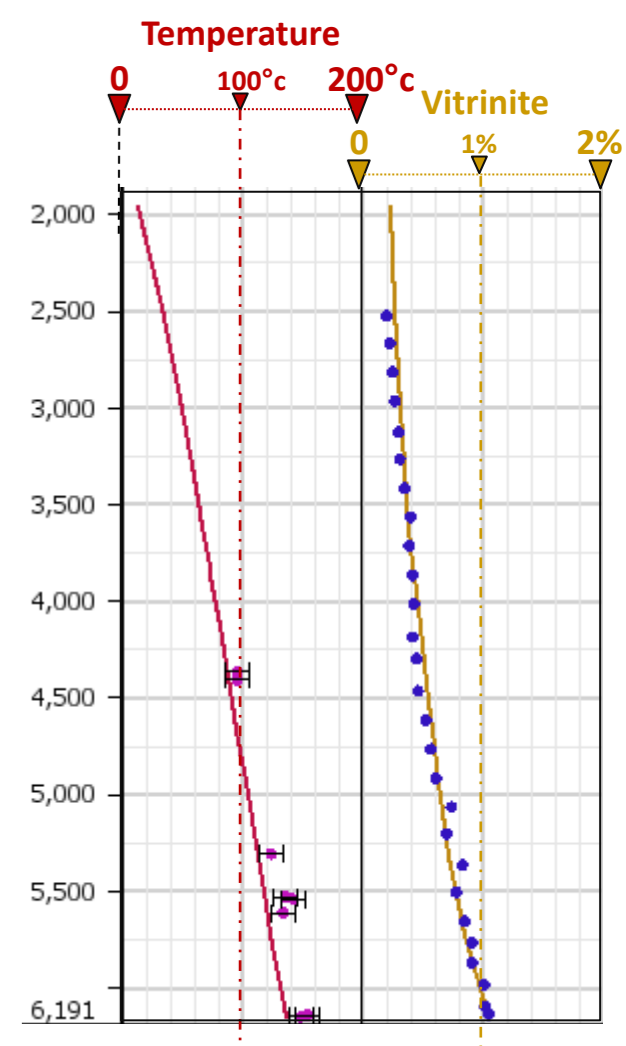
Moheida P-15



Glenelg J-48



Annapolis G-24



Bonnet P-23

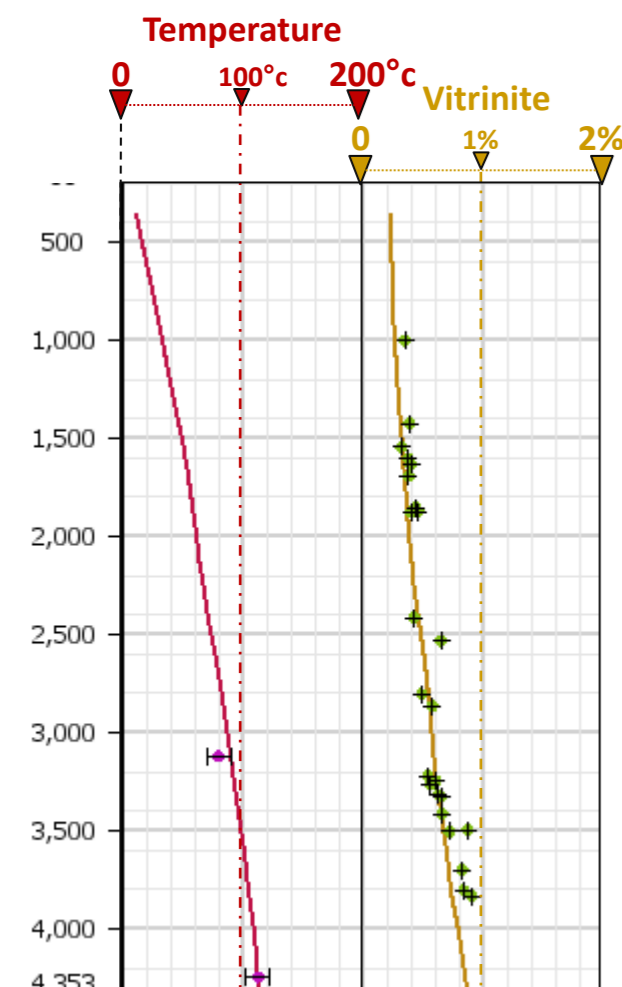


Figure 20: Thermal and Maturity calibration

Pressure Model Calibration

Pore pressure model simulates water flow in porous media using the Darcy equations to predict overpressures and to calculate the pressure gradients that drive hydrocarbon flows. The modeling takes into account capillary pressure, sedimentation rate, thermal cracking, secondary cracking and buoyancy (Archimedes force). The model was calibrated using 39 wells covering the entire study area. Results were compared with direct measurements from DMR, RFT, MLR, DST data. This plate shows a selection of 5 wells (yellow dots on the location map). The transgressive system tract highlighted in the sequence stratigraphic analysis (Chapter 3) coincided with the over-pressure kick seen in well measurements and were key elements for tuning the seal petrophysical parameters. Generally, these wells show a good model calibration.

Over-pressures in the basin correspond to efficient seals, dry gas columns and high sedimentation rate.

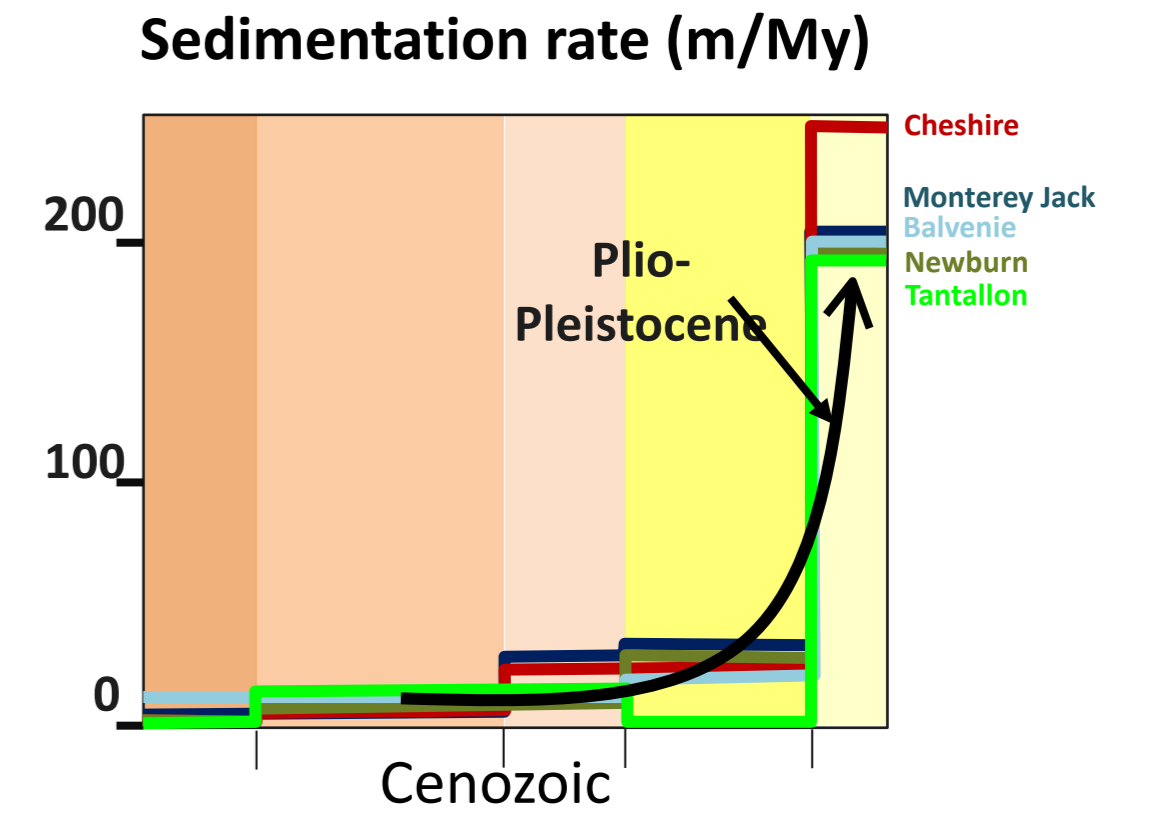
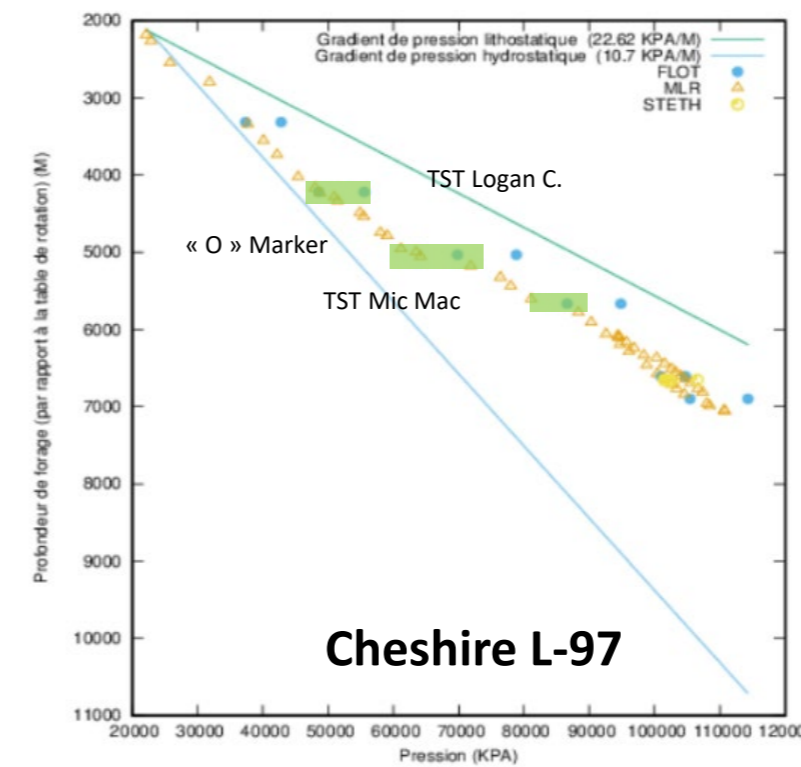
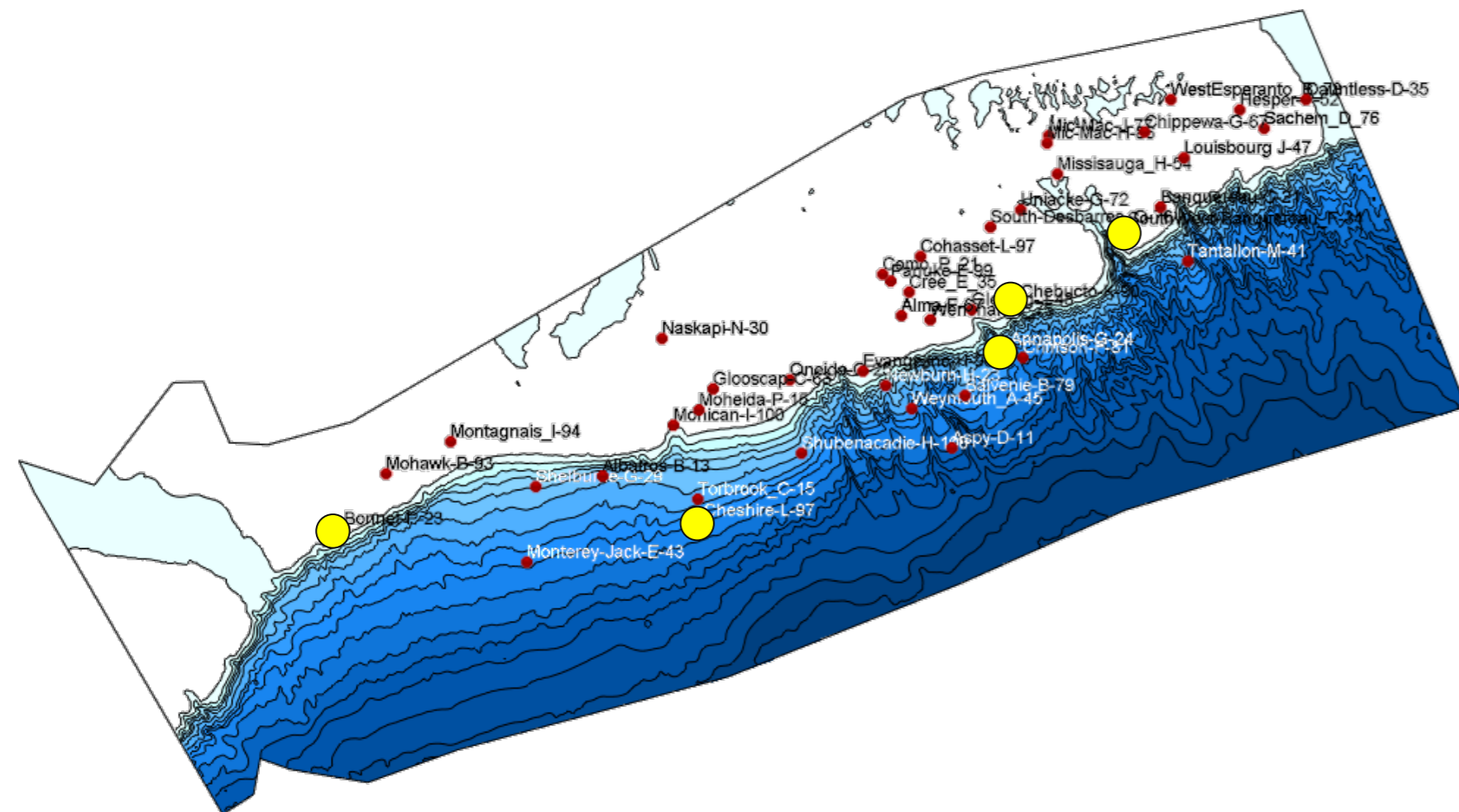


Figure 21: Example of Pore-pressure data and graph of sedimentation rate based on biostratigraphic data

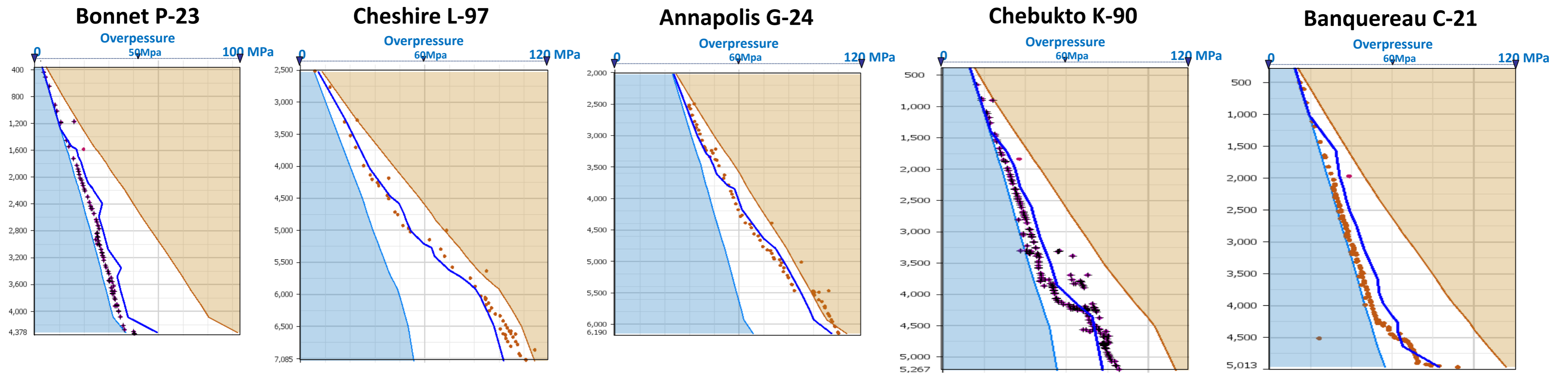
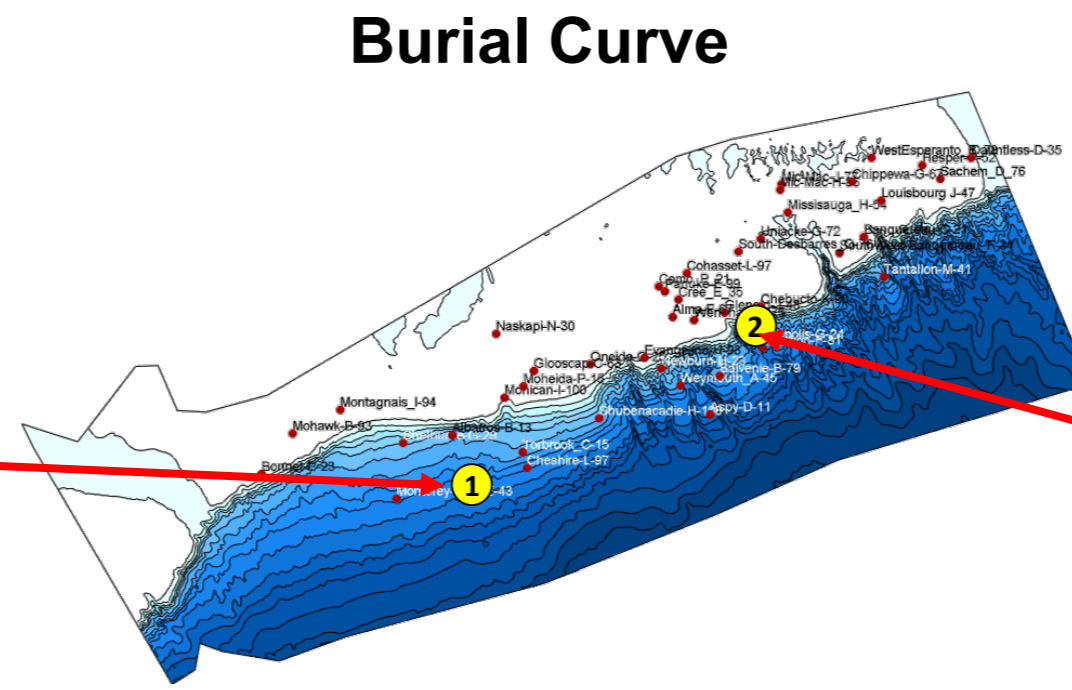
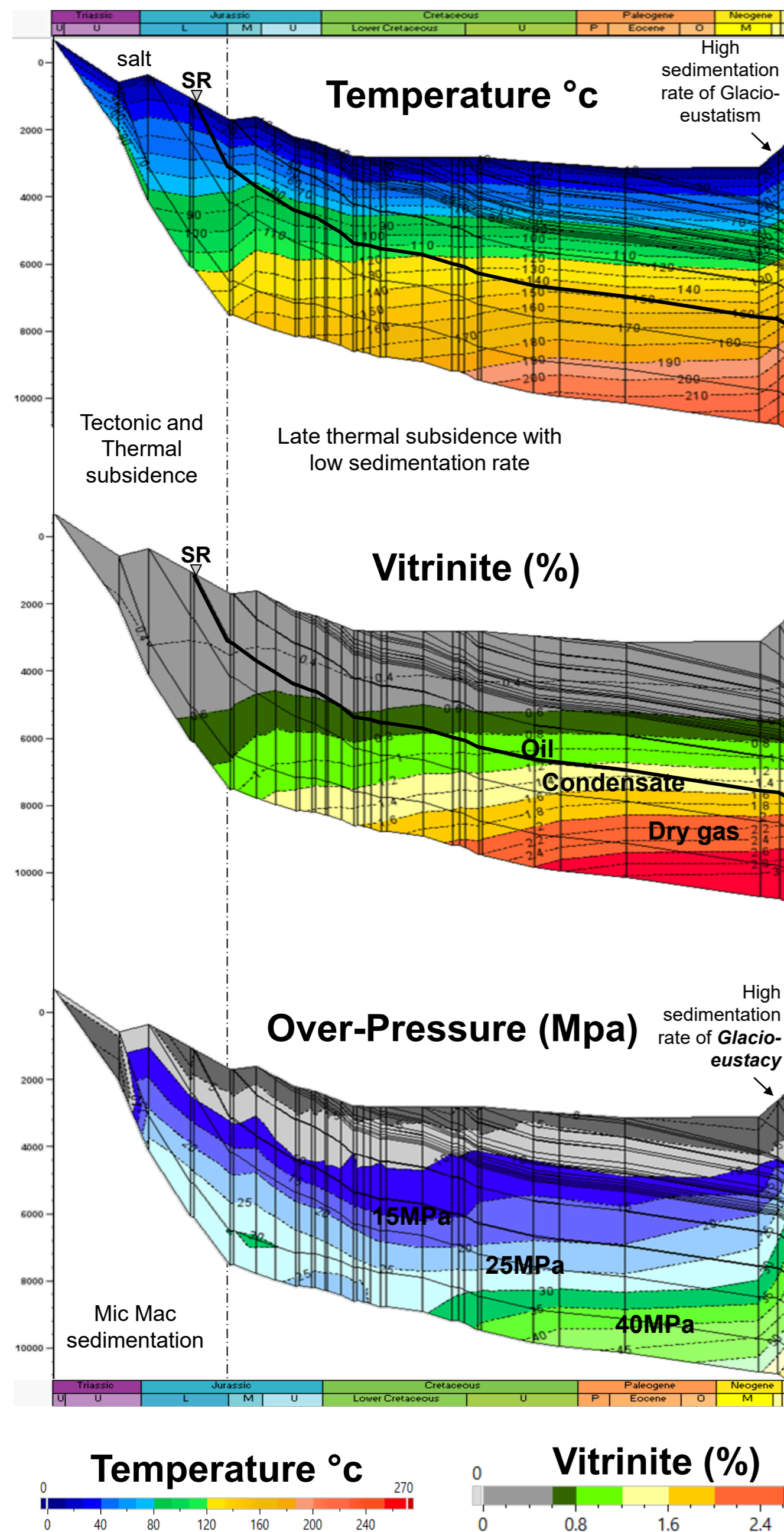


Figure 22: Pore-Pressure calibration



Burial Curve

Burial curves give the basin history at a specific location in the basin (yellow dots above). They display basement subsidence, paleobathymetries and sediment compaction. Here, Temperature, Vitrinite and Overpressure properties have been displayed.

The first curve (1), at the left, is representative of the western part of the basin where sedimentation rate generally is lower. A first stage of tectonic and thermal subsidence evolution, with strong subsidence rate, can be easily identified from late Triassic to Lower/Middle Jurassic, during which the Pliensbachian source rock was deposited. The second stage corresponds to a late thermal subsidence with low sedimentation. The final stage is a period of glacio-eustasy over the last 5My which causes a high sedimentation rate and generates an increase of over-pressure. At present day, the Pliensbachian source rock reaches 160°C and is in the condensate window and reaches over-pressure of more than 40MPa.

The second curve (2), at the right, is representative of the eastern part of the basin where sedimentation rates are higher. The first stage of tectonic and thermal subsidence is quite similar to the western part of the basin. The second stage of late thermal subsidence shows a strong sedimentation rate associated with the progradation of the shelf. Note that, paleobathymetry (water column) decreases during the end of Jurassic (Mic Mac Formation) and the Neocomian (Mississauga Formation) reflecting the progradation of the shelf. At present day, both source rocks are in a dry gas window where temperature exceed 200°C. Mic Mac Formation is predicted to have over-pressure between 50 to 70MPa, the Mississauga formation between 30 to 50MPa and the Logan Canyon formation lower than 10MPa.

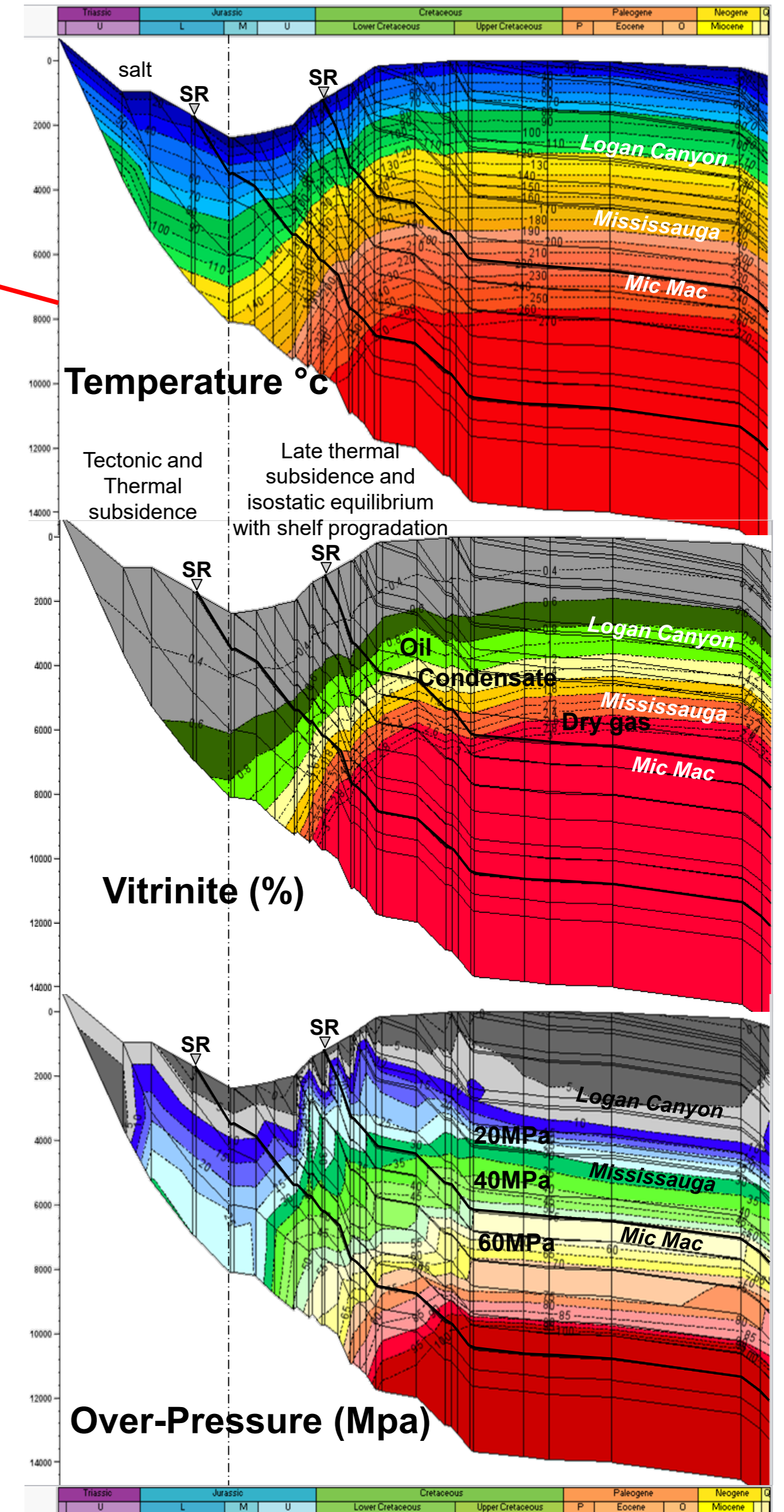


Figure 23: Burial curves with Temperature, Maturity and Over-pressure properties at two locations in the basin

Temperature

Temperature maps were extracted for each megasequence at reservoir level from Middle Jurassic (Mohican Formation) to MS6 (Logan Canyon). The very thick series of sediments in the eastern part generate high temperatures in the Jurassic series (Mohican and Mic Mac formations) exceed 200°C. Temperature maps from Mohican to MS6 show a lateral shift of maximum temperature that reflects the lateral shift of sediment depocenter through time. A biodegradation risk (where present day temperatures are below 80°C, blue in the color scale) exist for the MS6 (Upper part of Logan Canyon Formation) in the eastern part of the study area.

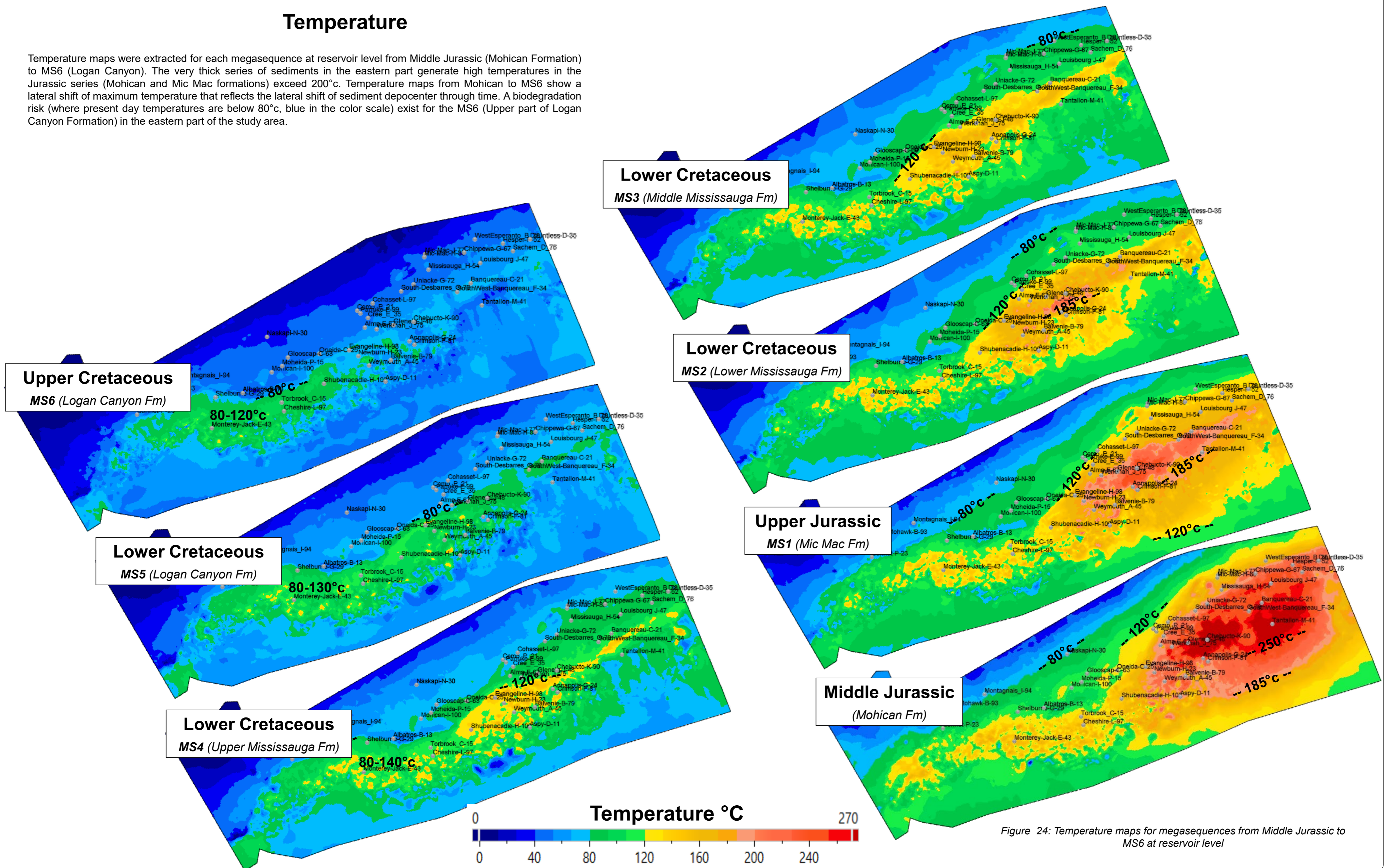


Figure 24: Temperature maps for megasequences from Middle Jurassic to MS6 at reservoir level

Over-Pressures

Overpressure maps were extracted for each megasequence at reservoir levels from Middle Jurassic (Mohican Formation) to MS6 (Logan Canyon). The very thick series of sediments in the eastern part generate high overpressures in the Jurassic series (Mohican and Mic Mac formations) exceeding 60MPa. Similar to the temperature maps (Plate 4.11), the overpressure from the Mohican to MS6 shows a lateral shift of maximum overpressure which reflects the lateral shift of sediment depocenter through time. Overpressures are mainly due to overburden stress where efficient seal levels exist, such as the “O” marker in the Lower Cretaceous. Additionally, gas generation can make a strong contribution especially in the eastern part of the study area where effective stress can be minimal very low (which could lead to top seal failure in such areas). The glacio-eustatic period from Late Miocene to Present day generates high sedimentation rates especially in the western part of the study area which leads to a rapid increase of overpressure (see burial curve page Plate 4.10).

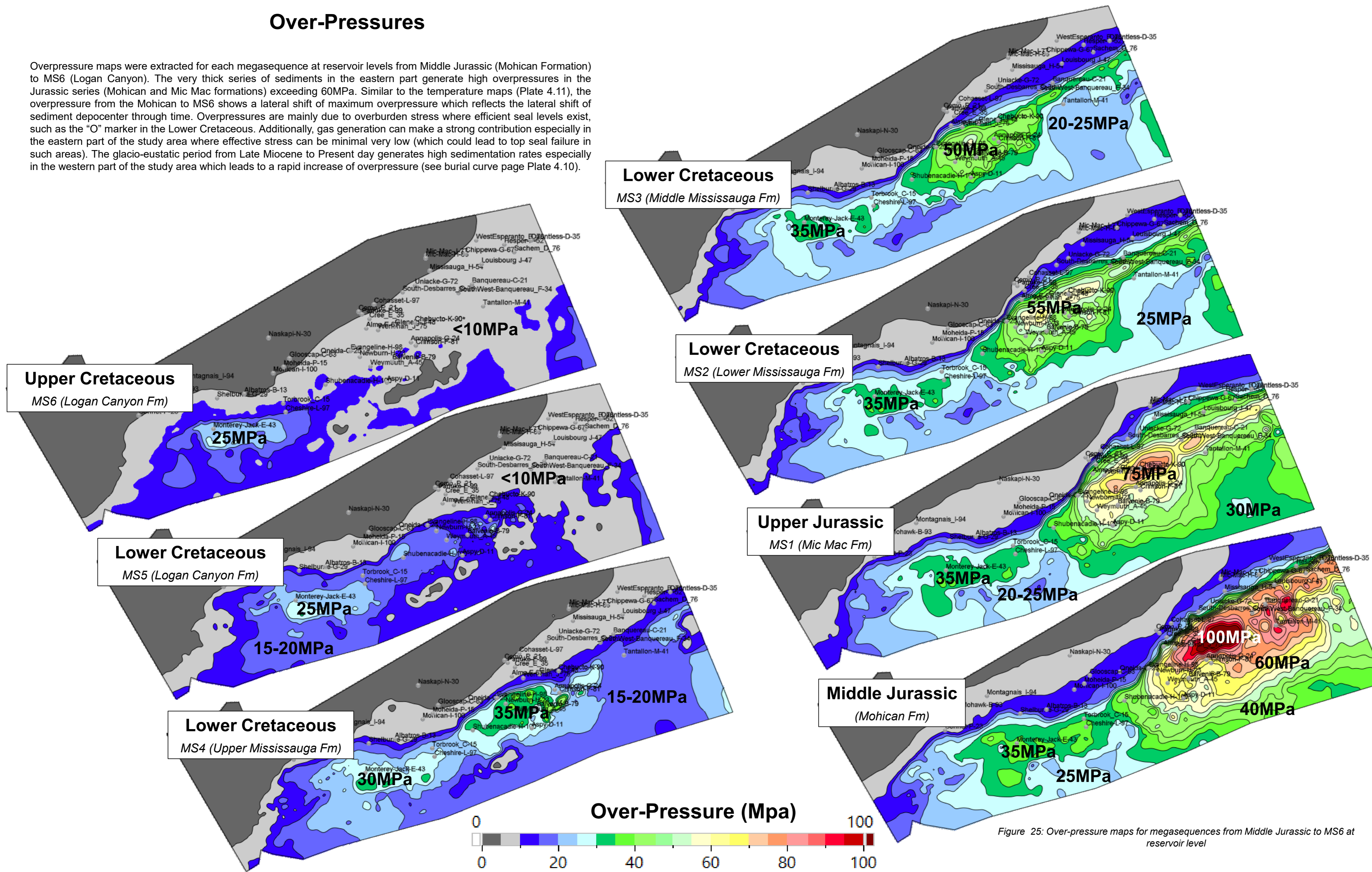


Figure 25: Over-pressure maps for megasequences from Middle Jurassic to MS6 at reservoir level

Pliensbachian Source Rock Temperature/Maturity/Generation/Expulsion/Timing

Source rock temperatures vary from 60°C in the very shallow inner shelf north-west of Naskapi, Montagnais and Mohawk, to 300°C in the main depot-center deeply buried around Tantallon, Banquereau and Chebucto in the east (Figure 26 A)

Pliensbachian source rock maturity is mainly in the oil window in the west and gas to dry gas window in the east where its depth can exceed 15km. Note that the very distal part (south-east) and the inner shelf (north-east) are still in condensate to oil window in the eastern part (Figure 26 B)

Source rock Transformation Ratio varies spatially in the western part from 0% to 100% in the mini basins and local depocenters. In the eastern part, the source rock is overcooked (100%) (Figure 26 C)

Hydrocarbon mass expelled from the Pliensbachian source rock varies from 300 to 1300 kg/m² (2 to 9 MBoe /km²) in the western part and reach 1500kg/m² in a large part of the eastern part (Figure 26 D)

The Generation/Expulsion Timing Map shows the age and location where the source rock transformation rate reaches more than 50%. This is the age of maximal generation/expulsion. Generation/Expulsion is dated to be late Cretaceous to Tertiary in the western part and late Jurassic to Early Cretaceous in the eastern part (Figure 26 E).

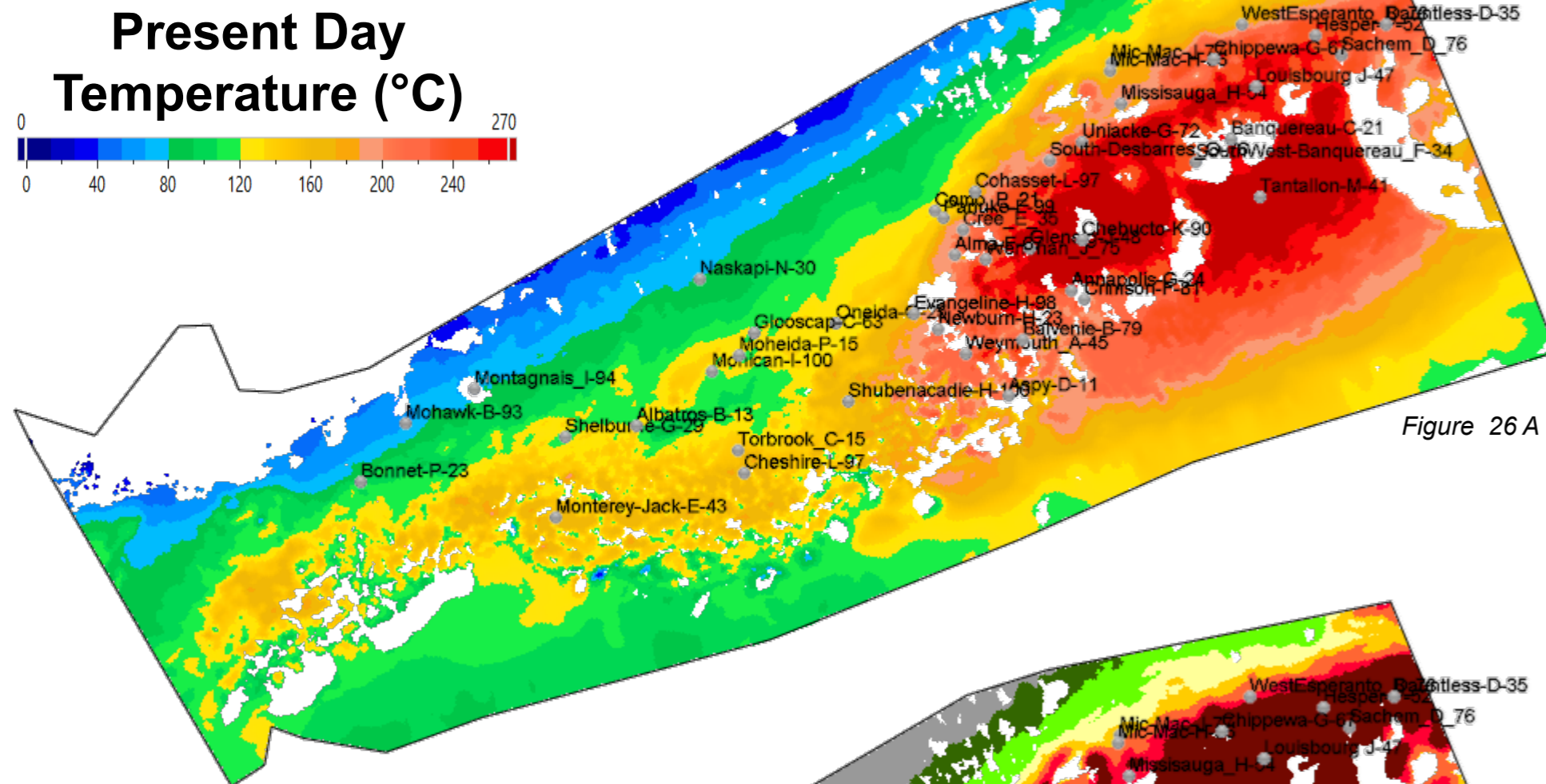


Figure 26 A

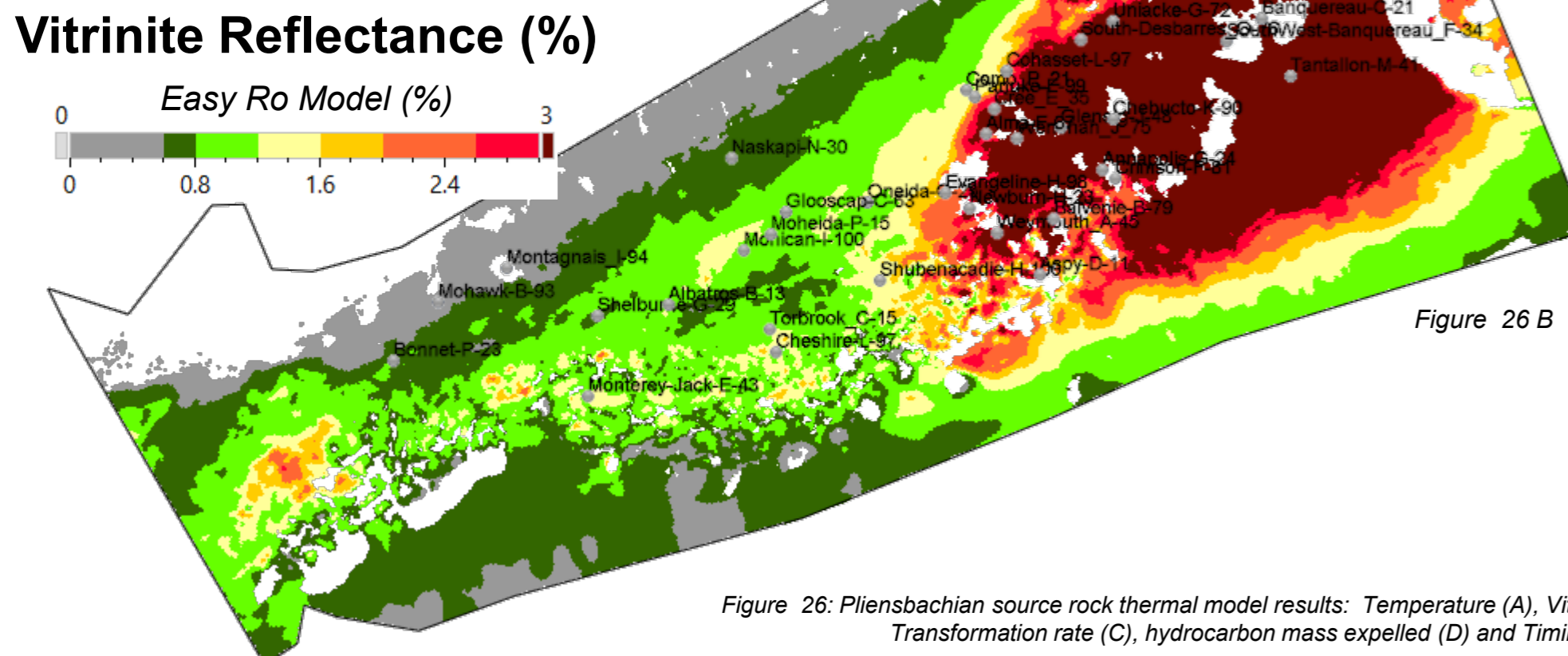


Figure 26 B

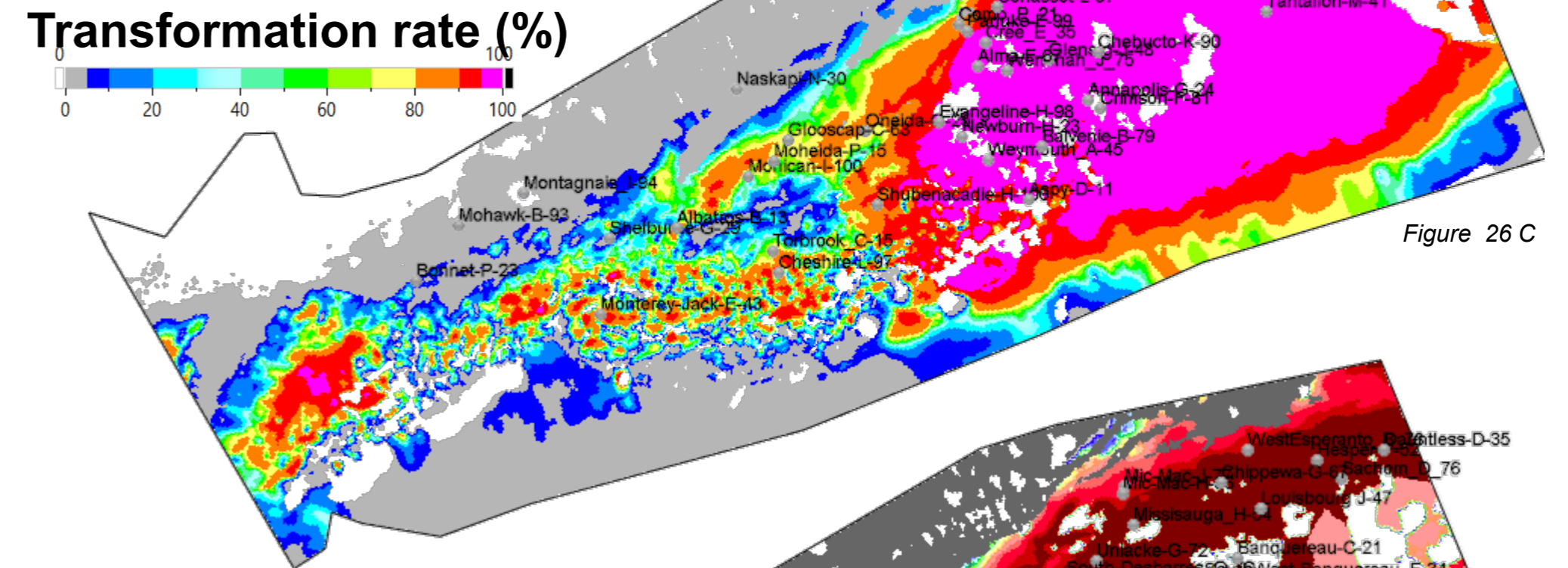


Figure 26 C

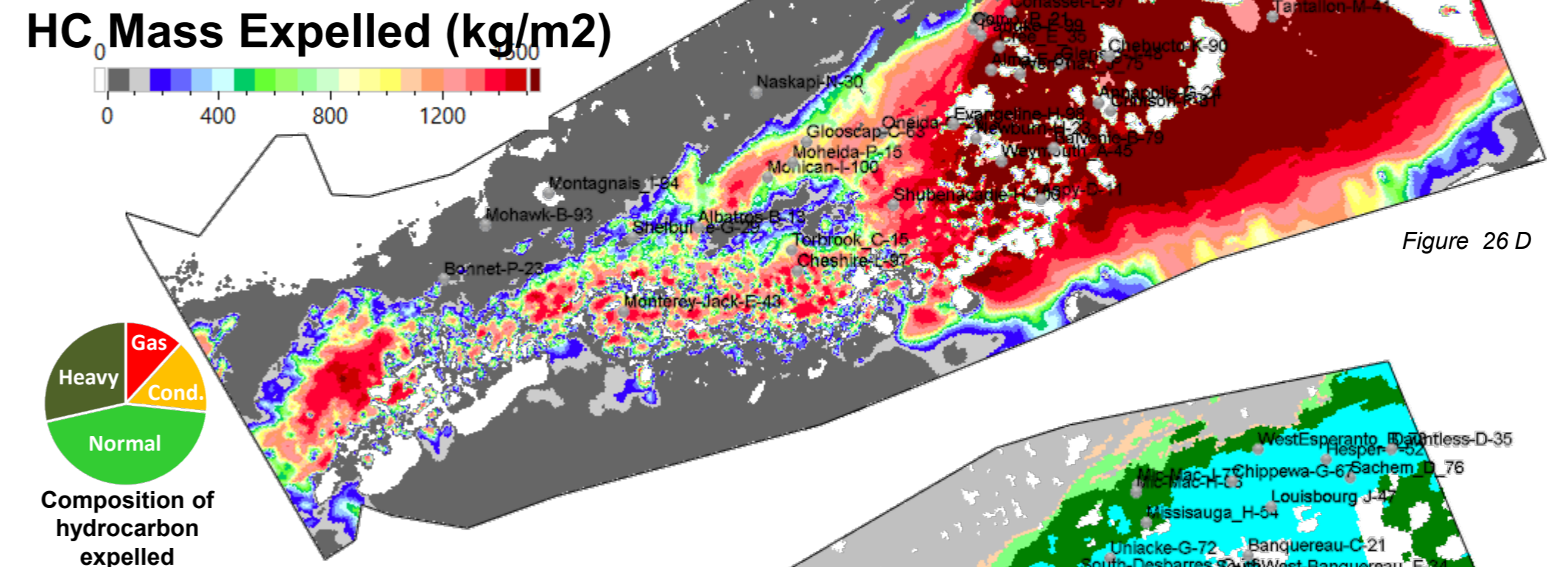
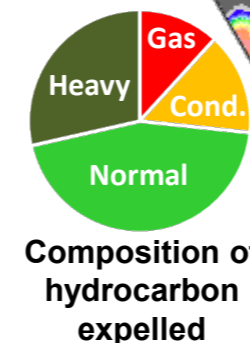


Figure 26 D



Composition of hydrocarbon expelled

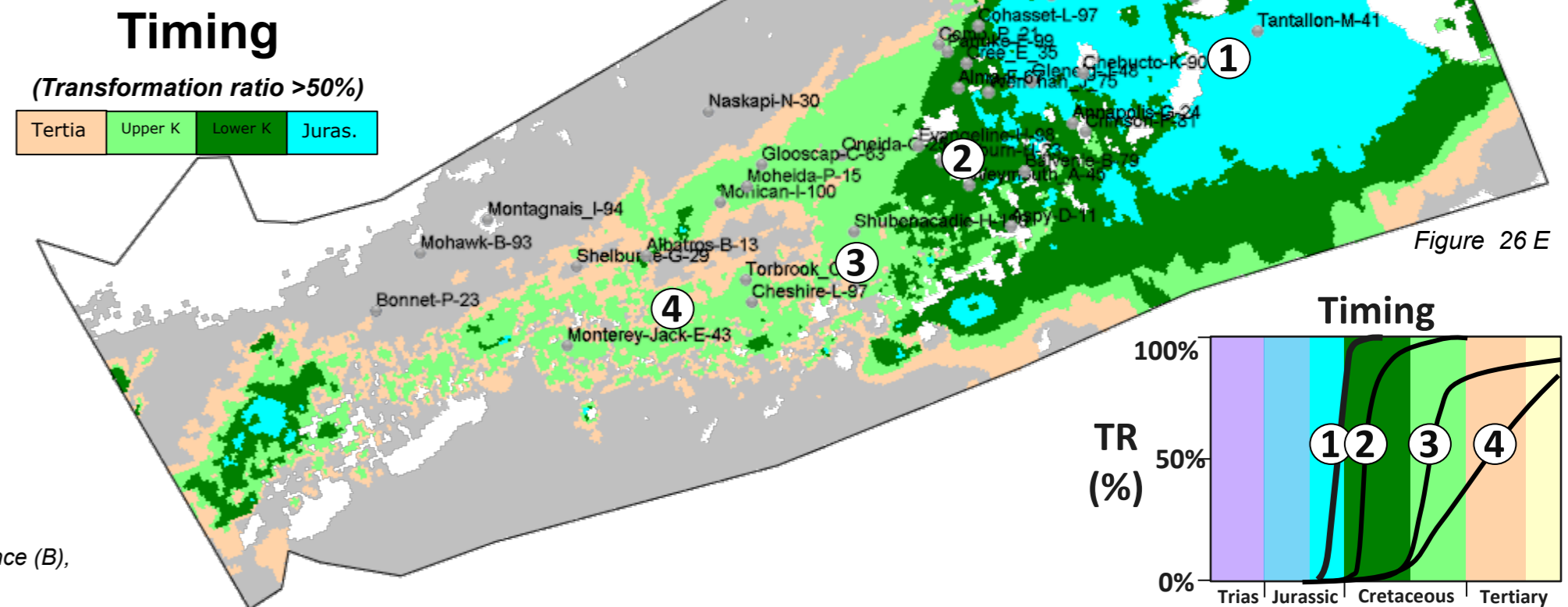


Figure 26 E

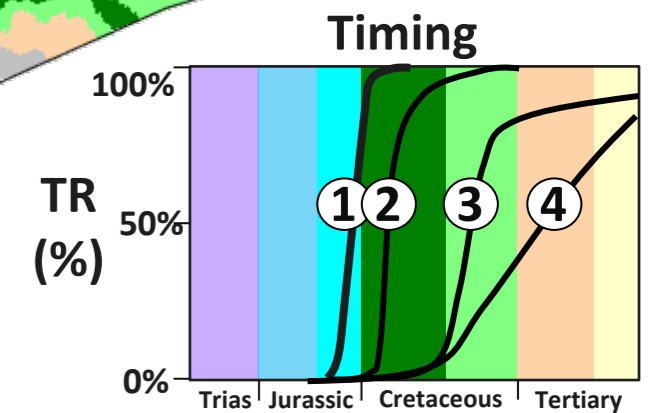


Figure 26: Pliensbachian source rock thermal model results: Temperature (A), Vitrinite Reflectance (B), Transformation rate (C), hydrocarbon mass expelled (D) and Timing (E)

Tithonian Source Rock

Temperature/Maturity/Generation/Expulsion/Timing

Source rock temperatures vary from 30°C in the very shallow inner shelf north-west of Bonnet, Montagnais and Mohawk, to 200°C in the main depocenter deeply buried around Annapolis and Chebucto in the east (Figure 27 A). Simulated vitrinite reflectance (Easy Ro%) shows a large area from oil to dry gas window in the eastern half of the study area whereas only very small areas are expected to be in oil window at mini basin locations in the western margin (Figure 27 B). Kerogen thermal cracking reaches 100% (Transformation Ratio) between Chebucto and Annapolis giving 800 kg/m² of hydrocarbon mass expelled whereas the western margin shows almost no potential (Figure 27 C and D). The main Tithonian kitchen is located in the eastern part of the basin where generation/expulsion is dated to be from early Cretaceous to Tertiary (Figure 27 E). Note that, vitrinite property is computed for the entire Tithonian interval and doesn't take into account the richness distribution. Hence mass expelled from the Tithonian west of the Shubenacadie well is modelled as low, because of poorer source rock parameters and thickness.

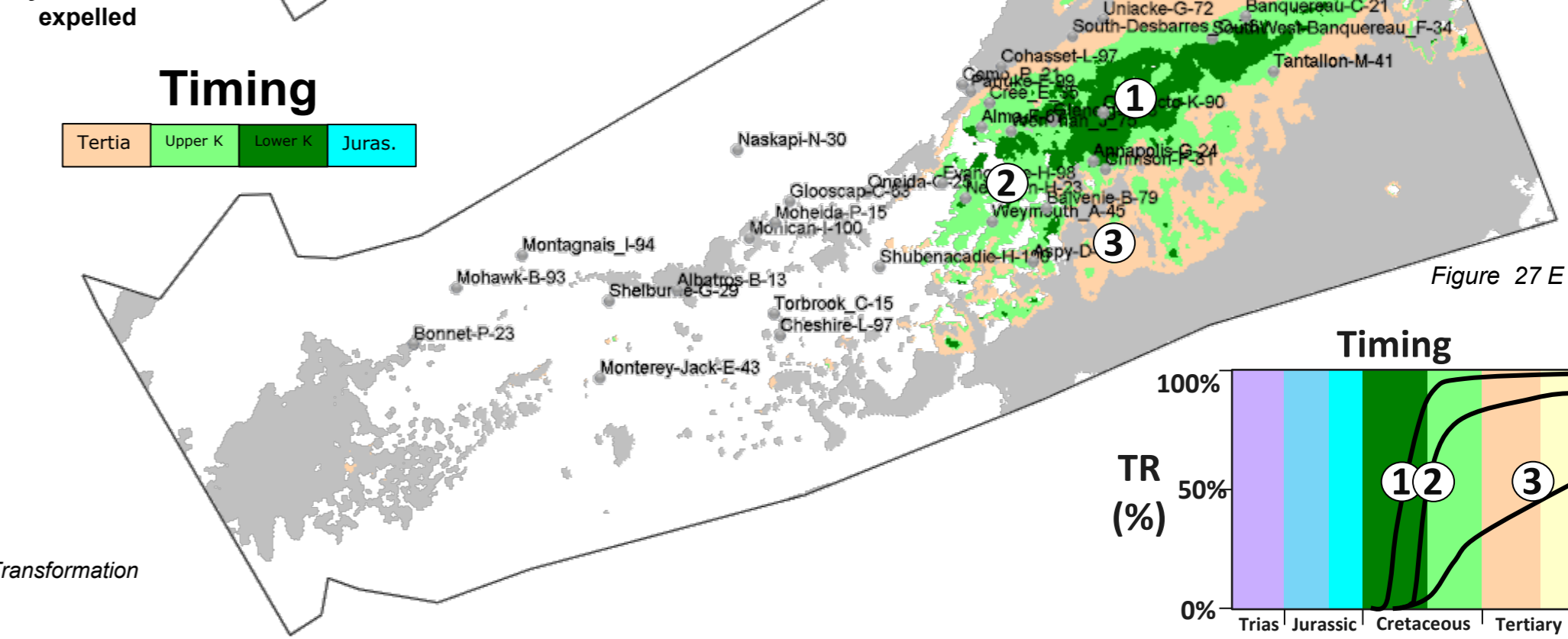
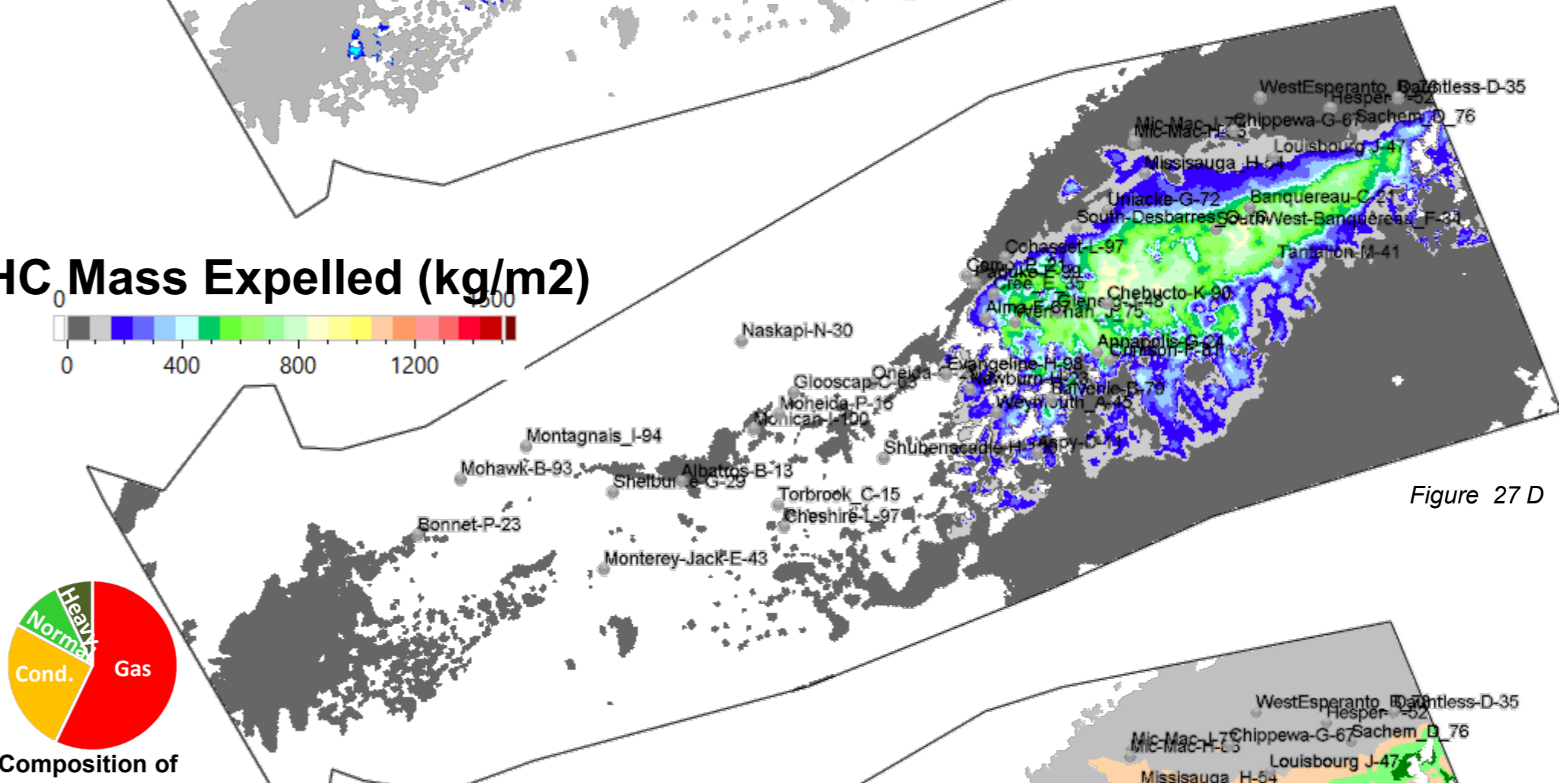
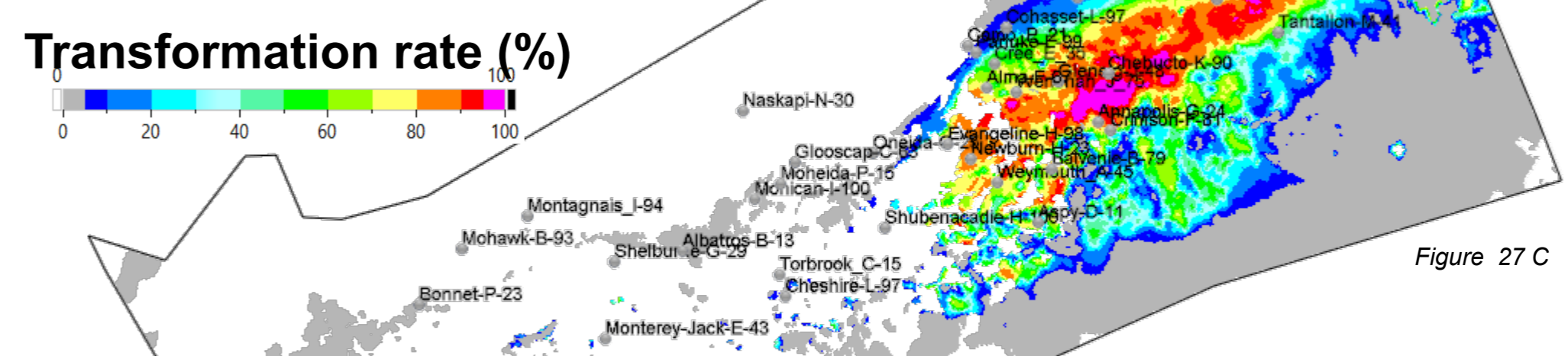
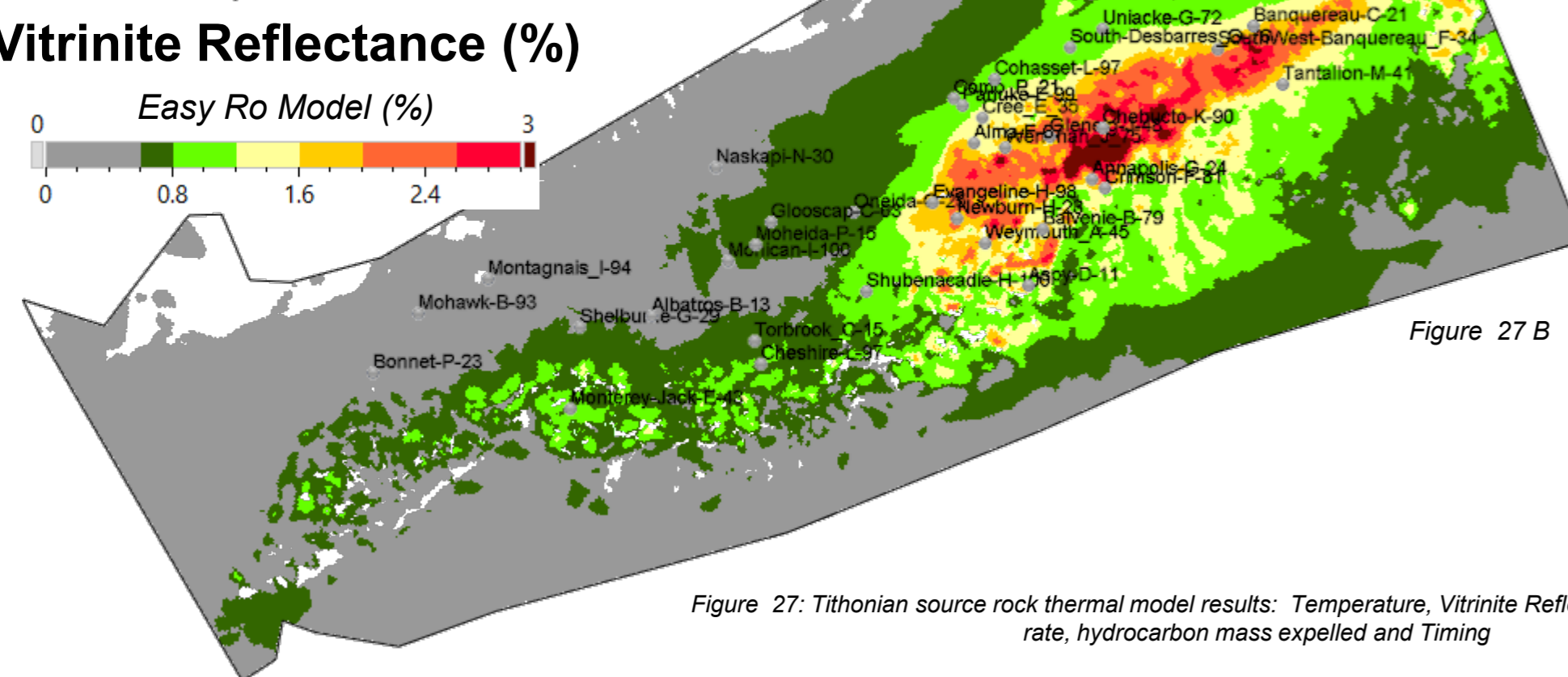
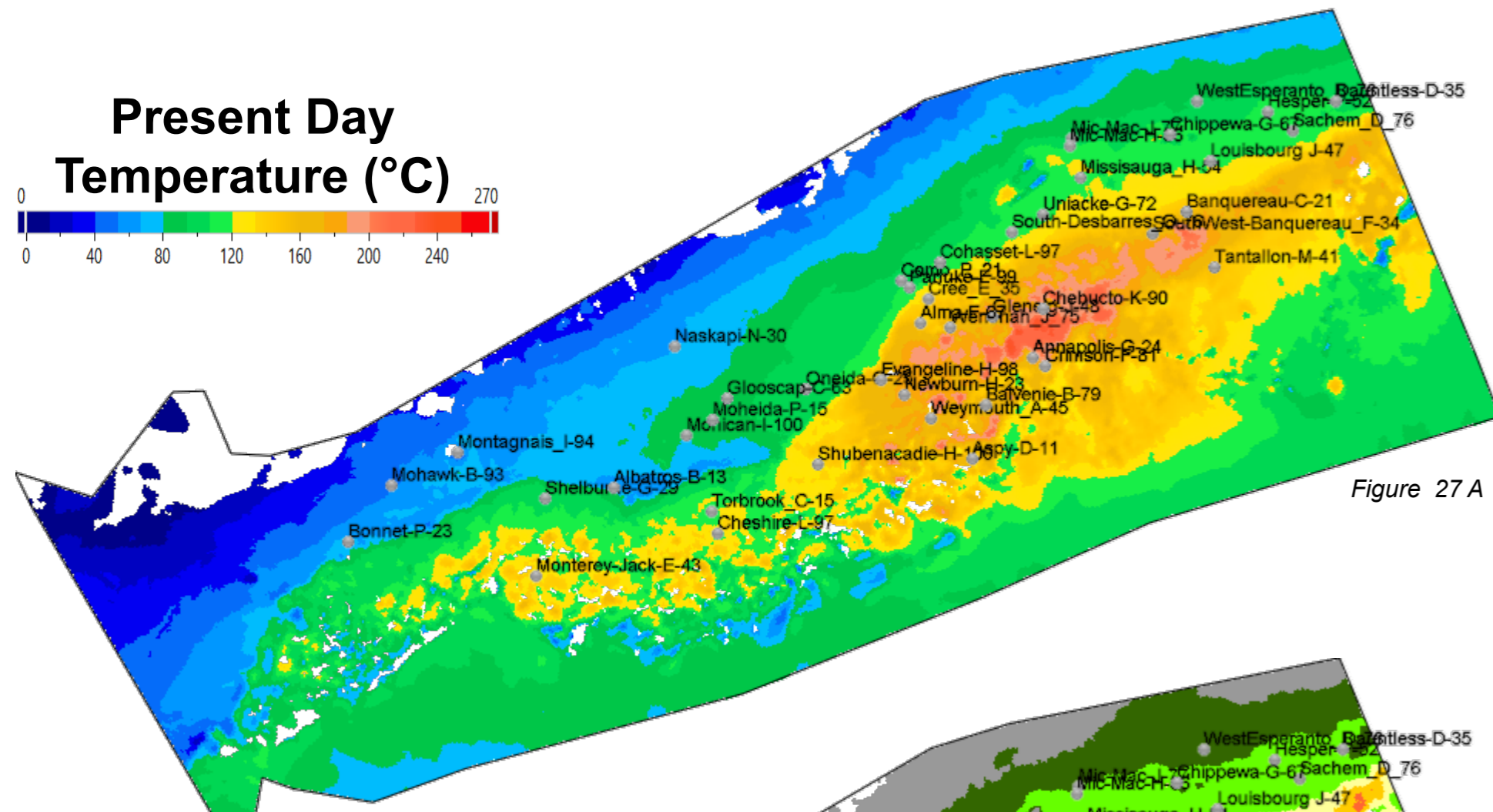


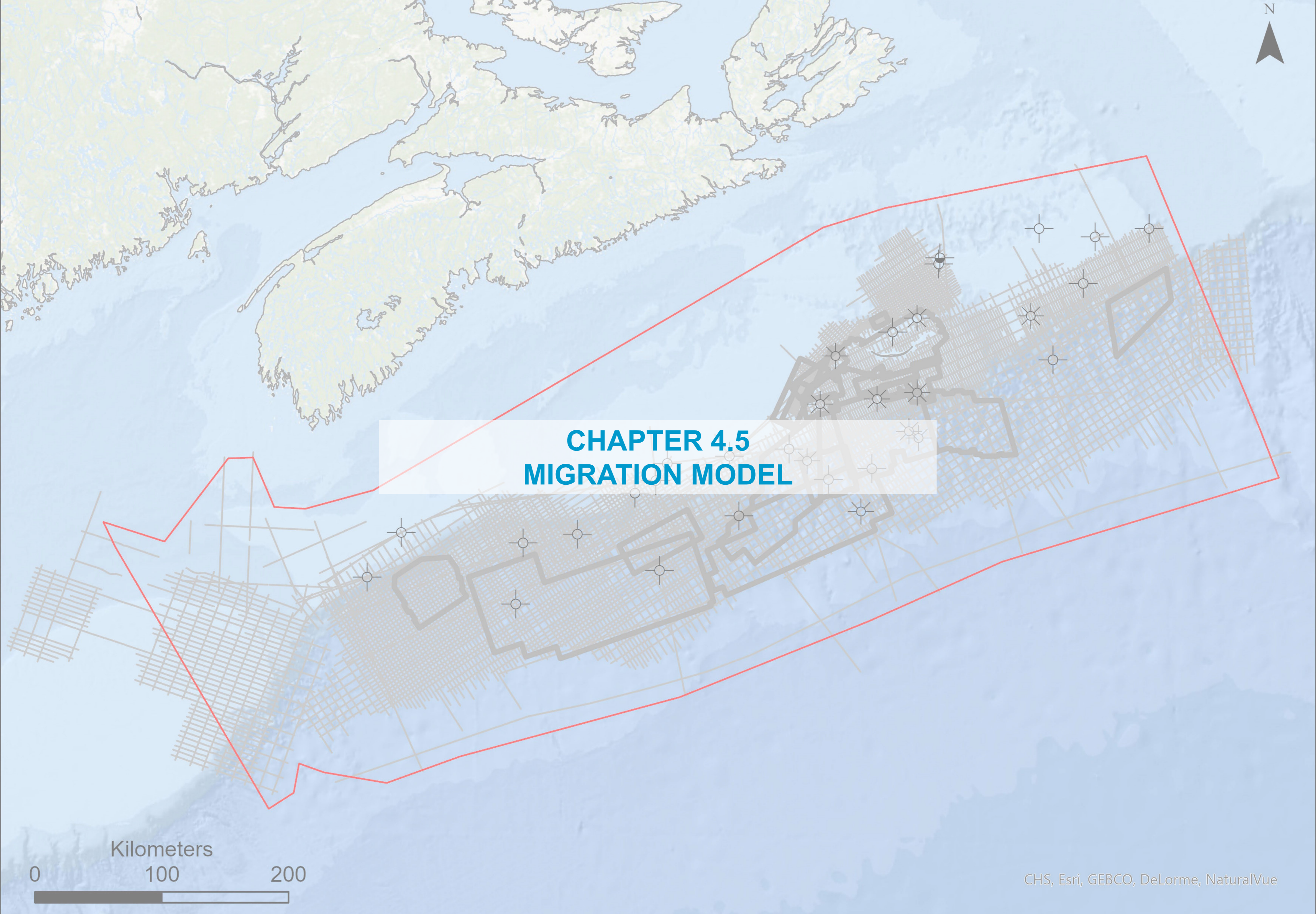
Figure 27: Tithonian source rock thermal model results: Temperature, Vitrinite Reflectance, Transformation rate, hydrocarbon mass expelled and Timing



CHAPTER 4.5 MIGRATION MODEL

Kilometers

0 100 200



3D migration model

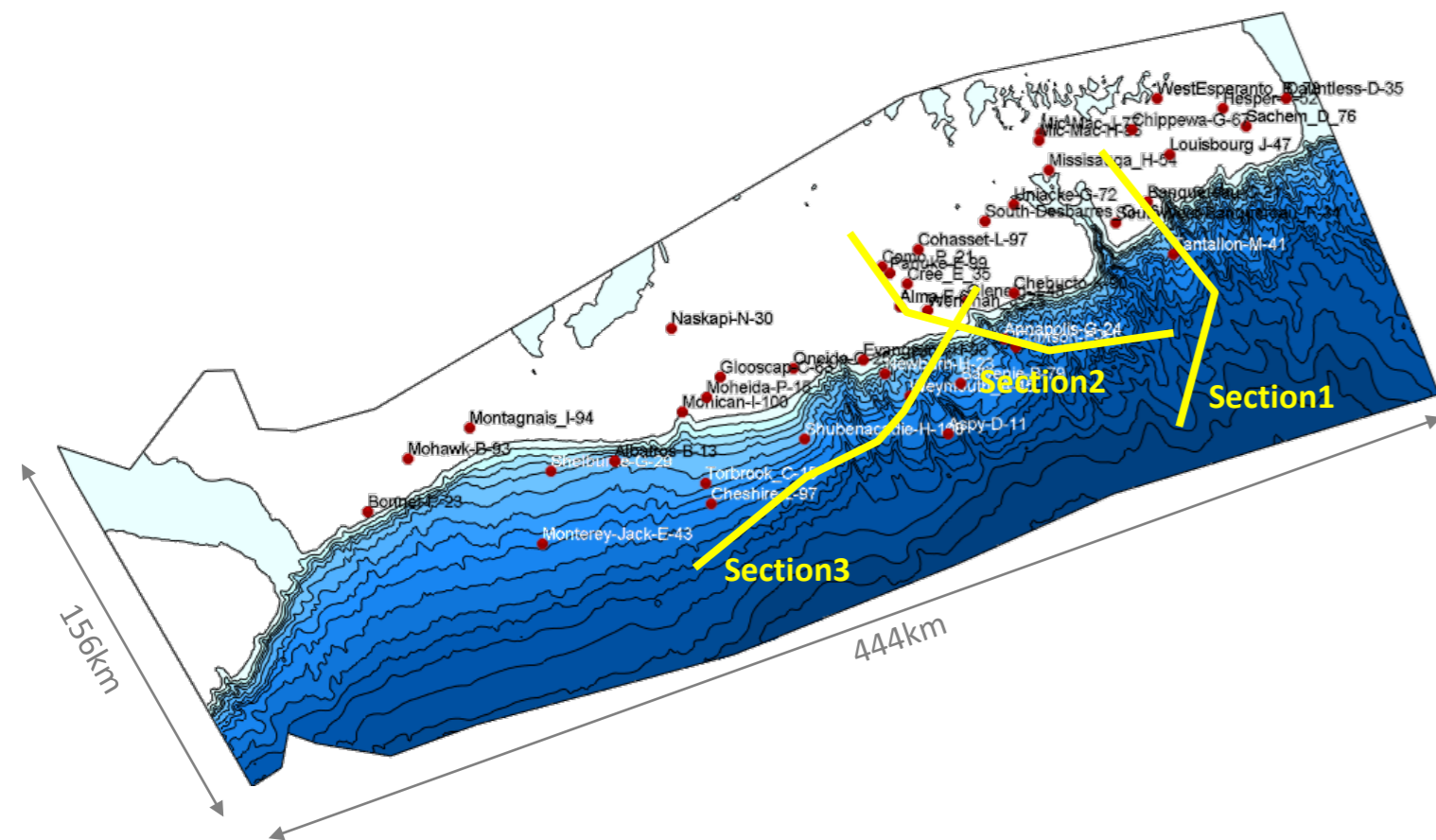
This 3D Migration modeling is an advanced petroleum system modeling that simulates processes of generation, expulsion, migration (Darcy), entrapment, secondary migration, secondary thermal cracking and preservation. Migration processes are performed using full Darcy capabilities of Temisflow that relate the flow (U_i) of phase i to the different driving forces (calculation of HCs and water movement through the porous water media). In this case, the grid resolution is 2km x 2km (cell size).

$$U_i = -\frac{Kk_{r,i}}{\mu_i} \left[\text{grad}(P - \rho_w g z) + \text{grad}(P_c) - (\rho_w - \rho_i) g \text{grad}(z) \right]$$

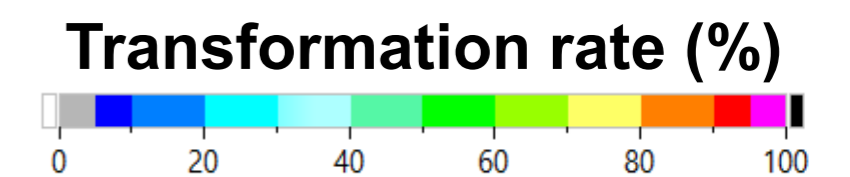
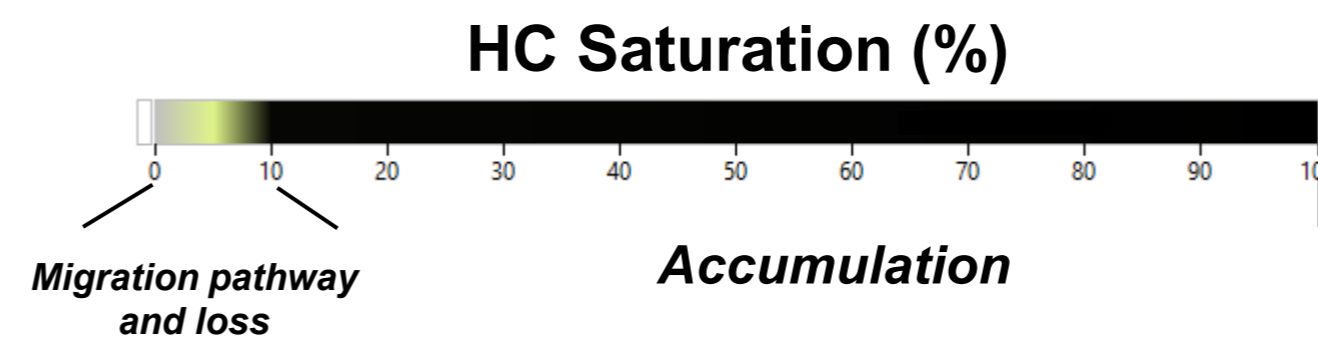
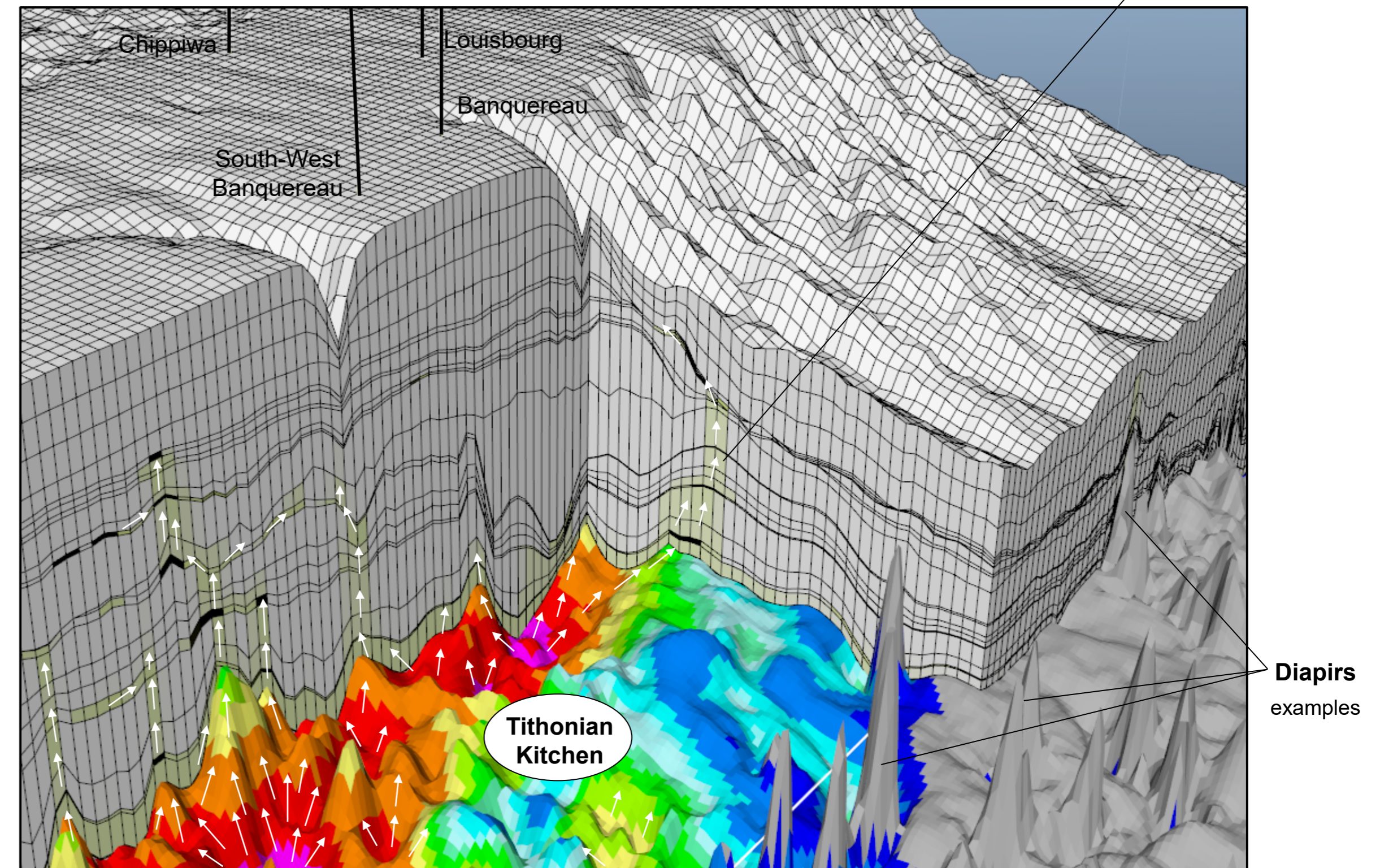
Intrinsic permeability K
 Relative permeability phase i
 Viscosity phase i
 Hydrodynamism
 Capillarity
 Buoyancy

On the right-hand side, the 3D view is showing the hydrocarbon migration and accumulations at present day around the Stonehouse lead (see Plate 6.11) and south of the Banquereau area. Black color in the grid indicates the hydrocarbon accumulations in reservoirs. White vector show the hydrocarbon flow and migration pathways. The map at the bottom part of the picture is the transformation ratio of Tithonian source rock which shows the effective kitchen area. Note that, mature Pliensbachian source rock also exists below this interval.

3 cross-sections extracted from the 3D migration model are presented in the following pages. These show hydrocarbon charge (saturation%), hydrocarbon phase (GOR) and migration history (HC flow) at present and through time. The location of the sections is shown in the map below.



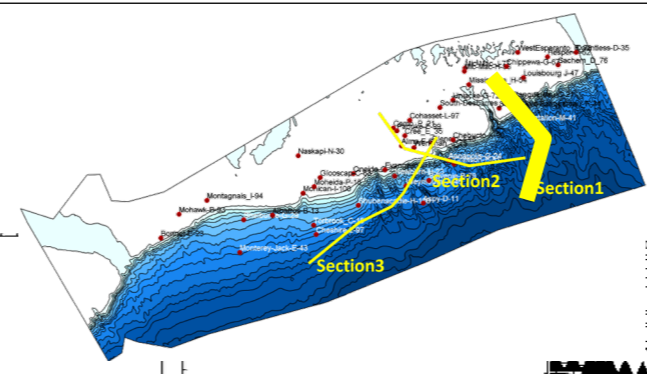
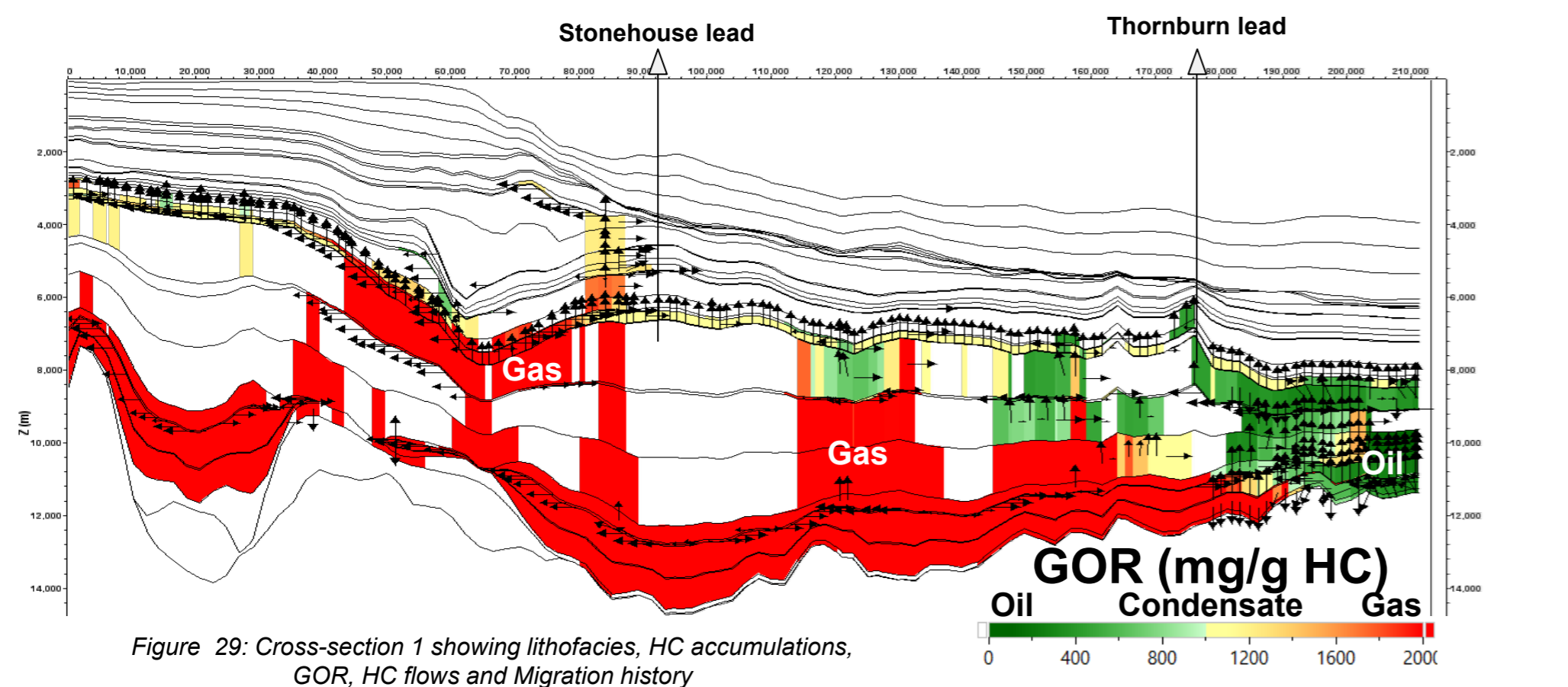
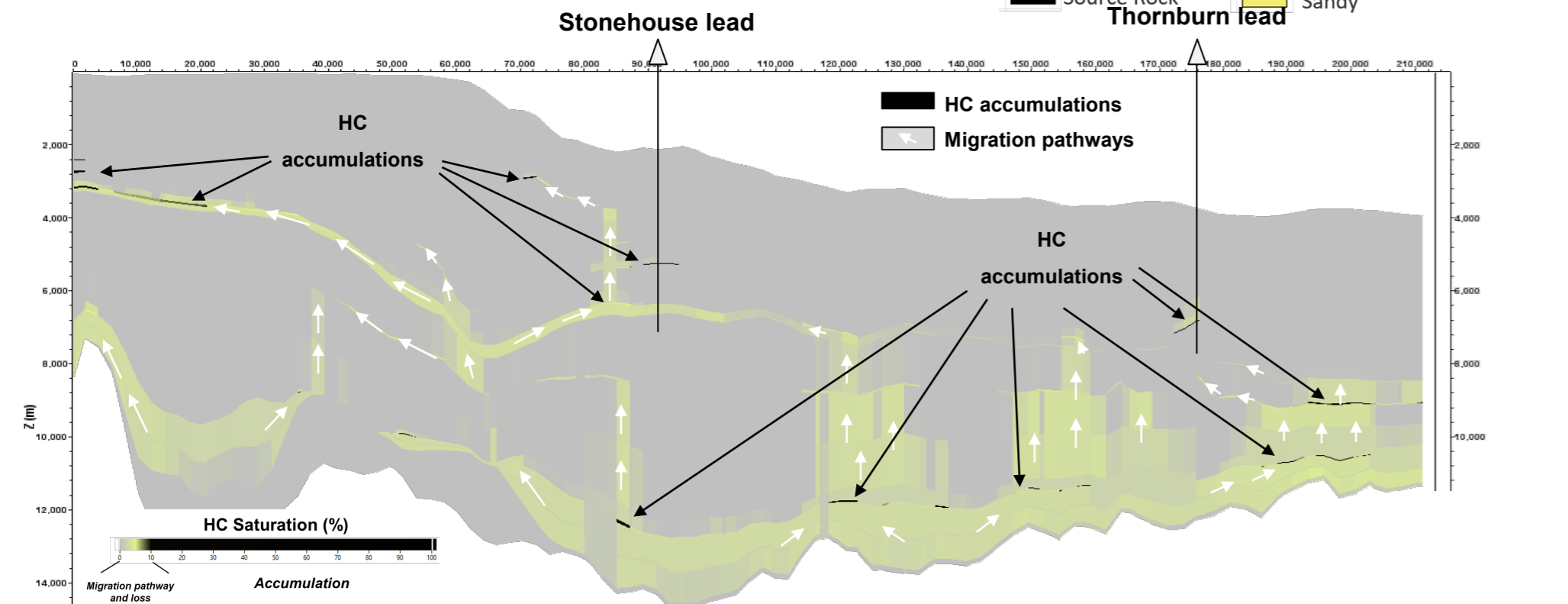
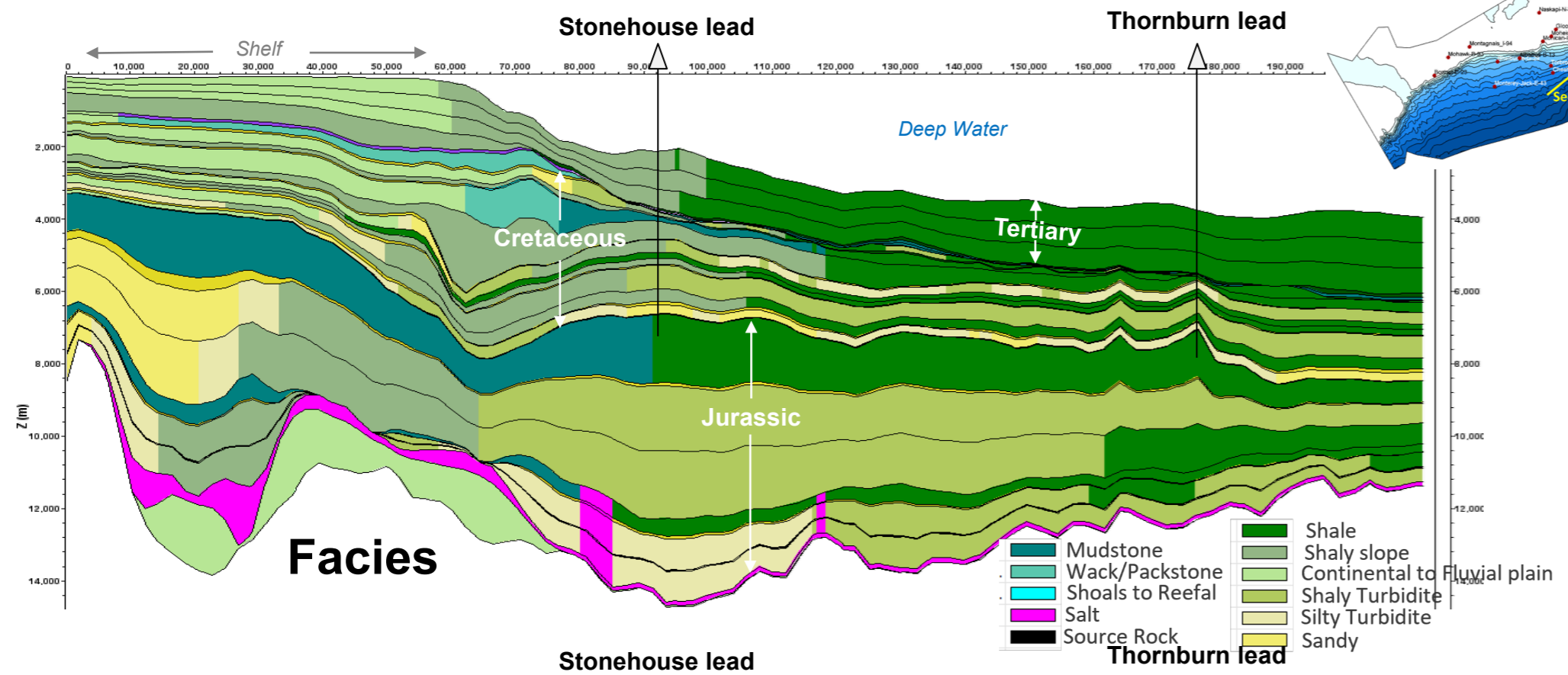
3D view on Temisflow model (Hydrocarbon migration/accumulations)



Accumulation

Figure 28: 3D view of migration modeling in the south Banquereau area showing Tithonian maturity, hydrocarbon flows and accumulations

Section 1



Migration history

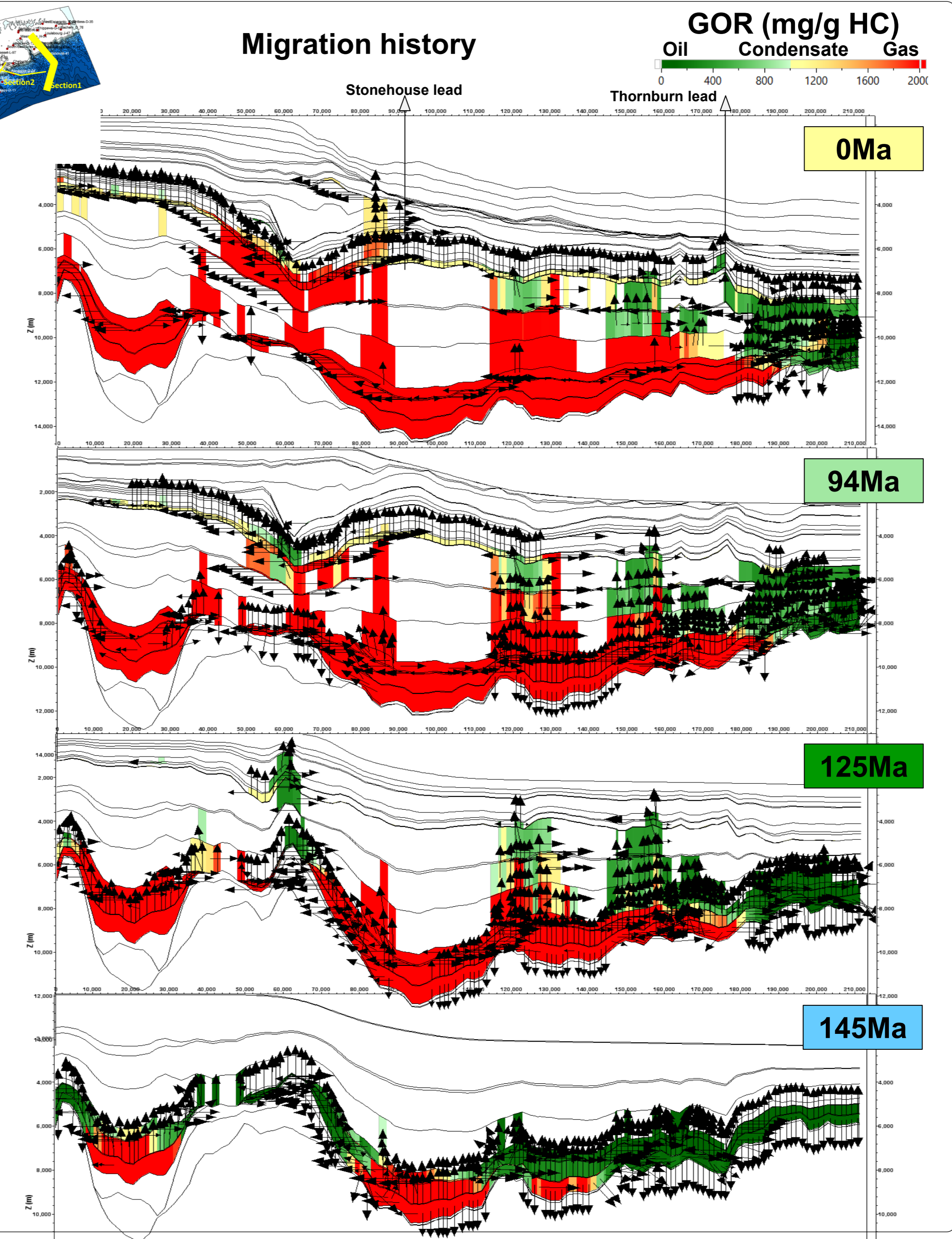
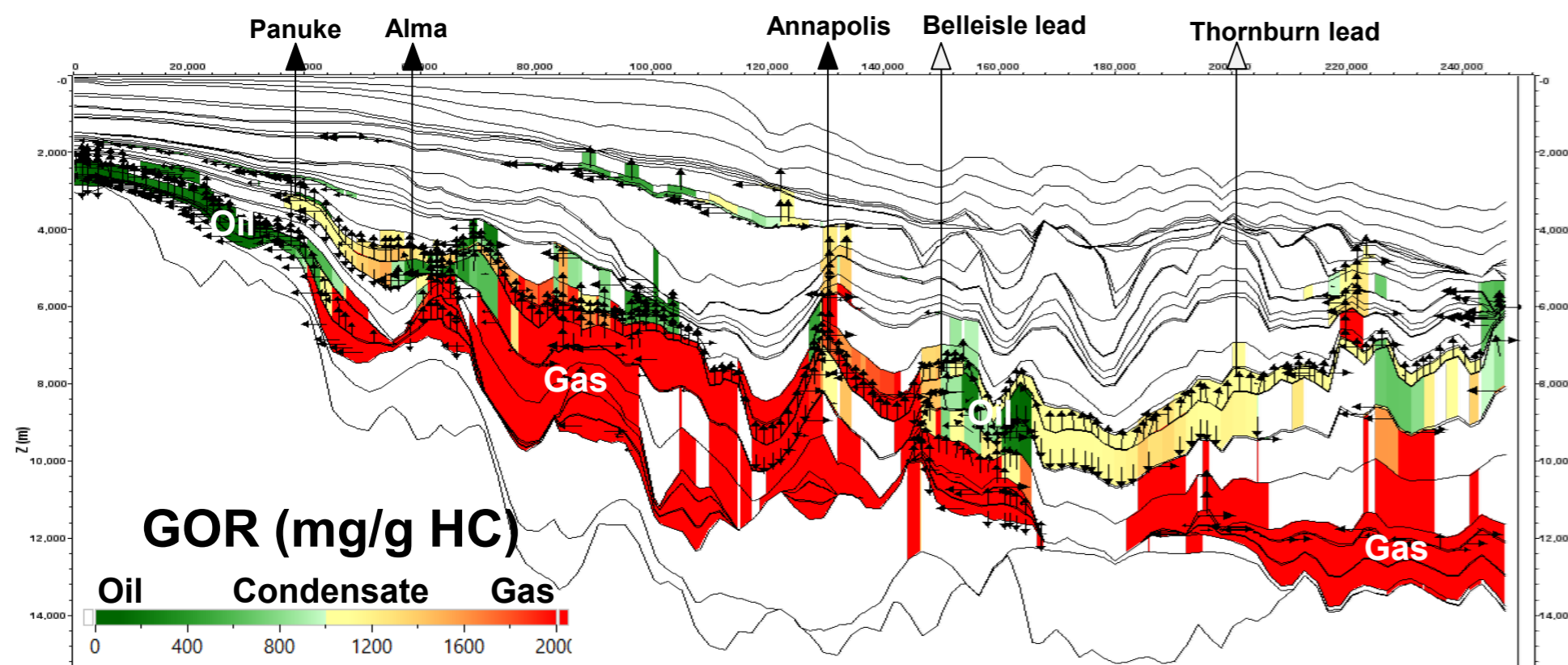
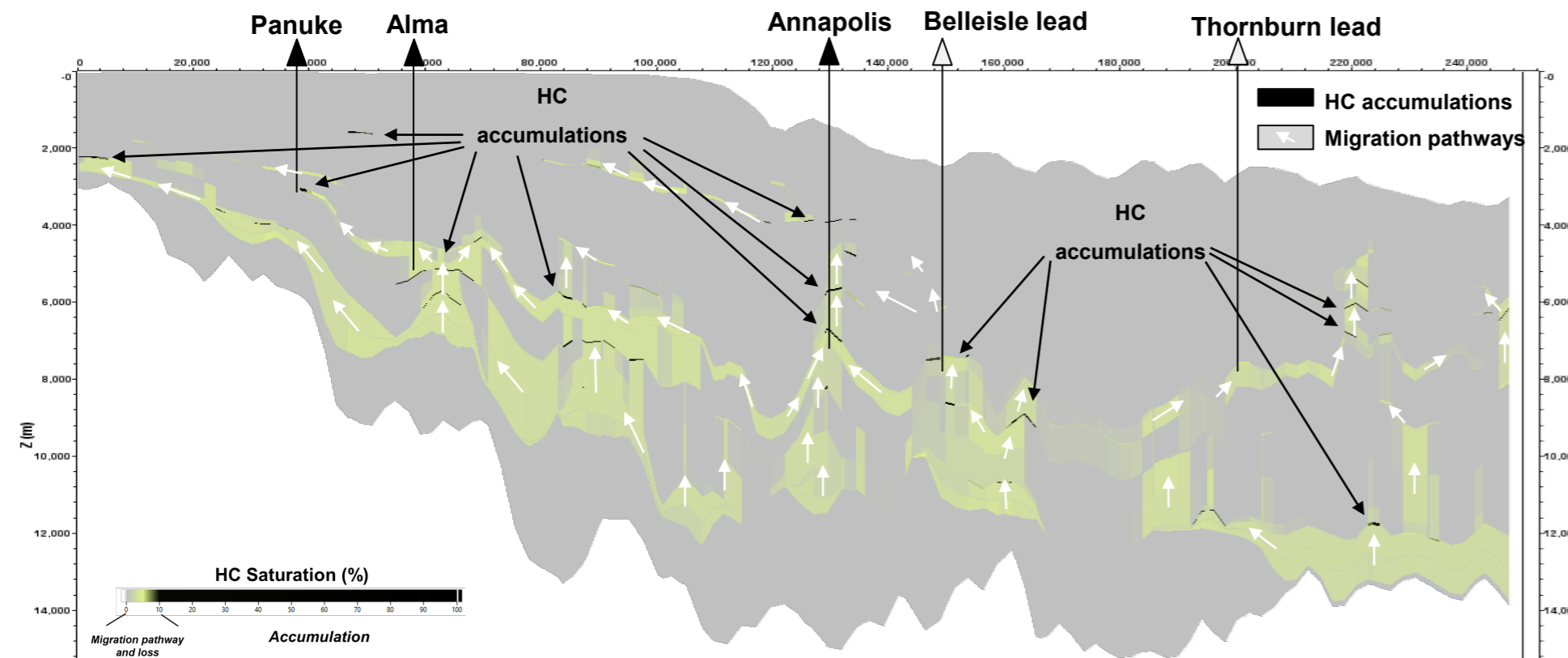
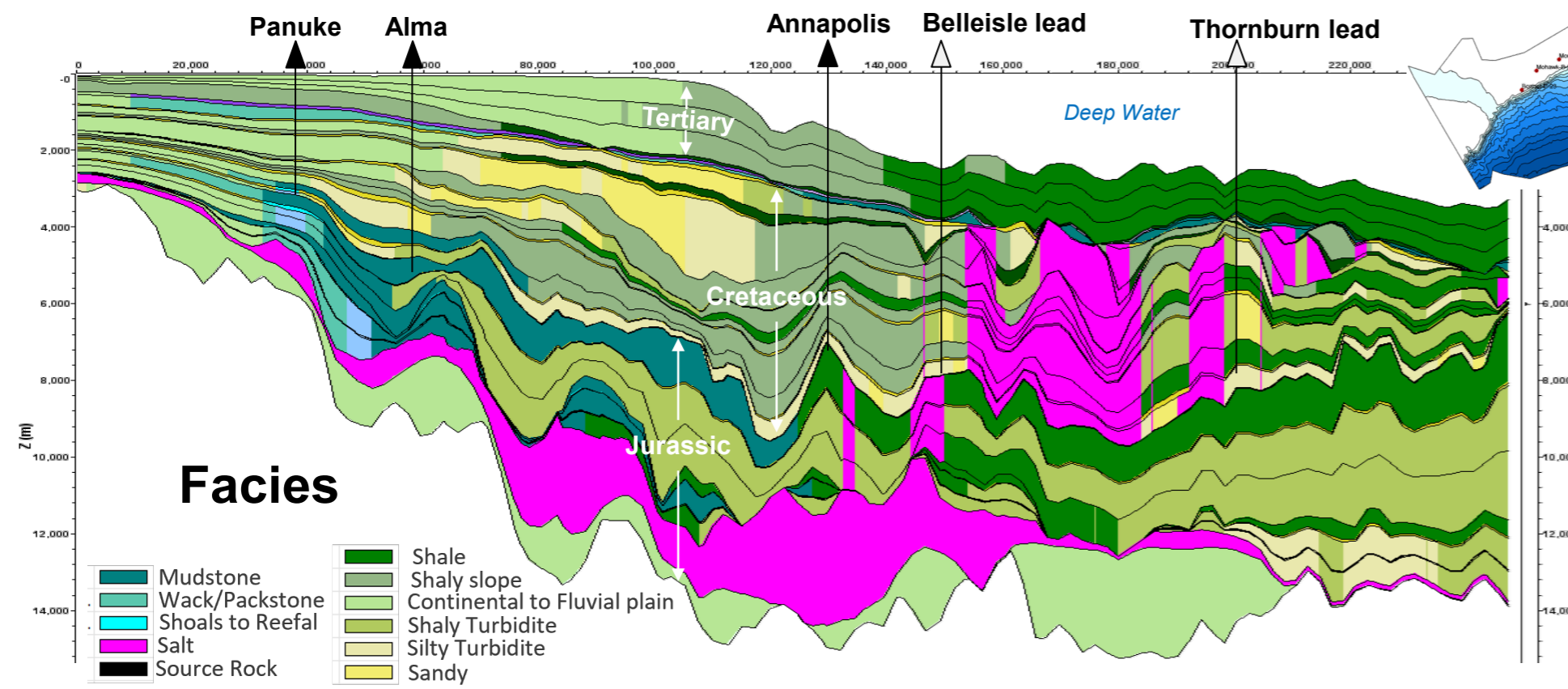


Figure 29: Cross-section 1 showing lithofacies, HC accumulations, GOR, HC flows and Migration history

Section 2



Migration history

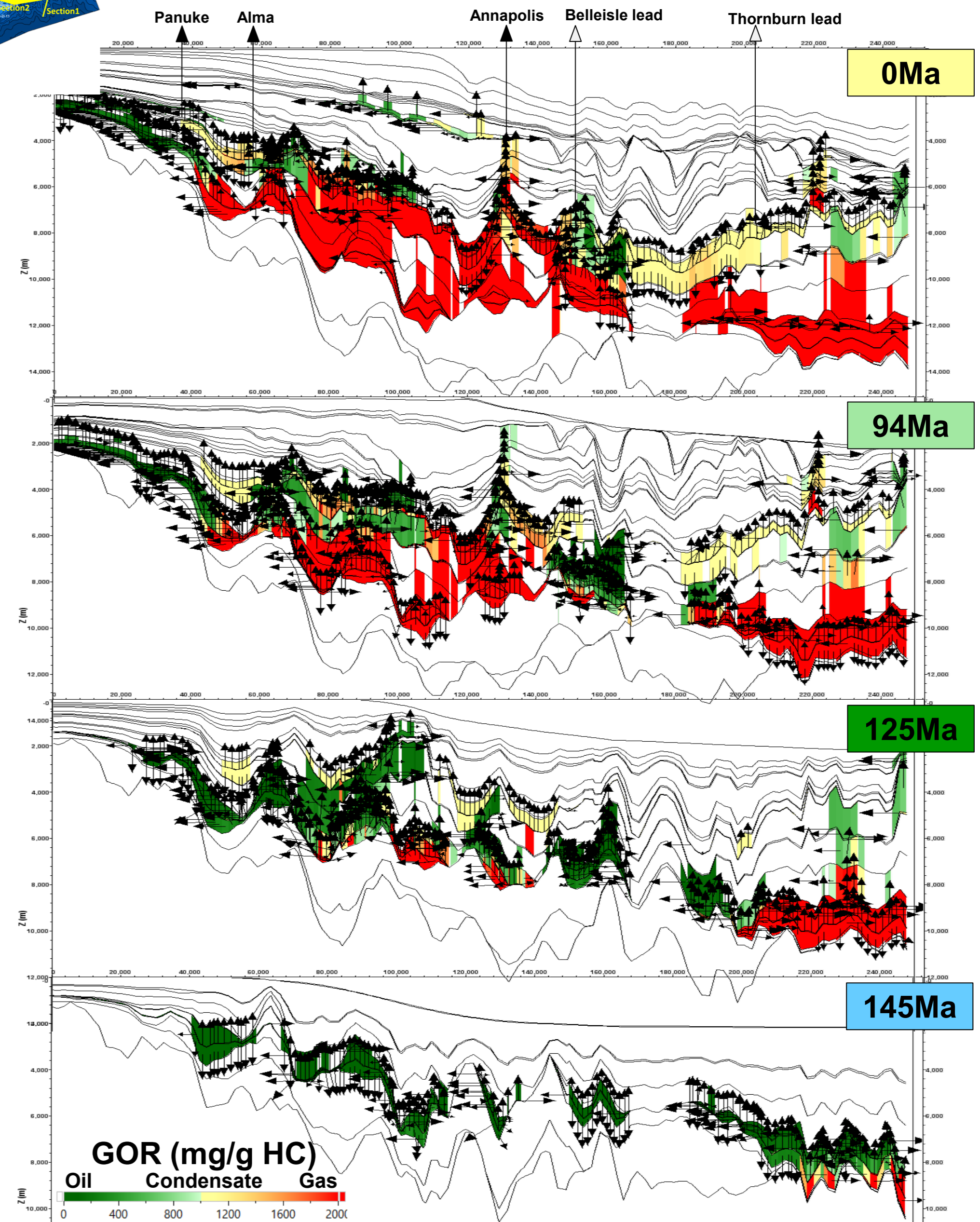
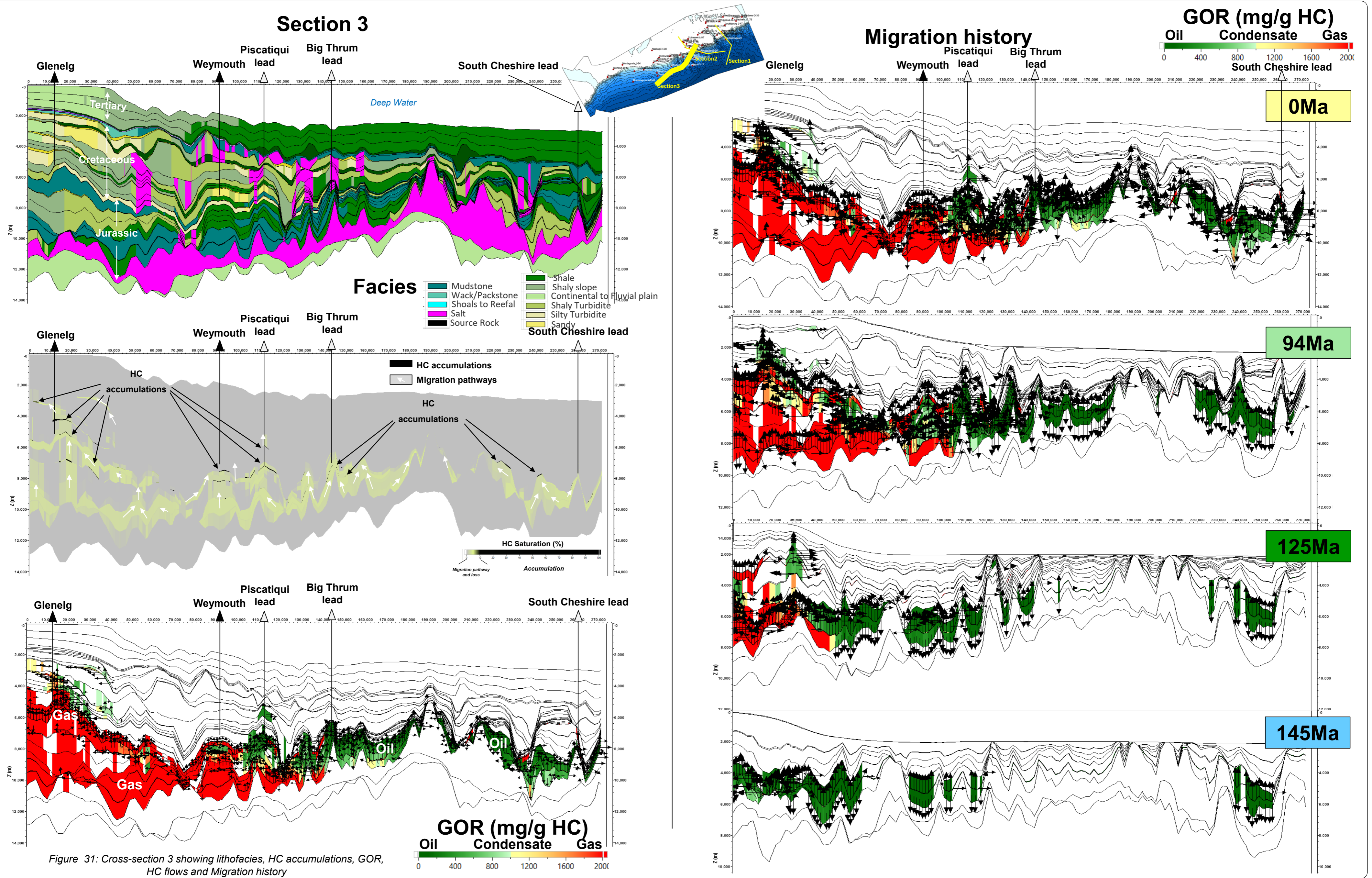


Figure 30: Cross-section 2 showing lithofacies, HC accumulations, GOR, HC flows and Migration history



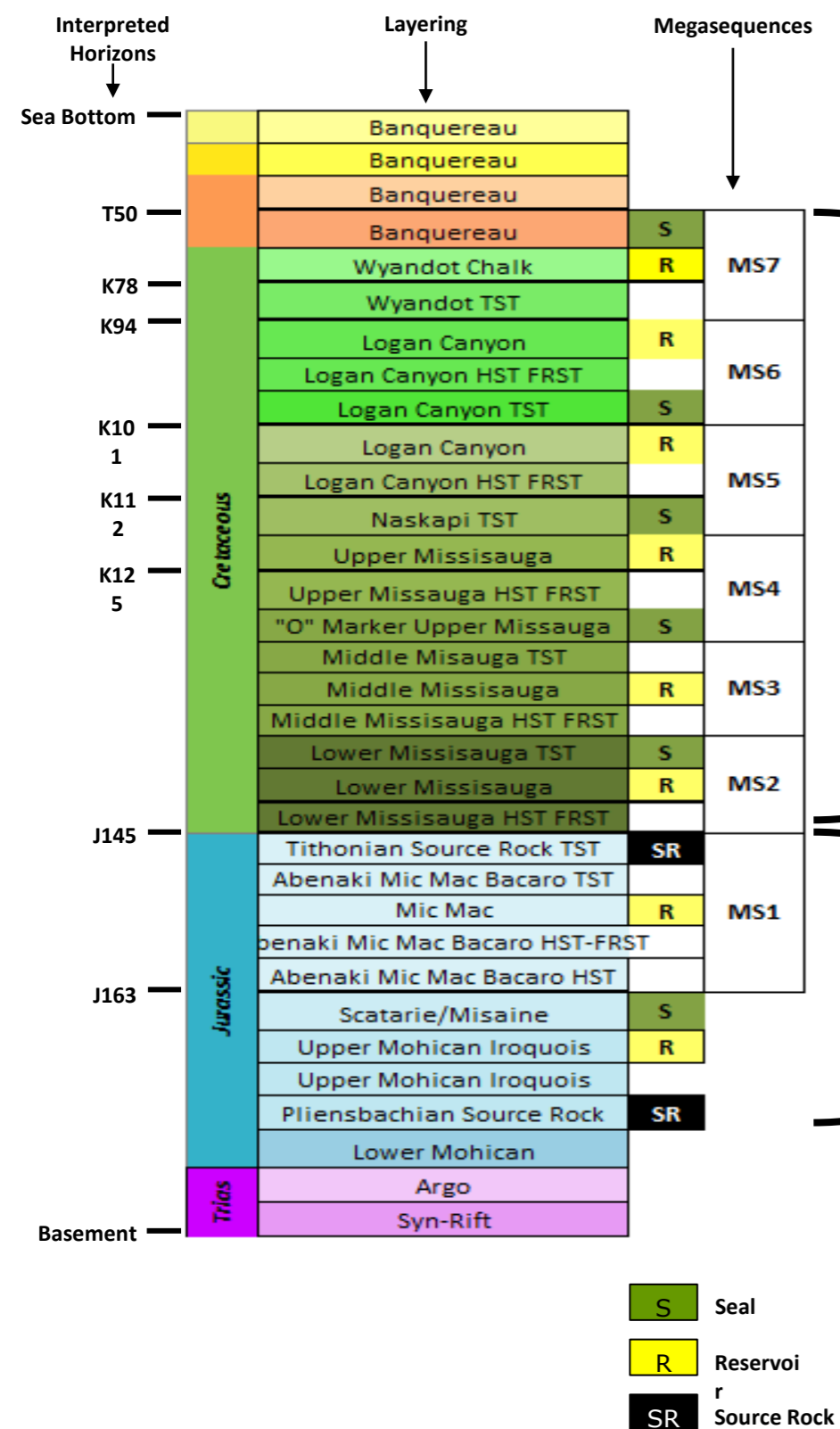
Hydrocarbon in place and Fluid type

The map of GOR shows the hydrocarbon charge in the basin (i.e. saturation > 1%) and the associated dominant phase (Oil, Condensate and Gas). This map indicates hydrocarbon traces, shows or accumulations.

The GOR was extracted for Jurassic and Cretaceous intervals. The first, Jurassic interval, is influenced by the charge of Pliensbachian source rock, and the second one, Cretaceous, is influenced by the charge of both Pliensbachian and Tithonian source rock.

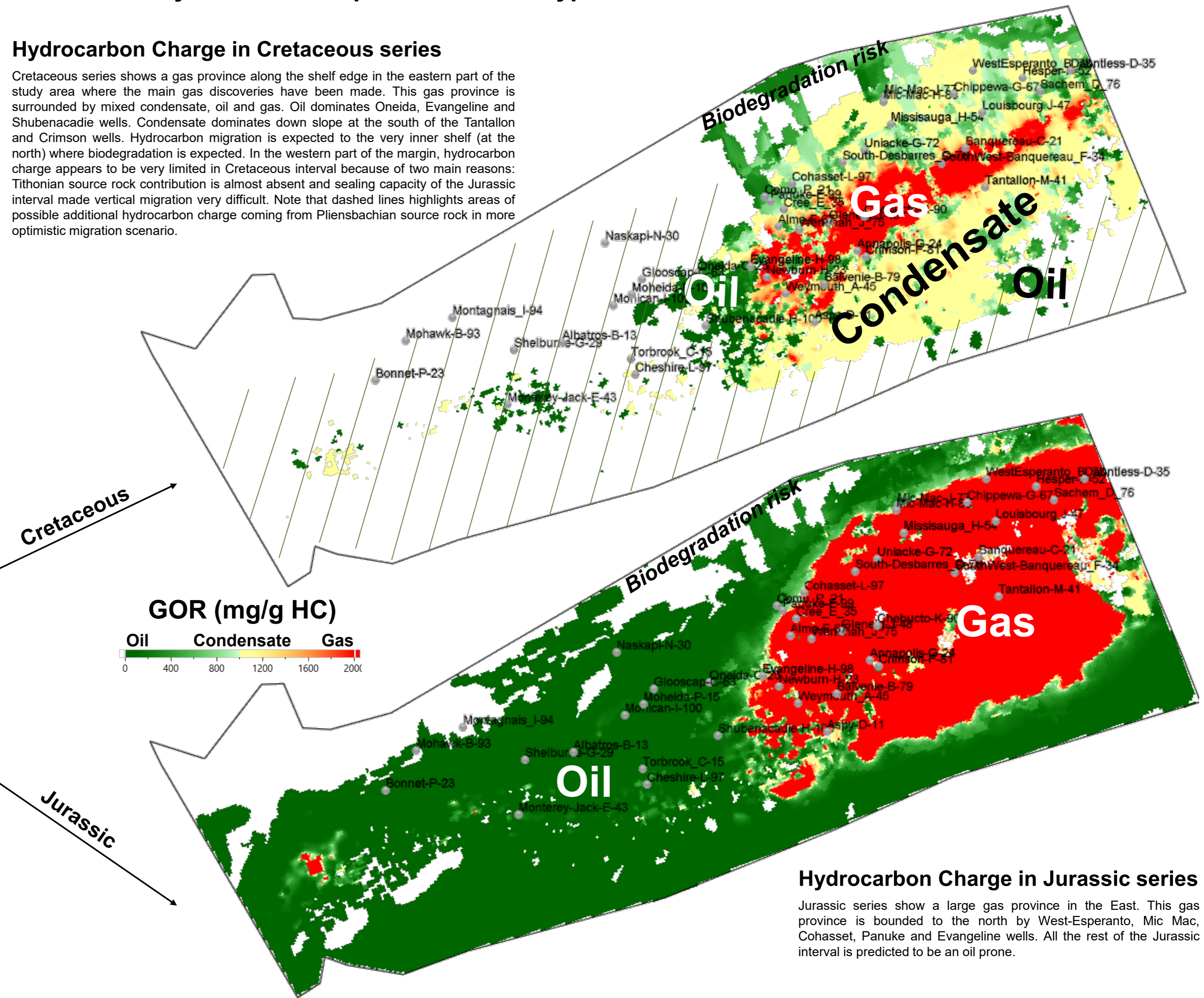
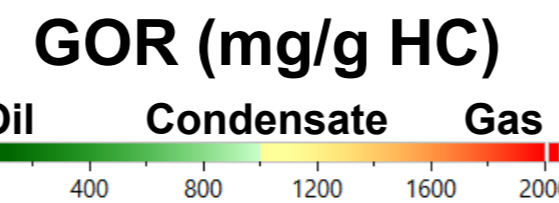
Hydrocarbon Charge in Cretaceous series

Cretaceous series shows a gas province along the shelf edge in the eastern part of the study area where the main gas discoveries have been made. This gas province is surrounded by mixed condensate, oil and gas. Oil dominates Oneida, Evangeline and Shubenacadie wells. Condensate dominates down slope at the south of the Tantallon and Crimson wells. Hydrocarbon migration is expected to the very inner shelf (at the north) where biodegradation is expected. In the western part of the margin, hydrocarbon charge appears to be very limited in Cretaceous interval because of two main reasons: Tithonian source rock contribution is almost absent and sealing capacity of the Jurassic interval made vertical migration very difficult. Note that dashed lines highlights areas of possible additional hydrocarbon charge coming from Pliensbachian source rock in more optimistic migration scenario.



Cretaceous

Jurassic



Hydrocarbon Charge in Jurassic series

Jurassic series show a large gas province in the East. This gas province is bounded to the north by West-Esperanto, Mic Mac, Cohasset, Panuke and Evangeline wells. All the rest of the Jurassic interval is predicted to be an oil prone.

Figure 32: Map of hydrocarbon in place (traces, shows, accumulations) and Fluid type



CHAPTER 4.6 WAY FORWARD

Kilometers

0 100 200



Lower and Middle Jurassic prospectivity

- Anticipated HC in Lower and Middle Jurassic to the west of Nova Scotia
- Planned activities in the Lower to Middle Jurassic interval
 - Seismic interpretation of intermediate horizons between Top Basement and J163 with fault interpretation
 - Geological model based on sedimentological and biostratigraphy analysis at wells and GDE mapping
 - 3D Forward Stratigraphic modelling to predict and characterize reservoir, sealing and source rock facies with risk analysis (P10, P50 and P90 maps). Several hypothesis for diapirism timing could be considered to assess the relationship between sediment flux and diapirism
 - 3D Petroleum System modelling based on Forward Stratigraphic model risk maps to delineate the HC accumulations and the associated risks

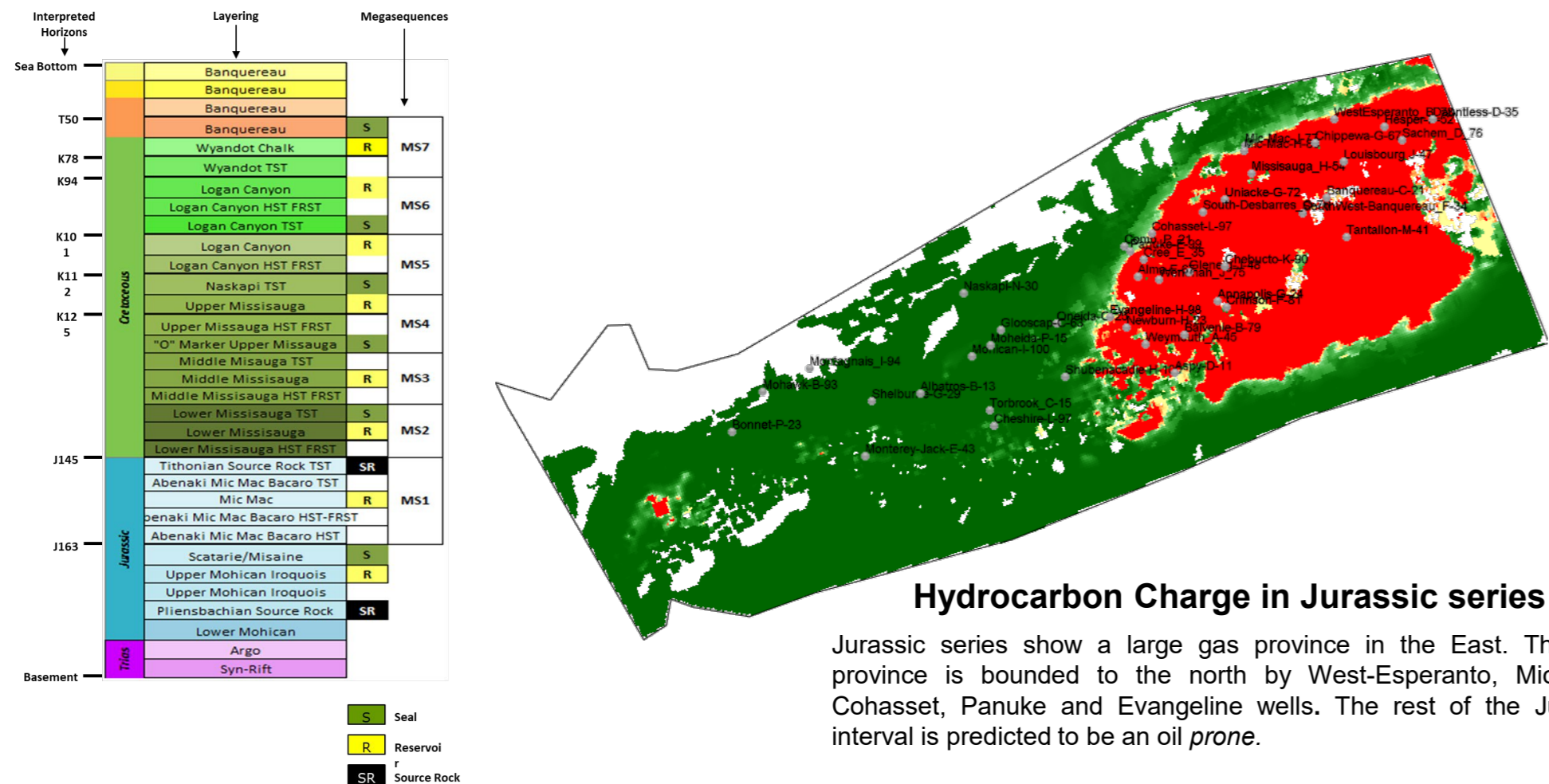


Figure 36: Map of hydrocarbon in place for the Jurassic interval

Reservoir and source rock prediction with DionisosFlow

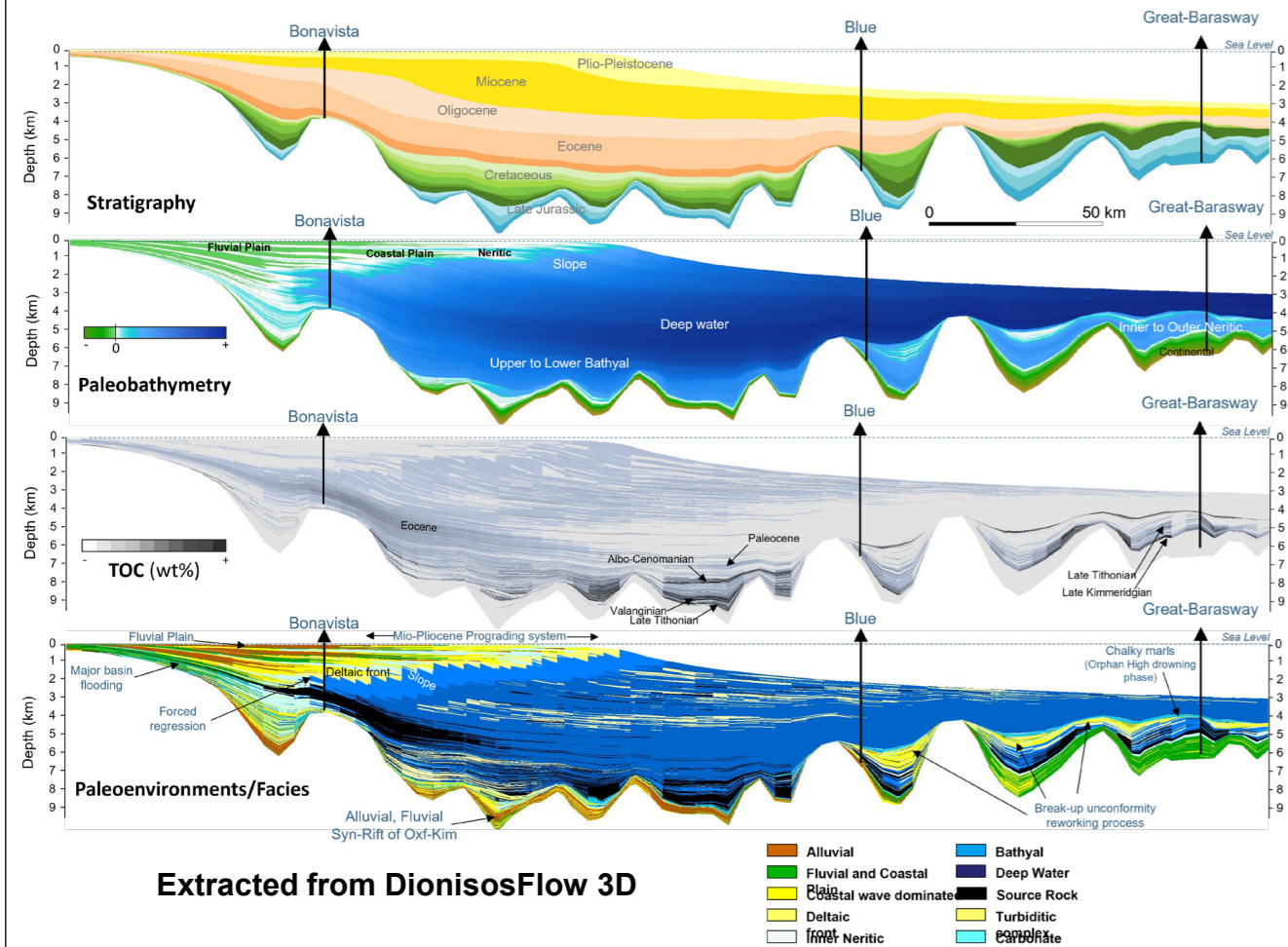
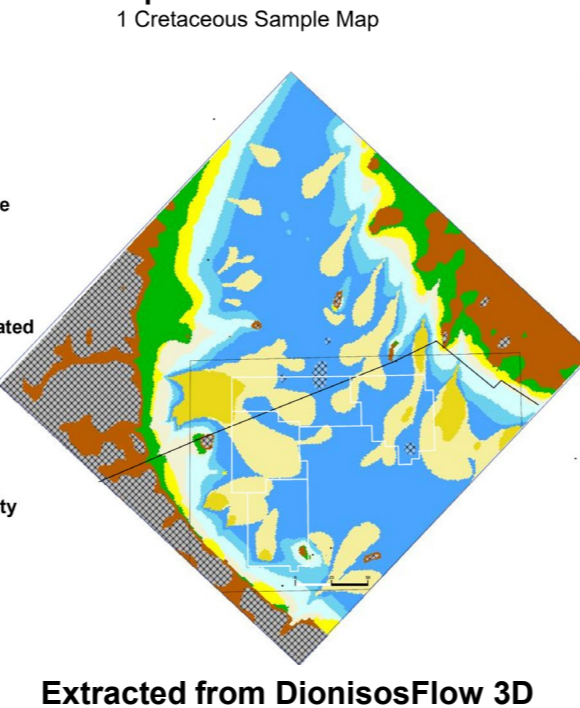


Figure 33: Example of DionisosFlow model from rifting to present day showing stratigraphy, paleo-bathymetry, lithofacies and organic matter content (Offshore Newfoundland & Labrador Resource assessment; Orphan Basin Area NL22-CFB01)

Gross Depositional Environments



Salt restoration at the scale of some of the 10 evaluated leads in Tangier 3D survey prospective area

- Estimate the ages of deformation of the salt
- Predict the distribution of transported clastic sediments during the salt deformation
- Delineate reservoir and seal bodies
- Planned activities for the salt deformation at the scale of the prospective area and interval
 - Seismic interpretation of salt bodies
 - Tuning the seismic interpretation of the key horizons accordingly
 - Seismic interpretation of intermediate horizons in the prospective area and interval
 - Velocity modeling and depth conversion
 - Seismic geomorphology based on horizons stack
 - Update of the petroleum system model including detailed timing of salt deformation

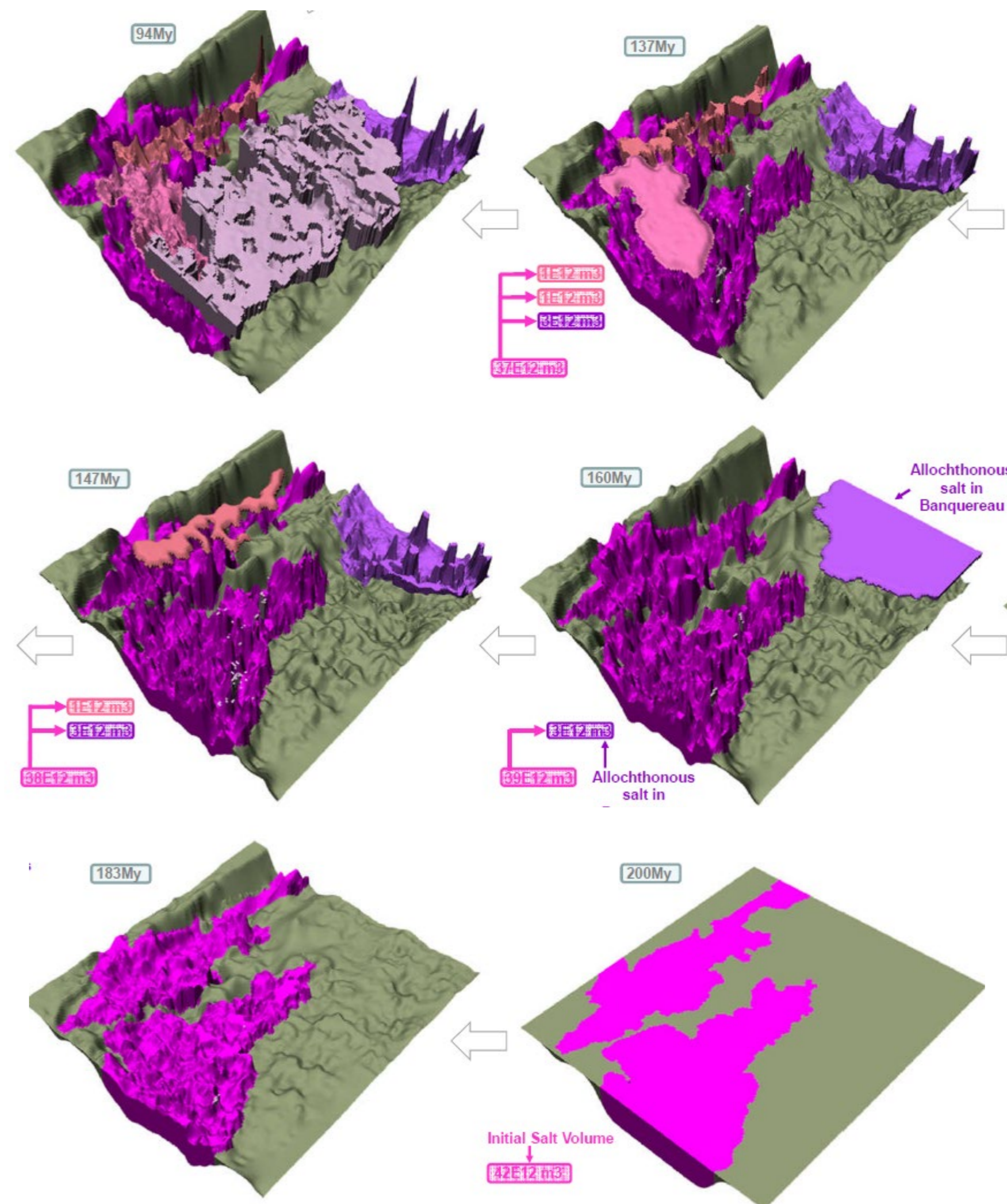


Figure 34: Example of salt restoration from emplacement to K94 in the Tangier prospective area